

Trade-off between simulation accuracy and complexity for mine compressed air systems

J Watkins



orcid.org/0000-0002-1832-1801

Dissertation submitted in fulfilment of the requirements for the degree *Master of Engineering in Mechanical Engineering* at the North-West University

Supervisor: Prof M Kleingeld

Graduation ceremony: May 2019

Student number: 24234222

ABSTRACT

Title: Trade-off between simulation accuracy and complexity for mine compressed air systems

Author: J Watkins

Supervisor: Prof. M Kleingeld

School: North-West University, Potchefstroom Campus

Faculty: Engineering

Degree: Master of Engineering in Mechanical Engineering

In South Africa, the industrial sector is responsible for a large portion of the country's total annual electricity consumption. The mining sector alone contributes approximately 15%, which makes it one of the largest electricity consumers in the country. A significant electricity consumer on a mine is compressed air.

Compressed air generation is a process with various challenges that can contribute to unnecessary operational expenses. Examples of these challenges are leakages and the continuous operation of compressors when compressed air is not required. Numerous other factors also contribute to compressed air generation being an expensive as well as a wasteful process.

Simulation software has the potential to identify problem areas within a compressed air network. Limited data availability on mines, however, often restricts the capability of simulation software. Simulation accuracy depends on the amount of available data to ensure accurate comparisons between actual system events and characteristics, as well as simulated predictions.

The need arose to determine the acceptability of simulation accuracy based on the availability of data on any mine. A method was developed to test simulation accuracies based on data availability. Three simulations, namely, a detailed, standard and simplified model were devised. The simulation models were created using actual data from Mine-A, which has been equipped to record a full variety of operational data. The recorded data was used to simulate the compressed air network of Mine-A accurately.

The three simulation models were each a simplified version of the previous one. Simplification entails reducing the number of simulation components. By reducing the number of components, the time and financial impact related to creating simulations can be reduced.

The study investigated the impact that a reduction in simulation complexity has on simulation accuracy. It was discovered that a simplified compressed air simulation model is able to achieve a simulation error of only 4.87%.

Finally, from the results gathered from this study, it can be concluded that simplifying compressed air simulations has little effect on simulation accuracy. Simplified compressed air simulations are therefore recommended because of the significant decrease in development time without compromising simulation accuracy.

Keywords: Compressed air network; Simulation model; Percentage error; Accuracy; Scenarios.

ACKNOWLEDGEMENTS

I would like to express my gratitude towards the following individuals and parties who made the completion of this study possible.

- First and foremost, to my Father, Lord and Saviour. Thank You for all You have done for me. I am truly grateful for the knowledge You have blessed me with to be able to complete this study.
- To ETA Operations (Pty) Ltd, Enermanage, and sister companies. Thank you for the funding of my post-graduate studies, as well as the opportunity to simultaneously develop myself as an engineer.
- To my mentor, Dr Philip Maré. Thank you for your continuous guidance and support throughout my studies.
- To my study leader, Prof. Marius Kleingeld. Thank you for all your assistance throughout my studies.
- To my family and friends. Thank you for your love, support, and understanding during my studies.
- To my parents, Percy and Sandra Watkins. Thank you for your continuous love and support throughout my life. It has made this study, as well as all my other goals in life possible.
- To my future in-laws, Fanie and Hanneke van Zyl. Thank you for your continuous love, motivation, and support throughout my studies. I am truly blessed to have you in my life.
- Lastly, to my fiancé and love of my life, Suné van Zyl. Thank you for your continuous love, support, patience, and understanding during these past couple of years. Without you, I would not have had the strength to complete this study.

TABLE OF CONTENTS

Abstract.....	ii
Acknowledgements	iv
Table of contents	v
List of figures.....	vii
List of tables.....	x
List of equations	xii
List of abbreviations	xiii
List of terms.....	xiv
Nomenclature	xv
Chapter 1 Introduction	1
1.1 Background	2
1.2 Mine compressed air systems	3
1.3 Integrated system simulation models in industry.....	7
1.4 Problem statement and objectives of this study	10
1.5 Overview of the study	11
Chapter 2 Literature study	12
2.1 Introduction.....	13
2.2 Compressed air network characteristics and fundamentals	14
2.3 Mine compressed air simulations.....	18
2.4 Determining simulation accuracy	27
2.5 Summary	31
Chapter 3 Methodology	32
3.1 Introduction.....	33
3.2 Compressed air network analysis.....	34
3.3 Development of models	44
3.4 Validation of models.....	59
3.5 Summary	64
Chapter 4 Results	66
4.1 Introduction.....	67
4.2 Impact of the simulation complexity	68
4.3 Variation of probability parameters	73
4.4 Analyses of simulation accuracy	79
4.5 Verification of simulation accuracy	84
4.6 Summary	90
Chapter 5 Conclusion.....	91
5.1 Study limitations	92
5.2 Recommendations.....	92
5.3 Conclusion	93
Chapter 6 References	95

Appendix A.....	103
Appendix B.....	106
Appendix C.....	109
Appendix D.....	112
Appendix E.....	114
Appendix F.....	116
Appendix G.....	119
Appendix H.....	123
Appendix I.....	126
Appendix J.....	143
Appendix K.....	149

LIST OF FIGURES

Figure 1: Compressed air system layout.....	3
Figure 2: Daily average airflow and pressure profile	6
Figure 3: Detailed simulation compressor data	35
Figure 4: Simplified available compressor data.....	37
Figure 5: Simulation setup procedure summary	38
Figure 6: Data acquisition procedure	40
Figure 7: Quality compressor running statuses data	42
Figure 8: Method used to develop compressed air simulations	43
Figure 9: Compressor specification illustration	47
Figure 10: Quadratic function for compressor characteristics curve (adapted from [59]).....	47
Figure 11: Available pipe dimensions	50
Figure 12: VK32 design specification – Simulation-A.....	52
Figure 13: VK50 design specification – Simulation-A.....	53
Figure 14: 2 × VK32 design specification – Simulation-C	55
Figure 15: 3 × VK32 design specification – Simulation-C	56
Figure 16: 2 × VK50 design specification – Simulation-C	57
Figure 17: 3 × VK50 design specification – Simulation-C	57
Figure 18: Simulation-A validation – supply flow	60
Figure 19: Simulation-A validation – power usage	61
Figure 20: Simulation-A validation – supply pressure	61
Figure 21: Simulation-B accuracy comparison – supply flow.....	68
Figure 22: Simulation-B accuracy comparison – power usage	69
Figure 23: Simulation-B accuracy comparison – supply pressure.....	69
Figure 24: Simulation-C accuracy comparison – supply flow.....	70
Figure 25: Simulation-C accuracy comparison – power usage	71
Figure 26: Simulation-C accuracy comparison – supply pressure.....	71
Figure 27: Mine-B compressed air layout	85
Figure 28: Mine-B simulation identification	86
Figure 29: Mine-B simplified compressed air layout	86
Figure 30: Mine-B simulation model.....	87
Figure 31: Mine-B power usage comparison.....	88
Figure 32: Mine-B compressor flow comparison	88

Figure 33: Mine-B level pressure comparison	89
Figure 34: GUI of PTB	107
Figure 35: PTB compressor input window	108
Figure 36: Simplified mine compressed air simulation method (adapted from [55]).....	110
Figure 37: Compressed air ring simulation development (adapted from [56])	110
Figure 38: Illustration of compressor relocation simulation (adapted from [11])	111
Figure 39: Simulation boundary condition selection (adapted from [32])	111
Figure 40: Schematic layout of Mine-A's compressed air network	113
Figure 41: AFT Arrow® simulation section screenshot.....	115
Figure 42: AFT Arrow® compressor component input variables	115
Figure 43: Simulation-A model screenshot	120
Figure 44: Simulation-B model screenshot.....	121
Figure 45: Simulation-C model screenshot.....	122
Figure 46: Simulation-B validation – supply flow	124
Figure 47: Simulation-B validation – power usage	124
Figure 48: Simulation-B validation – supply pressure	124
Figure 49: Simulation-C validation – supply flow	125
Figure 50: Simulation-C validation – power usage	125
Figure 51: Simulation-C validation – supply pressure	125
Figure 52: Supply flow increase comparison – Simulation-B – flow vs. time	127
Figure 53: Supply flow increase comparison – Simulation-B – power vs. time	127
Figure 54: Supply flow increase comparison – Simulation-B – pressure vs. time	127
Figure 55: Supply flow increase comparison – Simulation-C – flow vs. time	128
Figure 56: Supply flow increase comparison – Simulation-C – power vs. time	128
Figure 57: Supply flow increase comparison – Simulation-C – pressure vs. time	128
Figure 58: Supply flow decrease comparison – Simulation-B – flow vs. time	129
Figure 59: Supply flow decrease comparison – Simulation-B – power vs. time.....	129
Figure 60: Supply flow decrease comparison – Simulation-B – pressure vs. time	129
Figure 61: Supply flow decrease comparison – Simulation-C – flow vs. time	130
Figure 62: Supply flow decrease comparison – Simulation-C – power vs. time.....	130
Figure 63: Supply flow decrease comparison – Simulation-C – pressure vs. time	130
Figure 64: Supply pressure increase comparison – Simulation-B – flow vs. time	131
Figure 65: Supply pressure increase comparison – Simulation-B – power vs. time	131
Figure 66: Supply pressure increase comparison – Simulation-B – pressure vs. time	131

Figure 67: Supply pressure increase comparison – Simulation-C – flow vs. time	132
Figure 68: Supply pressure increase comparison – Simulation-C – power vs. time	132
Figure 69: Supply pressure increase comparison – Simulation-C – pressure vs. time	132
Figure 70: Supply pressure decrease comparison – Simulation-B – flow vs. time	133
Figure 71: Supply pressure decrease comparison – Simulation-B – power vs. time.....	133
Figure 72: Supply pressure decrease comparison – Simulation-B – pressure vs. time	133
Figure 73: Supply pressure decrease comparison – Simulation-C – flow vs. time	134
Figure 74: Supply pressure decrease comparison – Simulation-C – power vs. time.....	134
Figure 75: Supply pressure decrease comparison – Simulation-C – pressure vs. time	134
Figure 76: Pipe dimension increase comparison – Simulation-B – flow vs. time.....	135
Figure 77: Pipe dimension increase comparison – Simulation-B – power vs. time	135
Figure 78: Pipe dimension increase comparison – Simulation-B – pressure vs. time.....	135
Figure 79: Pipe dimension increase comparison – Simulation-C – flow vs. time.....	136
Figure 80: Pipe dimension increase comparison – Simulation-C – power vs. time	136
Figure 81: Pipe dimension increase comparison – Simulation-C – pressure vs. time.....	136
Figure 82: Pipe dimension decrease comparison – Simulation-B – flow vs. time	137
Figure 83: Pipe dimension decrease comparison – Simulation-B – power vs. time.....	137
Figure 84: Pipe dimension decrease comparison – Simulation-B – pressure vs. time	137
Figure 85: Pipe dimension decrease comparison – Simulation-C – flow vs. time	138
Figure 86: Pipe dimension decrease comparison – Simulation-C – power vs. time.....	138
Figure 87: Pipe dimension decrease comparison – Simulation-C – pressure vs. time	138
Figure 88: Multiple parameter increase comparison – Simulation-B – flow vs. time.....	139
Figure 89: Multiple parameter increase comparison – Simulation-B – power vs. time	139
Figure 90: Multiple parameter increase comparison – Simulation-B – pressure vs. time.....	139
Figure 91: Multiple parameter increase comparison – Simulation-C – flow vs. time.....	140
Figure 92: Multiple parameter increase comparison – Simulation-C – power vs. time	140
Figure 93: Multiple parameter increase comparison – Simulation-C – pressure vs. time.....	140
Figure 94: Multiple parameter decrease comparison – Simulation-B – flow vs. time	141
Figure 95: Multiple parameter decrease comparison – Simulation-B – power vs. time.....	141
Figure 96: Multiple parameter decrease comparison – Simulation-B – pressure vs. time	141
Figure 97: Multiple parameter decrease comparison – Simulation-C – flow vs. time	142
Figure 98: Multiple parameter decrease comparison – Simulation-C – power vs. time.....	142
Figure 99: Multiple parameter decrease comparison – Simulation-C – pressure vs. time	142

LIST OF TABLES

Table 1: Compressed air operated components	4
Table 2: Air properties at 25°C and 100 kPa [39]	15
Table 3: Absolute roughness of pipe materials (adapted from [11])	17
Table 4: Simplified compressed air simulation development – summary	21
Table 5: Compressed air ring simulation development	22
Table 6: Periodic simulation process of analysis [32]	24
Table 7: Summary of previously developed methods.....	25
Table 8: Baseline simulation accuracies	33
Table 9: PTB simulation data requirements.....	41
Table 10: Simulation comparison parameters.....	44
Table 11: Mine-A compressed air network summary.....	45
Table 12: Description of required simulation data	46
Table 13: Simulation-A accuracy comparison.....	64
Table 14: Simulation-B accuracy comparison.....	64
Table 15: Simulation-C accuracy comparison.....	64
Table 16: Simulation-B accuracy analysis.....	70
Table 17: Simulation-C accuracy analysis.....	72
Table 18: Single probability parameter variations.....	73
Table 19: Flow demand variation results – Simulation-B	75
Table 20: Flow demand variation results – Simulation-C	75
Table 21: Compressor set point variation results – Simulation-B	76
Table 22: Compressor set point variation results – Simulation-C	76
Table 23: Pipe dimension variation results – Simulation-B	76
Table 24: Pipe dimension variation results – Simulation-C	77
Table 25: Multiple parameter variation results – Simulation-B	77
Table 26: Multiple parameter variation results – Simulation-C	78
Table 27: Simulation-B – Parameter variation accuracy comparison	80
Table 28: Simulation-C – Parameter variation accuracy comparison	80
Table 29: Financial impact of simulation complexity	82
Table 30: Simulation component count comparison	83
Table 31: Impact of simulation complexity on simulation speed	83
Table 32: Summary of simulation development method	84

Table 33: Mine-B validation comparison	89
Table 34: VK32 design specifications	117
Table 35: VK32 corrected flow values	117
Table 36: VK50 design specifications	117
Table 37: VK50 corrected flow values	117
Table 38: Multiple VK32 design specifications	118
Table 39: Multiple VK32 corrected flow values	118
Table 40: Multiple VK50 design specifications	118
Table 41: Multiple VK50 corrected flow values	118
Table 42: Simulation-B – flow demand variation – max percentage error.....	144
Table 43: Simulation-C – flow demand variation – max percentage error.....	144
Table 44: Simulation-B – supply pressure variation – max percentage error.....	145
Table 45: Simulation-C – supply pressure variation – max percentage error.....	146
Table 46: Simulation-B – pipe dimension variation – max percentage error	146
Table 47: Simulation-C – pipe dimension variation – max percentage error	147
Table 48: Simulation-B – multiple parameter variation – max percentage error	147
Table 49: Simulation-C – multiple parameter variation – max percentage error	148
Table 50: Mine-B 24-hour raw data.....	150
Table 51: Mine-B power usage comparison	151
Table 52: Mine-B flow comparison.....	152
Table 53: Mine-B pressure comparison.....	153

LIST OF EQUATIONS

Equation 1: Pressure drop calculation using the Darcy–Weisbach equation.....	16
Equation 2: Darcy friction factor using the Colebrook–White equation	16
Equation 3: Reynolds number calculation	17
Equation 4: Resultant error calculation (MAE)	27
Equation 5: Relative error calculation (MAE)	28
Equation 6: Resultant error calculation (MRD)	28
Equation 7: Relative error calculation (MRD)	29
Equation 8: Corrected flow calculation	48
Equation 9: Mass flow calculation.....	48
Equation 10: Temperature ratio calculation.....	48
Equation 11: Pressure ratio calculation.....	48
Equation 12: Corrected flow detailed equation	49
Equation 13: Electric motor power required by centrifugal compressors	104
Equation 14: Compressor power required to compress air	104
Equation 15: Mechanical energy required to compress air.....	104
Equation 16: Polytrophic constant calculation	105
Equation 17: Air mass flow rate calculation.....	105
Equation 18: Density of compressed air calculation.....	105

LIST OF ABBREVIATIONS

CH	Compressor House
DSM	Demand-side Management
GUI	Graphical User Interface
MAE	Mean Absolute Error
MRD	Mean Residual Difference
R	Rand (South African Currency)
PTB	Process Toolbox

LIST OF TERMS

Baseline	Baseline simulation models are reference simulation models other simulation models are compared with. Usually, a baseline simulation model is a replica of a mining system for a specific time period.
Blast shift	Period when explosives are detonated to break the rockface underground.
Bypass valve	Regulating valve that allows one to open or close compressed air flow to various locations in the compressed air network.
Compressor house	Building that contains the compressors that supply compressed air to the shaft.
Demand flow	Quantity of compressed air consumed by end users to perform various mining operations.
End user	Components/equipment that require compressed air to perform various mining operations.
Peak drilling period	Period when pneumatic rock drill activity and compressed air consumption are at their highest.
Supply flow	Quantity of compressed air supplied by the compressors to the mine compressed air network.
Supply pressure	Pressure at which compressed air is supplied to the mine compressed air network.
VK32	Small compressor used within the compressed air network of Mine-A.
VK50	Large compressor used within the compressed air network of Mine-A.

NOMENCLATURE

#	Shaft
—	Dimensionless
%	Percentage
°	Degree
Ø	Diameter
/	Division (per)
R	Universal gas constant
ρ	Density
®	Registered
C	Celsius
H	Hour
K	Kelvin
kg	Kilogram
kJ	Kilojoule
km	Kilometre
kPa	Kilopascal
kW	Kilowatt
m	Metre
mm	Millimetre
m ³	Cubic metre
MW	Megawatt
s	Seconds

Chapter 1 Introduction



1

“Science without religion is lame, religion without science is blind” – Albert Einstein

¹ Adapted from Mapio [Online]. Available: <https://mapio.net/s/45266961/> [Accessed: 04 August 2018].

1.1 Background

The industrial sector is responsible for 41.5% of global energy consumption [1]. In 2010, Eskom, which supplies 95% of South Africa's electricity, stipulated that the mining sector was responsible for 15% of the utility's annual output [1], [2], [3].

Compressed air energy is regarded as one of the essential industrial utilities because it is irreplaceable for a number of production practices. However, compressed air generation is also regarded as one of the most expensive processes [4]. Compressed air generation consumes approximately 17% of the total energy used in the mining sector [5]. A different study indicates that compressed air generation contributes 10% to global industrial sector energy consumption [6].

Due to the high electricity consumption, energy cost savings on compressed air systems are important. Strategies need to be investigated and implemented to mitigate the high energy consumption of these systems. Examples of such initiatives are supply-/demand-side management, as well as pipe replacement or leak-fixing [7], [8], [9].

Simulation models are typically used to evaluate the feasibility and indicate the expected impact of these initiatives. Simulation models are actual systems represented digitally [10]. It is therefore vital to ensure that the correct simulation models are developed with acceptable accuracies.

1.2 Mine compressed air systems

The bulk of the mining industry uses compressed air in mining operations. Compressed air is typically supplied by one or more compressors and sent underground via an air reticulation network. The air reticulation network interconnects the processing plant and shaft in what is called the compressed air network [11].

Multiple compressors operating together to supply compressed air from the same location is referred to as a compressor house [12]. The compressor house supplies compressed air to underground areas via pipes with diameters of up to 700 mm [11]. Depending on the size of the mine, these pipe networks can be as much as forty kilometres long [1]. Typically, mines have more compressors available than required to supply enough air to underground levels. These compressors serve as backup should a compressor break or undergo routine maintenance.

Figure 1 illustrates a basic layout of an integrated mine compressed air network. As seen in Figure 1, compressed air can be supplied from multiple compressors in multiple compressor houses. This is made possible by the pipe network interconnecting the different shafts. Compressed air is sent underground to the different levels for mining activities to take place.

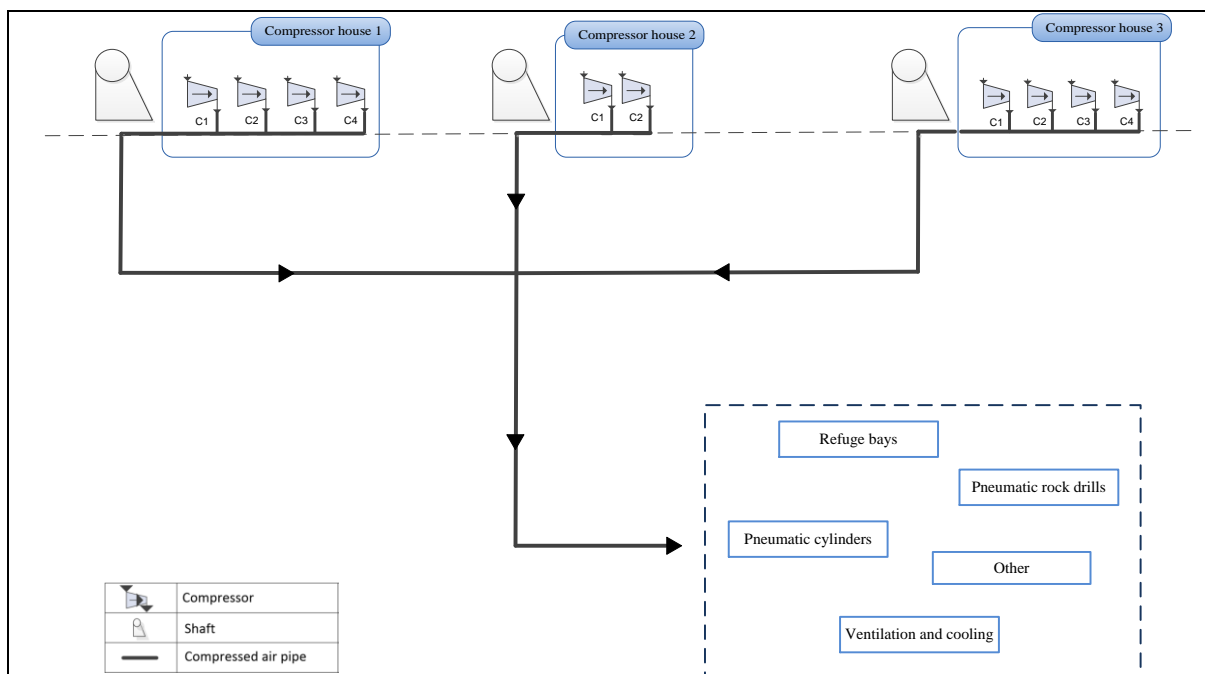







Figure 1: Compressed air system layout

There are multiple mining activities that depend on compressed air to be able to function. Table 1 summarises some of the flow and pressure requirements of the leading components underground that rely on compressed air for everyday functions [1], [11], [13], [14], [15], [16].

Table 1: Compressed air operated components

Description	Image	Flow requirements [kg/s]	Pressure requirement [kPa]
Refuge chambers ²		0.0014 per person	200–300
Pneumatic rock drills ³		Up to 0.42	400–600
Pneumatic cylinders ⁴		Up to 0.14	350–600
Mechanical loaders ⁵		0.12–0.30	400–500
Ventilation and cooling ⁶		1.6	100–650 (50 mm pipe)

² Refuge chambers: Johannesburg, South Africa. [Online]. Available: http://bbp-mp.co.za/?page_id=200 [Accessed: 24 June 2018].

³ Pneumatic rock drills: Johannesburg, South Africa. [Online]. Available: <https://mg.co.za/article/2016-03-15-mining-companies-black-shareholder-case-in-court> [Accessed: 24 June 2018].

⁴ Pneumatic cylinders: Johannesburg, South Africa. [Online]. Available: <http://www.bostongear.com/products/couplings-shaft-accessories-and-pt-products/fluid-power-products/pneumatic-cylinders> [Accessed: 24 June 2018].

⁵ Mechanical loaders: Johannesburg, South Africa. [Online]. Available: <https://www.asme.org/about-asme/who-we-are/engineering-history/landmarks/212-cimco-rocker-shovel-loader-model-12b> [Accessed: 24 June 2018].

⁶ Ventilation and cooling: Johannesburg, South Africa. [Online]. Available: <https://www.cutandcouple.com/products/industrial-hose-fittings/compressed-air-industrial-rubber-hose/> [Accessed: 24 June 2018].

Refuge chamber:

In underground mining, refuge chambers are a requirement to guarantee the safety of miners when accidents occur [17], [18], [19]. Refuge chambers serve as sanctuary for mineworkers in the event of an emergency. Compressed air is used in refuge chambers to supply the chamber with a constant flow of fresh air and maintain a positive pressure within the chamber. This prevents harmful gases such as smoke from a fire to enter the chamber.

The ideal pressure to prevent harmful gases is between 100 kPa and 500 kPa [20]. The chamber requires an opening for air to exit the chamber. If not, the result will be a continuous pressure increase within the chamber [21]. However, the larger the opening is, the more air escapes the refuge chamber. It is, therefore, essential to allow just enough air out of the chamber to supply continuous fresh air to the occupants.

Pneumatic rock drills:

Pneumatic rock drills are one of the essential components that require compressed air. Drills use compressed air to advance the rockface in the haulages and working areas. This is done by drilling many holes where explosives are placed [22]. The explosives are detonated whereby rock is broken and removed from underground. Rock drills are also used to drill the holes required for roof structure support.

Pneumatic cylinders:

After the material is blasted with explosives in the working areas, it is sent to a loading box. Pneumatic cylinders are mainly used in the working areas to dump the material from the loading boxes into carriages [1]. By using compressed air, the pneumatic cylinder pushes the loading box open, allowing the material to fall into the carriage. After the carriage is full, the cylinder retracts until a new empty carriage is available.

Mechanical loaders:

Mechanical loaders are used to remove material from work areas. The loaders use compressed air to operate pneumatic cylinders. The cylinders expand and contract to create a lifting action. The loaders then travel with the material to a specific location to dump it until the areas are cleared.

Ventilation and cooling:

As a mine's depth increases and it becomes warmer, it becomes difficult to supply sufficient quantities of fresh air to working areas [23]. Low airflow quantities cause the areas to heat up. According to the Mine Health and Safety Inspectorate, a hot environment is classified as one with temperatures ranging from 27.5–32.5°C wet bulb [24]. Mineworkers use compressed air pipes to supply fresh ventilation air to the area [13], [25]. When the compressed air leaves the pipes, expansion takes place, creating a cooling effect.

Summary:

It is evident that many components depend daily on compressed air. These components can consume air at a combined rate of up to 50 kg/s during peak drilling periods [12]. Figure 2 illustrates the daily average flow and corresponding daily average pressure profile of a deep-level gold mine.

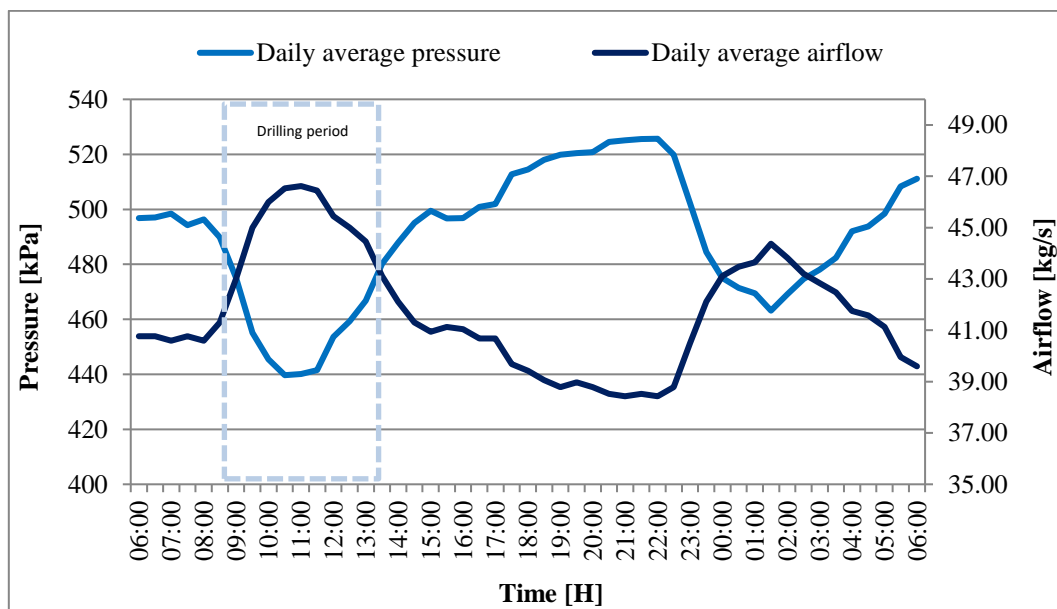


Figure 2: Daily average airflow and pressure profile

As seen in Figure 2, the compressed air usage is significant. The high air usage results in lower compressed air pressures.

With compressed air being one of the most expensive utilities, it is essential for mines to minimise wastage. However, compressed air wastage such as leaks rarely receives attention. Leaks are only addressed if the air shortage and pressure losses interfere with mining operations [6].

1.3 Integrated system simulation models in industry

1.3.1 Preamble

Simulation models have played an essential role in the evolution of power systems into the complex networks we have today. Transient network analysers was amongst the first simulators used to study electric power systems. These analysers were once considered outstanding but did have several disadvantages. One particular disadvantage was that the analysers had limited capability to simulate complex networks.[26].

The more complex a simulation is, the more difficult it is to create. However, if successful, the compound simulation will yield highly accurate results. The problem is that creating a sophisticated and accurate system simulation is a time-consuming process. Simulation engineers, therefore, tend to create simplified simulation models that have a suitable accuracy percentage [27]. This means that the simulation model has a percentage error small enough to neglect. However, the smaller the model size, the higher the percentage error [28]. Thus, it is important to determine whether the errors are small enough to deem simplified simulations as accurate.

1.3.2 Simulations used in the industry

The mining sector uses old technology as well as equipment that is no longer efficient [29]. Improvement strategies for the equipment and systems can be identified by creating simulation models of the entire mine compressed air system. With the available technology, simulation models are able to predict the performance of mining systems accurately.

Van Rensburg et al. stated in 2007 that simulations are the most effective way of predicting the impact that system changes have on energy efficiency calculations [30]. However, optimisation using simulations is a new approach in the mining sector [31]. This results in many potential problems faced with simulation models.

In 2017, Friedenstien [32] explained how estimations were used to determine the feasibility of energy interventions before the necessary tools existed. The problem was that estimations were calculated using simplified models. Simplification leads to increased errors. Estimations, therefore, only increase expected errors further.

In a compressed air simulation study done by Bredenkamp, Van der Zee and Van Rensburg in 2014 [33], it was found that software packages, such as KYPipe, are able to predict compressor power usage to within a 12% simulation error. It was, however, discovered that the simulated models did not account for factors such as compressed air leaks. After the leaks were repaired and the simulation repeated, the average simulation error reduced to only 9%.

In 2014, Holman, Heyns and Pelzer created a simulation model of a mine's cooling system [34]. A total simulation model error of 2.5% was obtained. The simulation model was validated by comparing actual parameters with simulated parameters. It was, however, found that their individual component percentage error comparisons ranged between 0.1% and 32.1%. According to Holman et al. [34], the model was deemed accurate "based on discussions with experienced personnel". Their validation did not consider the total error but rather the average error.

In 2017, Gölbaşı and Demirel [35] developed a simulation algorithm to determine optimal time intervals between component inspections to ensure that no unnecessary maintenance problems are encountered. Gölbaşı and Demirel determined that cost savings of up to 6.2% can be realised using the simulation model. Definitive values could, however, not be given because of simulation percentage errors.

In 2007, Van Rensburg et al. developed a procedure for skilled technicians to use for simulation modelling [30]. They stated that a user must create a simple simulation as this would reduce project cost due to fewer personnel requirements. In the same study, Van Rensburg et al. mentioned that the total savings achieved were also simulated and included in the financial analysis. The focus was placed on the value the simulation model possesses in terms of financial impact. Validation of the model, however, lacked sufficient confirmation.

Upadhyay and Askari-Nasab mentioned in 2017 that simulation models are designed and created to address specific problems [31]. Industrial simulations, therefore, do not focus on developing methods to address similar problems in the future. The focus is placed on current issues and, once resolved, the simulation model is discarded.

In the above-mentioned studies, simulations form an essential part of the industrial sector. As previously discussed, simulation models can be used for a wide variety of purposes. The simulation models created for industrial uses, unfortunately, do not account for different factors such as compressed air leaks. It is also clear that percentage errors between actual and

simulated values are miscalculated. The average total outputs are compared instead of comparing each component individually. Because of the percentage error uncertainty, absolute values cannot be given when determining factors such as power usage or financial savings.

Few methods are being developed to address similar problems in the future. Simulations are merely created to address current problems until they are resolved. In addition to this, simplified simulation models are being created to save time. This is being done without knowing the impact of simplifying a simulation model on the simulation accuracy.

1.3.3 Simulation requirements

It is essential that simulation models are calibrated correctly to ensure the most accurate results. This is done by calibrating the simulation model according to component design specifications. Any simulation performance achieved below requirement is an indication of inefficient equipment. Relevant and accurate simulation data is, therefore, critical when calibrating a simulation model [36].

Calibration accuracy depends on the amount of available data. The more data is available, the higher the simulation accuracy will be. The problem, however, is that it is difficult to predict how accurate a simulation model will be when limited data is available. This creates a need to identify simulation accuracies based on various degrees of data availability. In doing so, one can simultaneously identify the accuracy of complex simulations when compared with less complex ones.

Thus, a method is required that determines the effect that various degrees of data availability (or simulation complexity) have on simulation accuracy. Three simulation models, each with varying amounts of data inputs, need to be compared with one another. This will identify the accuracy of the less complicated models with little available data when being compared with the more complex model.

The effect of various changes to each network also needs to be simulated. This is to ensure that the simulation accuracy of the three different models do not deteriorate as various changes are implemented.

1.4 Problem statement and objectives of this study

1.4.1 Objective of this study

The objective of this study is to evaluate the impact of complexity on simulation accuracy. The objective is therefore to determine if a simplified simulation model is viable to use in an industry where data availability is limited.

1.4.2 Scope of the work

The problem statement is that the impact simulation complexity has on simulation accuracy must be analysed. A process to create compressed air simulation models is, therefore, required. Three compressed air simulations with varying complexity must be created to gradually illustrate the effect of simplification on simulation accuracy. A method must be developed to identify three simulation types based on the simulation complexity or data availability. The method must also identify the expected accuracy of the three simulation types. Various scenarios must be implemented on the three simulation types to ensure the accuracies of the models remain viable. Finally, the model developed to determine the accuracy of the three simulation types must be verified to ensure its validity.

1.4.3 Summary

This dissertation focuses on the variation of simulation complexity to evaluate the simulation accuracy. This will serve as an indication as to the level of detail required to ensure accurate results while minimising resource expenditure. Additionally, it serves as an indication of what level of simulation accuracy can be expected when limited mine data is available.

1.5 Overview of the study

Chapter 1: Introduction – This chapter provides an overview towards the need for the study. Emphasis is placed on the energy consumption of compressed air generation in the industrial sector. The need to accurately simulate compressed air networks to quantify savings opportunities is therefore identified. An intricate surface compressed air networks system is replicated and simplified within this study to determine the degree of simplification required for accurate results.

Chapter 2: Literature study – This chapter is used to provide knowledge on compressors and compressed air networks. Various simulation software packages are shown, and one capable of simulating compressed air networks is selected. Previous simulation studies are investigated to identify shortcomings. Lastly, an investigation is done to determine the accuracy of simulation models when being compared with actual data.

Chapter 3: Methodology – This chapter provides an in-depth analysis towards the development of three simulation models. A method is developed that allows one to identify the level of simulation complexity. An expected error can then be predetermined based on the simulation complexity.

Chapter 4: Results – The three simulation models developed in Chapter 3 are compared with one another within this chapter. Various changes to the compressed air network are simulated in all three models. The percentage deviation of necessary measurements is investigated and compared with the baseline simulation model. This determines the impact simulation simplification has on the accuracy.

Chapter 5: Conclusion and recommendation – The simulation accuracies and findings are summarised in this chapter. The limits of the study are identified and discussed along with recommendations for further studies.

Chapter 2 Literature study



7

“A man who dares to waste one hour of time has not discovered the value of life” – Charles Darwin

⁷ Adapted from Brand South Africa [Online]. Available: <https://www.brandsouthafrica.com/resources-downloads/media-library/images/rml-content/business-industry> [Accessed: 04 August 2018].

2.1 Introduction

This chapter consists of comprehensive analyses into the operation of the compressed air network components. The fundamental characteristics of compressors are illustrated with mathematical calculations. The total requirements are calculated to ensure that the previously mentioned requirements are met.

The influence that the compressed air pipe network has on pressure losses is analysed in detail. Mathematical calculations illustrate the effect various pipe materials and lengths have on compressed air pressure. These losses are incorporated into the simulations used in this study.

Various simulation software packages used in previous studies with the capability of simulating compressed air networks are briefly discussed. One of these simulation packages, namely, Process Toolbox® (PTB), is selected and discussed further as it is used for all simulation purposes within this study.

Previous methods developed to simulate compressed air systems are thoroughly investigated as part of the comprehensive literature review. These methods are analysed and shortcomings identified. From the shortcomings, a need is identified to create a new method that allows the user to create compressed air simulations.

Lastly, an investigation is done to accurately determine the required percentage difference of simulation models when compared with actual data.

2.2 Compressed air network characteristics and fundamentals

2.2.1 Preamble

This section consists of an in-depth analysis of the operational requirements as well as outputs of compressors. The requirements of the compressed air users are investigated and discussed. The theoretical calculations illustrated in this section are used by the simulation software to determine various outputs.

The compressed air network is discussed along with various materials and pipe lengths found in a compressed air network today. Pressure losses are calculated to determine the direct impact that pipe material and pipe length have on the compressed air delivery side.

2.2.2 Compressed air demand and minimum requirements

Compressed air is consumed by a large number of end users on deep-level mines. In 2012, Marias identified these various end users [1]. The end users can range from surface to underground operations, requiring a combination of high-pressure and flow outputs [14]. Various research is done regarding the required compressed air pressure and compressed air flow, as illustrated in Table 1.

The compressors are typically located on the surface of an underground gold mine. It is, therefore, essential that the compressor and pipe configurations are correct. This is to ensure there is an adequate air supply to underground with the least amount of losses.

2.2.3 Compressed air fundamental calculations

The process of producing compressed air is considered polytropic, which describes any reversible process that involves both heat and work transfer, where certain properties are kept constant throughout the process. [37]. Various calculations are performed to determine fundamental compressor requirement and outputs. The theoretical calculations are illustrated in Appendix A.

Equation 13 to Equation 18 in Appendix A are used to determine all the necessary compressor requirements to compress air. This is an important part of simulation. It illustrates how the simulation software is able to accurately simulate compressors.

Various parameters such as airflow rates and compressor efficiencies however are not calculated. This is because airflow rates are normally measured at the compressor discharge [11]. Efficiencies also vary from one compressor to the other. A compressor and motor efficiency of between 0.7 and 0.9 are, however, acceptable assumptions if specifications are not available [11], [38].

Table 2 illustrates the various air properties used throughout Equation 13 to Equation 18. These properties can vary depending on atmospheric conditions. For illustration purposes, air temperature and pressures of 25°C and 100 kPa respectively are used.

Table 2: Air properties at 25°C and 100 kPa [39]

Property	Value
R [kJ/kg·K]	0.287
ρ [kg/m ³]	1.169
C_p [kJ/kg·K]	1.004
C_v [kJ/kg·K]	0.171
n [–]	1.400

Air properties vary depending on air temperature and pressure [39]. Therefore, a constant value cannot be used throughout the calculations. The values indicated by Table 2, however, can serve as estimate values should air conditions be unavailable. With the information discussed in this section, the power required by a compressor to compress air can be determined.

2.2.4 Compressed air reticulation network

A compressed air reticulation network consists of many interconnecting pipelines. As discussed in Chapter 1, these pipelines can have lengths of up to forty kilometres. The impact of friction over such a distance becomes significant. Friction over longer pipe sections with smaller diameters results in higher pressure losses [40], [41]. The compressors need to overcome the friction to supply adequate amounts of compressed air to the end users. The Darcy–Weisbach equation, displayed in Equation 1, determines the pressure drop in sizeable compressed air networks [11].

Equation 1: Pressure drop calculation using the Darcy–Weisbach equation

$$\Delta P = \frac{f_D \rho_{air} L Q_{air}^2}{82.76 D_{inner}^5}$$

Where:

- ΔP = Pressure drop [kPa]
 f_D = Darcy friction factor [–]
 ρ_{air} = Density of air [kg/m³]
 L = Pipe length [m]
 Q_{air} = Air volume flow rate [m³/s]
 D_{inner} = Pipe inside diameter [m]

Equation 2 calculates the Darcy friction factor with a dimensionless parameter known as the Reynolds number. Equation 2 is referred to as the Colebrook–White equation [11], [42].

Equation 2: Darcy friction factor using the Colebrook–White equation

$$\frac{1}{\sqrt{f_D}} = -2 \log_{10} \left(\frac{e}{3.7 D_{inner}} + \frac{2.51}{Re \sqrt{f_D}} \right) \text{ for } Re > 4000$$

Where:

- f_D = Darcy friction factor [–]
 e = Absolute pipe roughness [m]
 D_{inner} = Pipe inside diameter [m]
 Re = Reynolds number [–]

Higher pipe surface roughness causes pipe friction to increase [43]. Absolute roughness is dependent on the type of material used, as well as the condition of the material in the compressed air pipe network.

Factors like rust and oxidation due to moisture and temperature can alter the properties of the material, but will be neglected for the purpose of this study. Table 3 summarises various material roughness values of pipes used in the mining industry [11].

Table 3: Absolute roughness of pipe materials (adapted from [11])

Material	Roughness [mm]
Wrought iron	0.045
Commercial steel	0.045
Galvanised iron	0.15
Cast iron	0.26
Riveted steel	0.9–9.0

The Reynolds number is calculated using Equation 3 [11], [14], [44].

Equation 3: Reynolds number calculation

$$Re = \frac{u_{air} D_{inner} \rho_{air}}{\mu_{air}}$$

Where:

Re = Reynolds number [–]

D_{inner} = Pipe inside diameter [m]

ρ_{air} = Density of air [kg/m^3]

u_{air} = Average air velocity [m/s]

μ_{air} = Viscosity of air [$kg/m \cdot s$]

Using the equations discussed in this section, the pressure loss over a large compressed air network can be determined. This becomes particularly useful in the event of large surface compressed air pipe networks. It allows one to determine optimal compressor placement throughout the network to supply adequate air to all shafts.

2.3 Mine compressed air simulations

2.3.1 Preamble

Simulation models are used to investigate potential optimisation strategies or energy cost-saving initiatives. It is, therefore, possible to accurately simulate compressed air networks [45]. A baseline simulation model is required of the system to be investigated.

Mining system simulation models can be a series of integrated components. These components are dependent on one other as the outlet conditions of one component become the inlet conditions of the next [46]. It is essential that each individual component is calibrated accurately for the baseline simulation model.

2.3.2 Simulation software

Simulation speed and accuracy are highly dependent on parameter settings; this applies especially to complex simulation systems [47]. There are various simulation software packages commercially available to simulate mining systems. However, it is becoming increasingly difficult to select a simulation package due to the large number of available packages [48]. Few simulation software packages, however, allow access to real-time system data, or simulate integrated systems [27], [49]. Therefore, processed data must be entered manually into the simulation package. This is a time-consuming process and creates limitations for simulating mining systems.

The simulation package must be a transient simulation tool capable of calculating the simulation's response to system changes. The package must deliver various simulation outputs at certain time steps to compare with actual data. Finally, the package must be easy to use. This will ensure that no unnecessary time is wasted while creating the simulation model.

The following simulation packages can be used to simulate mining operations [32]:

- PTB®
- AFT Arrow®
- KYPipe GAS®
- Flownex®

KYPipe and Flownex are examples of simulation software that do not have an interface for viewing real-time system data [49]. Flownex is able to process batch data which will work, but will take a long time. PTB, described in Appendix B, is a simulation package that meets all the requirements for compressed air simulation. Thus, it is used for all simulation purposes within this study.

2.3.3 Compressed air simulation studies

2.3.3.1 Overview

In 2007, Marais, Mathews and Pelser [50] determined that the effect of implementing demand-side management (DSM) can be evaluated using simulations entirely; therefore, real-time tests are no longer required. However, without real-time tests, the error margins of simulations cannot be determined.

Studies done by Van Niekerk [51], and Kleingeld and Van Niekerk [52] in 2013 indicated how simplified compressed air simulation models are able to determine cost-saving benefits in a short amount of time. The problem, however, is that the simulation models were not verified by a more detailed simulation model.

The relationship between parameters in compressed air systems can be quantified through simulation techniques [1], [53]. Compressor models can be developed to simulate the performance of individual components [54]. However, the shortage of instrumentation and information makes this problematic. Mine compressed air networks are highly complex systems, making it a time-consuming process to gather the necessary information to simulate the system [1].

Marais stated that in order to enable fast estimated energy savings on compressed air networks, a simplified calculation method is required [1]. Complex simulation models are more difficult and time-consuming to construct than simplified simulations. The problem with simplified simulations, as stated earlier, is their accuracy.

A method is required to identify the expected accuracy of compressed air simulations based on the level of simulation complexity. The complexity of the simulation model must be based on the available information on a mine and must not be determined by the user.

2.3.3.2 Method to design a simplified compressed air simulation

In 2017, Maré, Bredenkamp and Marais [55] developed a method for creating a simplified compressed air simulation model. The model simulated various scenarios of a mine compressed air network. The scenarios identified possible improvements to underground compressed air pressures supplied to different mining levels. In addition to the improved pressures, the model identified possible reductions in annual electricity cost.

Maré et al. used all the compressors operating on the mining complex. Each compressor in the model was calibrated accurately to represent actual conditions on the compressed air network. The method Maré et al. used identifies critical elements that need to be considered for compressed air systems. These elements include the following (adapted from [55]):

- Dynamic operation of mining complex;
- Compressed air system configuration;
- Condition and constraints;
- Data availability and accuracy;
- Compressor specification;
- Operation boundary conditions;
- Simulated period.

The method developed to create simplified compressed air simulation models consists of a step-by-step process. According to Maré et al., these steps are to be repeated until the simulation baseline is within 5% of actual system operations [55].

Table 4 summarises the method developed by Maré et al. A detailed description can be seen in Figure 36 of Appendix C.

Table 4: Simplified compressed air simulation development – summary

Step	Description
1	Select level of detail required in the simulation
2	Acquire necessary information
3	Select simulation application
4	Select project properties
5	Construct systems in simulation
6	Calibrate the simulation model
7	Run simulation
8	Evaluate results

The simulation developed from the method designed by Maré et al. had the ability to increase the compressed air pressure underground by 51 kPa. In addition to the pressure increase, the simulation realised an annual electricity saving of up to R1.5 million.

In the above-mentioned method to develop simplified compressed air simulations, the user determined the level of detail required in the simulation model. The accuracy of the simulation model, therefore, depends on the user and not the availability of mine information.

2.3.3.3 Compressed air ring simulation model development

In 2016, Pascoe, Groenewald and Marais [56] used compressed air simulations to determine the effect of DSM initiatives on the annual electricity cost of a mine. In their model, a control philosophy was implemented on bypass valves to limit compressed air supply. The philosophy was implemented during periods when compressed air was not required.

Pascoe et al. used a less detailed simulation setup procedure that allows a compressed air simulation to be calibrated. They developed a series of steps in their study that should be followed iteratively until the desired output for each step is achieved.

A description of the development method of Pascoe et al. is summarised in Table 5 and displayed in Figure 37 of Appendix C.

Table 5: Compressed air ring simulation development

Step	Description
1	Build initial simulation
2	Build additional simulation
3	Calibrate flow
4	Calibrate power
5	Calibrate pressure
6	Iterate steps
7	Determine accuracy

The simulation model developed by Pascoe et al. could realise annual electricity savings of up to 31 MW. This led to an annual electricity cost saving of R1.9 million. Additionally, Pascoe et al. simulated the effect of replacing a large compressor with two smaller compressors. Their investigation showed that an annual electricity cost saving of up to R20 million could be realised.

However, the simulation developed by Pascoe et al. verifies its accuracy according to the residual difference method described in Section 2.4. Improvements to this method can assist with simulation accuracy.

2.3.3.4 Optimising energy consumption of mine compressed air systems

In 2012, Marais [1] described simulating large and complex networks as a “nearly impossible” task. This is because it is challenging to gather all the necessary information to create the simulation model. Marais focused on developing an approach to simplify compressed air systems, which would enable users to analyse complex systems easily. This results in the fast identification of cost-saving opportunities.

In his initial method, Marais calculated the compressed air mass flows by taking various factors such as heat ratios, line pressures and line temperature increase into account. In his simplified approach, however, Marais used the initial approach he developed and assumed constant values for most of the simulation inputs. The assumptions allowed him to only look at critical factors influencing the power usage of the compressors.

The simplified method implied that a 10% reduction in absolute pressure should theoretically result in an electrical saving of up to 18%. This, however, only applied to pressures ranging from 300 kPa to 700 kPa. This method is described by Marais as a general “rule of thumb” as the results are not definitive.

Marais developed a simplified simulation model based on assumptions made in the theoretical mathematical calculations. Verification with more detailed simulation models was not done as Marais was trying to avoid detailed simulations throughout his study. The accuracy of Marais’ “rule of thumb” is something that requires more thorough investigations.

2.3.3.5 Relocation of mine compressors through simulation

In 2014, Bredenkamp [11] developed theoretical simulations to determine what a network’s response would be to reconfiguration. Bredenkamp used the simulation package KYPipe to determine ideal compressor locations. His research indicated that a simulation model was created. The study, however, does not give a detailed description of the method he used to develop his models.

During his simulation development, Bredenkamp included specifications such as compressor location and design. He also included pipe dimensions and materials used but neglected to include pipe bends and elbows. The developed simulation model, illustrated in Figure 38 in Appendix C, could identify R170 million in electrical energy savings.

The simulation results were verified by using calibrated measuring equipment to measure actual parameters on a mine. Bredenkamp verified his simulations with the residual difference method described in Section 2.4. As previously indicated, this method is not the most reliable way of verifying simulation accuracy.

2.3.3.6 Simulating compressed air for operational improvements

Friedenstein [32] developed a simulation methodology that allowed him to perform various investigations on mine compressed air systems. Two separate investigations identified improvements to the different compressed air networks.

In his first investigation, Friedenstein was able to identify R900 000 in energy cost savings. This was after network intervention investigations were performed on the compressed air network. His second investigation identified energy cost savings of R5.2 million by merely reducing the air usage in refuge bays.

The method developed by Friedenstein indicates how simulation boundaries should be selected based on data availability. Like Maré et al., Friedenstein also explains that the boundary conditions largely depend on the level of desired simulation accuracy. The boundary conditions used by Friedenstein are illustrated in Figure 39 in Appendix C.

The method describes a process similar to the process mentioned earlier by Pascoe et al. Friedenstein discusses the selection and calibration of individual components. Unlike Maré, Friedenstein lacks a clear method to achieve his simulation model (as seen in Table 6).

Table 6: Periodic simulation process of analysis [32]

Step	Description
1	Locate data source
2	Update simulation inputs and simulate
4	Export data after simulating
5	Analyse
6	Repeat

His verification method was done using the mean absolute error described in Section 2.4, resulting in more accurate comparisons. His simulations, similar to that of the above-mentioned studies, were deemed accurate if they had a percentage difference of less than 5%.

2.3.3.7 Summary of previously developed methods

Table 7 summarises the previous methods developed by other authors for creating compressed air simulations. Table 7 furthermore indicates the process and shortcomings of each.

Table 7: Summary of previously developed methods

Author	Method	Shortcoming
Maré et al. [55]	Method to design a simplified compressed air simulation	The user determines simulation accuracy and not the available data
Pascoe et al. [56]	Compressed air ring simulation method development	Inaccurate verification method is used resulting in inaccurate comparisons
Marais [1]	Optimising energy consumption of mine compressed air systems	Assumptions are made to simplify simulations, potentially compromising on accuracy
Bredenkamp [11]	Relocation of mine compressors through simulations	Inaccurate verification method is again used resulting in inaccurate comparisons
Friedenstein [32]	Simulating compressed air for operational improvements	An unclear method is described to simulate various scenarios

As seen in Table 7, previous studies tend to focus on calibrating simplified simulations until an acceptable percentage error is obtained. Previous studies do not focus on the accuracy of complex simulation models. Therefore, a new method is required to evaluate the impact of data availability on simulation accuracy.

2.3.4 Summary

As discussed in this section, various simulation packages exist that can simulate mine compressed air systems. The simulation package, PTB, was selected for this study based on its ability to simulate complex mine compressed air systems accurately.

Previous studies described the development of mine simulation models as a way of improving systems in a short amount of time. System simulations allow one to quantify and compare various parameters. Simulation models are also used to investigate the performance of individual components.

A problem with most simulation developments is the shortage of information available on a mine. Complex simulations are not created due to the lack of information as well as the time it takes to create them. Simplified simulation models are made due to insufficient information and to reduce the amount of time spent on model development.

In previous methods to develop simplified simulation models, the user determined the level of desired complexity. Previous studies did not determine the impact of a lack of information on the accuracy of a simulation model.

Therefore, a new method needs to be developed that allows the user to predetermine the expected error based on the available information. This will assist in preventing unnecessary time spent calibrating a simulation model more accurately than theoretically possible.

2.4 Determining simulation accuracy

2.4.1 Preamble

This section discusses how percentage error is calculated between simulated data and measured data. Incorrect percentage difference calculations are explained as well as the impact they have on the reliability of the results. Determining the maximum acceptable percentage difference is also briefly discussed.

2.4.2 Simulation accuracy

Many statistical indices exist that are used by engineers to determine the difference between two data sets [57]. This study uses two methods to determine the accuracy of the simulation models. These methods include the mean absolute error (MAE) method and the mean residual difference (MRD) method [32].

a) MAE method

The MAE method (or median regression), is widely used to accurately determine percentage errors during forecasting [58]. One example is the quality measurement during forecasting of electricity consumption, similar to that of this study. The MAE method determines the average percentage error of all individual data points in a series. The resultant error is then calculated by determining the average of all individual data point errors as indicated by Equation 4 [32].

Equation 4: Resultant error calculation (MAE)

$$MAE = \frac{1}{K} \sum_{k=1}^K |A_k - S_k|$$

Where:

MAE	$=$ Mean absolute error [–]
K	$=$ Total number of data points [–]
k	$=$ Specific data point [–]
A_k	$=$ Actual data point [–]
S_k	$=$ Simulated data point [–]

By dividing each error of that time step with the actual value of the same time step, the relative error percentage can be calculated as illustrated by Equation 5 [32].

Equation 5: Relative error calculation (MAE)

$$Error_{\%} = \frac{1}{K} \sum_{k=1}^K \left| \frac{A_k - S_k}{A_k} \right| (100\%)$$

Where:

$Error_{\%}$	= Percentage error [%]
K	= Total number of data points [–]
k	= Specific data point [–]
A_k	= Actual data point [–]
S_k	= Simulated data point [–]

The MAE method is regarded as the more accurate percentage error calculation method as it uses all the available data points in a series to determine the average error. The MRD method is not as accurate as the MAE method when calculating percentage errors. This is discussed in the next section.

b) MRD method

The MRD method calculates an error using average values from the actual and simulated data series as indicated by Equation 6 [32].

Equation 6: Resultant error calculation (MRD)

$$MRD = \left| \frac{1}{K} \sum_{k=1}^K (A_k - S_k) \right|$$

Where:

MRD	= Mean residual difference [–]
K	= Total number of data points [–]
k	= Specific data point [–]
A_k	= Actual data point [–]
S_k	= Simulated data point [–]

The percentage error of the system is then calculated by dividing the percentage error of the series by the actual data as illustrated by Equation 7 [32].

Equation 7: Relative error calculation (MRD)

$$Error_{\%} = \left| \frac{1}{K} \sum_{k=1}^K \left(\frac{A_k - S_k}{A_k} \right) \right| (100\%)$$

Where:

$Error_{\%}$	= Percentage error [%]
K	= Total number of data points [–]
k	= Specific data point [–]
A_k	= Actual data point [–]
S_k	= Simulated data point [–]

The MRD method does have a disadvantage for transient simulations [32]. The percentage error is calculated using the total average values of a series. It is, therefore, possible that positive and negative values in a transient simulation can cancel one another out. This will result in higher accuracy comparisons than there actually are. This can be misleading as one may think that the simulation model is accurately calibrated when it is in fact not.

2.4.3 Impact of complexity on simulations

Determining the percentage error of a simulation depends on the size of a model. The larger the simulation model, the larger the impact inaccuracies will have on the simulated results. Based on previous studies, creating complex mining simulations is not a feasible process [32].

Complex simulations require detailed information that is often not available on a mine [1]. The process of gathering detailed information is also a time-consuming process. In the event that a complex simulation investigation is unfeasible, valuable time would have been wasted to create the complex model.

2.4.4 Acceptable percentage error

In 2017, Friedenstien investigated 15 different simulation case studies. The average accepted percentage error between the 15 case studies was calculated to be roughly 9% [32]. However, the percentage error depends on the type of simulation outputs being simulated. One would

generally want accurate results when comparing annual electricity consumption as opposed to the average amount of water in a dam. Thus, acceptable percentage error mostly depends on the individual using the results.

2.5 Summary

As seen in this chapter, the amount of power required by a compressor to create compressed air can be determined accurately using calculations. The calculations allow one to determine the total power required to deliver adequate amounts of air to the various consumers.

Sizeable compressed air networks are susceptible to pressure losses. Within this chapter, calculations are made to accurately determine the impact more extended pipe networks have on the compressed air pressure.

Pressure losses also occur due to friction caused by the roughness of the pipes being used. The roughness of a pipe depends on the material. The higher the roughness of a pipe is, the more significant the pressure loss will be.

Previous compressed air simulation studies have developed methods to design simplified simulation models. The studies show that the percentage difference between simulated and actual values is usually below 9%. These methods, however, do not determine the level of expected simulation accuracy as the user identifies the amount of detail and, in doing so, determines the accuracy.

Finally, the MAE proves to be the best suitable way to determine simulation percentage errors. The percentage error calculations in this study will, therefore, be done using the MAE method.

Chapter 3 Methodology



8

“Nothing in life is to be feared, it is only to be understood. Now is the time to understand more, so that we may fear less.” – Marie Curie

⁸ Adapted from Brand South Africa [Online]. Available: <https://www.brandsouthafrica.com/resources-downloads/media-library/images/rml-content/business-industry> [Accessed: 04 August 2018].

3.1 Introduction

Numerous methods have been developed to create compressed air simulations. The purpose of the simulations is to identify areas where energy usage can be reduced. This is, however, only feasible if production remains unaffected by the system changes. The problem with simulation models is that there is no method for identifying the expected accuracy of the simulation by investigating the available data. There is often limited mine instrumentation available to provide data for doing compressed air simulations. Insufficient data can lead to inaccurate simulation models.

This chapter develops a method to create accurate compressed air simulation models. The method is used to create three similar simulations, each with varying amounts of data inputs. This determines the direct impact that data availability has on simulation accuracy. The three simulation models are calibrated to within a percentage error less than the previously discussed 9%. Table 8 summarises the percentage difference of the three baseline simulation models.

Table 8: Baseline simulation accuracies

Description	Percentage error [%]
Simulation-A	2.88
Simulation-B	4.50
Simulation-C	4.87

Finally, a new method is developed that identifies the type of simulation model that can be created. The method identifies the simulation accuracy that can be expected based on the available data. The newly developed method is displayed in Figure 5 of Section 3.2.2.4.

3.2 Compressed air network analysis

3.2.1 Preamble

A simulation model that consist of a large number of individual components is considered a complex simulation model. To simulate a complex compressed air network accurately, an in-depth analysis of the system is required. Sufficient data and network information need to be obtained before any simulation model can be constructed. The data and information will enable one to develop simulation models swiftly and accurately.

3.2.2 Network analysis

This section describes the process followed to determine the level of complexity of the compressed air simulation. Three levels of simulation complexity are identified within this section, namely, Simulation-A, Simulation-B, and Simulation-C.

3.2.2.1 Simulation-A

Simulation-A serves as a digital copy of the replicated mine's compressed air network. The simulation model is therefore under the assumption that it perfectly mimics the actual mine compressed air network outputs. All components must, therefore, replicate actual conditions.

For Simulation-A to replicate the compressed air network of Mine-A, a considerable amount of data is required. The more available data there is, the higher the simulation accuracy will be. Below is a description of the required data to create a highly accurate simulation model.

a) Individual compressor data

By acquiring individual compressor data, a group of compressors can be simulated accurately. This is done by comparing each compressor's outputs of the simulation model with actual compressor data. The outputs lower the probability of dissimilarities in simulation results in the event of small changes brought forth to a single compressor. Individual compressor data requirements include the following:

- Compressor power usage
- Compressor supply pressure
- Compressor characteristic curve
- Compressor efficiency

Figure 3 illustrates the measured individual compressor data.

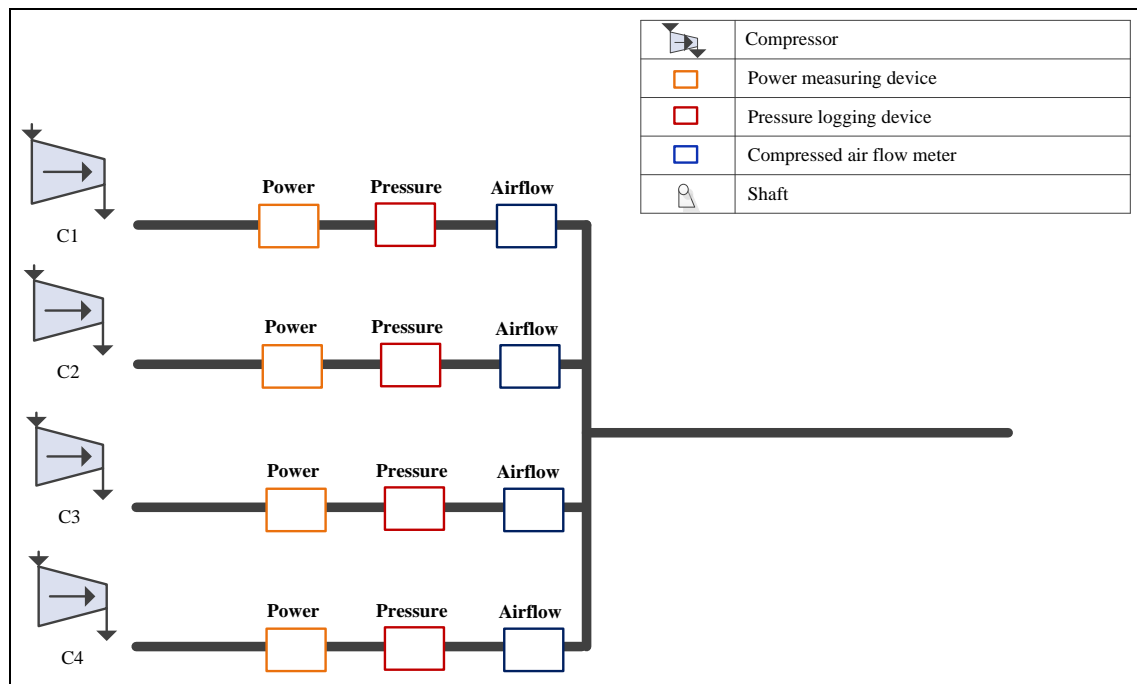


Figure 3: Detailed simulation compressor data

b) Individual pipe section dimensions

By individually simulating each pipe section, the risk of making an error when calculating average pipe dimensions is lowered. The risk is particularly applicable to sizeable compressed air networks where many pipe sections are present. Accurate simulation data is ensured as the compressed air network is replicated precisely.

Required pipe section dimensions include the following:

- Pipe length
- Pipe diameter
- Pipe surface roughness

c) Compressed air demand

The simulation is the most accurate when the compressed air demand to each underground level for each shaft is available as the exact whereabouts of all the generated compressed air is known. Therefore, the air demand to each underground level can be compared, which leads to an accurate comparison of the compressed air demand of each shaft.

3.2.2.2 Simulation-B

The availability of data is often limited to the instrumentation on a mine. It is not always possible to include all parameters. Thus, a less complicated model must be used to simulate the mine compressed air system as accurately as possible.

Below is a description of the minimum data required to simulate a compressed air network as accurately as possible to create a less detailed model, namely, Simulation-B.

a) Individual compressor data

Simulation-B requires the same individual compressor data as Simulation-A. The data will yield accurate simulation results when simplifying other sections of the compressed air network.

b) Average pipe section dimensions

When simulating a sizeable compressed air network, pipe sections can become challenging to simulate individually. The exact dimensions of larger compressed air network pipe sections are not always available. Average pipe lengths and diameters are often all that are available. The simulation model can be simplified by reducing the number of pipe components.

c) Compressed air demand

It is possible that the compressed air demand is not available for each level. However, it is essential to know the total compressed air demand of each shaft in the compressed air network. It is not as accurate as when measuring the usage per underground level, but it gives an accurate air usage per individual shaft.

3.2.2.3 Simulation-C

Simulation-C, a simplified model, is used when the availability of data on mines is limited. Thus, as few components as possible are used to try and simulate the compressed air networks as accurately as possible. Below is a description of limited data availability used in Simulation-C.

a) Compressor house data

Mines will often have one instrument for each parameter on the surface instead of one for each component. The single instrument means that each parameter is measured after the compressors' supply has already converged into the same network as indicated by Figure 4.

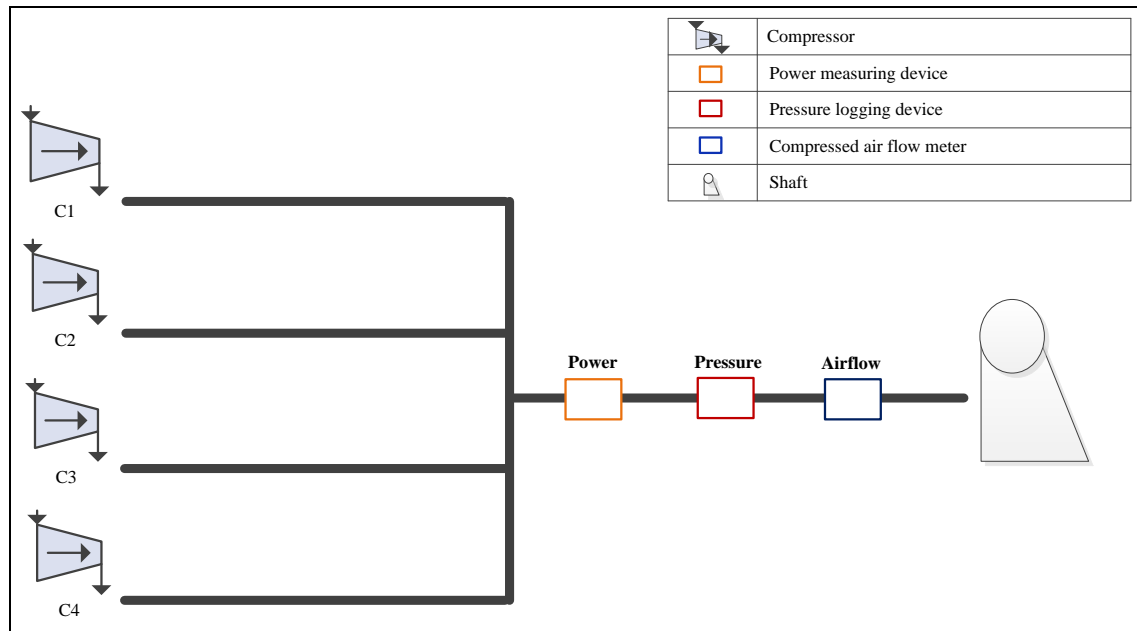


Figure 4: Simplified available compressor data

b) Average pipe section dimensions

The pipe dimension conditions for Simulation-C are the same as for Simulation-B (discussed previously in Section 3.2.2.2).

c) Compressed air demand

The compressed air demand conditions for Simulation-C are the same as for Simulation-B (discussed previously in Section 3.2.2.2).

3.2.2.4 Simulation setup summary

Figure 5 summarises the simulation setup procedure based on the availability of compressed air network data on mines. Figure 5 serves as an indication as to which simulation model can be created based on the available mine data.

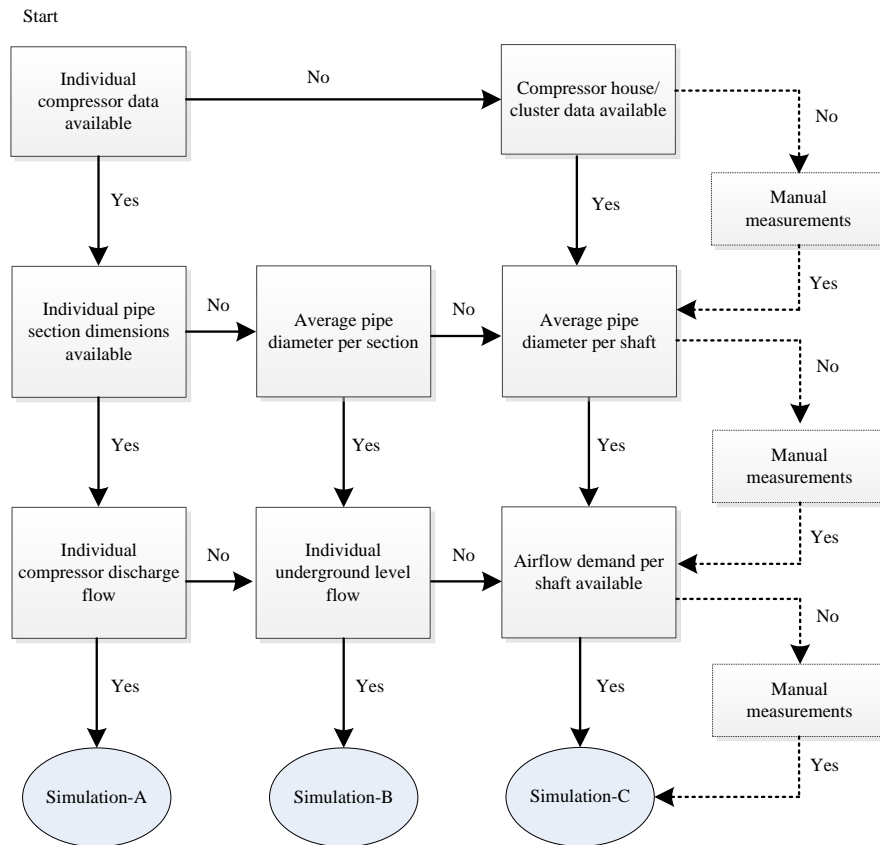


Figure 5: Simulation setup procedure summary

It is important to note that Mine-A simulations used in this study are that of the surface compressed air only. Simulation-A will therefore not use compressed air demand per level but only per shaft.

3.2.3 Simulation purpose

Simulation models are used to identify various savings initiatives. A simulation model should be created with a particular purpose in mind. For the parameters discussed in this section, specific measurements should be emphasised to ensure the accuracy of the simulation results. There are multiple parameters that can be investigated; however, this study focuses on compressed air flow, pressure and compressor power.

a) Flow

To ensure correct simulation flow calculations, detailed supplied and demand flow information is required. This will ensure that the correct distribution of compressed air flow is supplied to the simulation model. Various scenarios can then be simulated to distribute adequate amounts of air to other locations on the compressed air network.

b) Pressure

Most mines measure compressed air pressure either on the surface at the compressor discharge or underground. This is helpful for simulations as there are detailed measurements throughout the network. In order to simulate pressure readings accurately, one must ensure that the simulation compressors are able to supply adequate amounts of air at the correct pressure. Compressor specifications are not a necessity.

c) Power

Determining the power usage when supplying air at correct pressures and flows requires detailed compressor specifications. It is important to ensure that the size, characteristics and efficiency of each compressor are available, which will ensure accurate power measurements during simulation.

3.2.4 Data acquisition

Figure 6 shows the required diagram procedure to obtain the necessary data for creating a simulation model replica of Mine-A.

Each simulation package requires different data to create an accurate compressed air simulation model. The procedure illustrated in Figure 6 allows one to gather the essential data required by most simulation packages. Any additional information required by the simulation package must also be obtained.

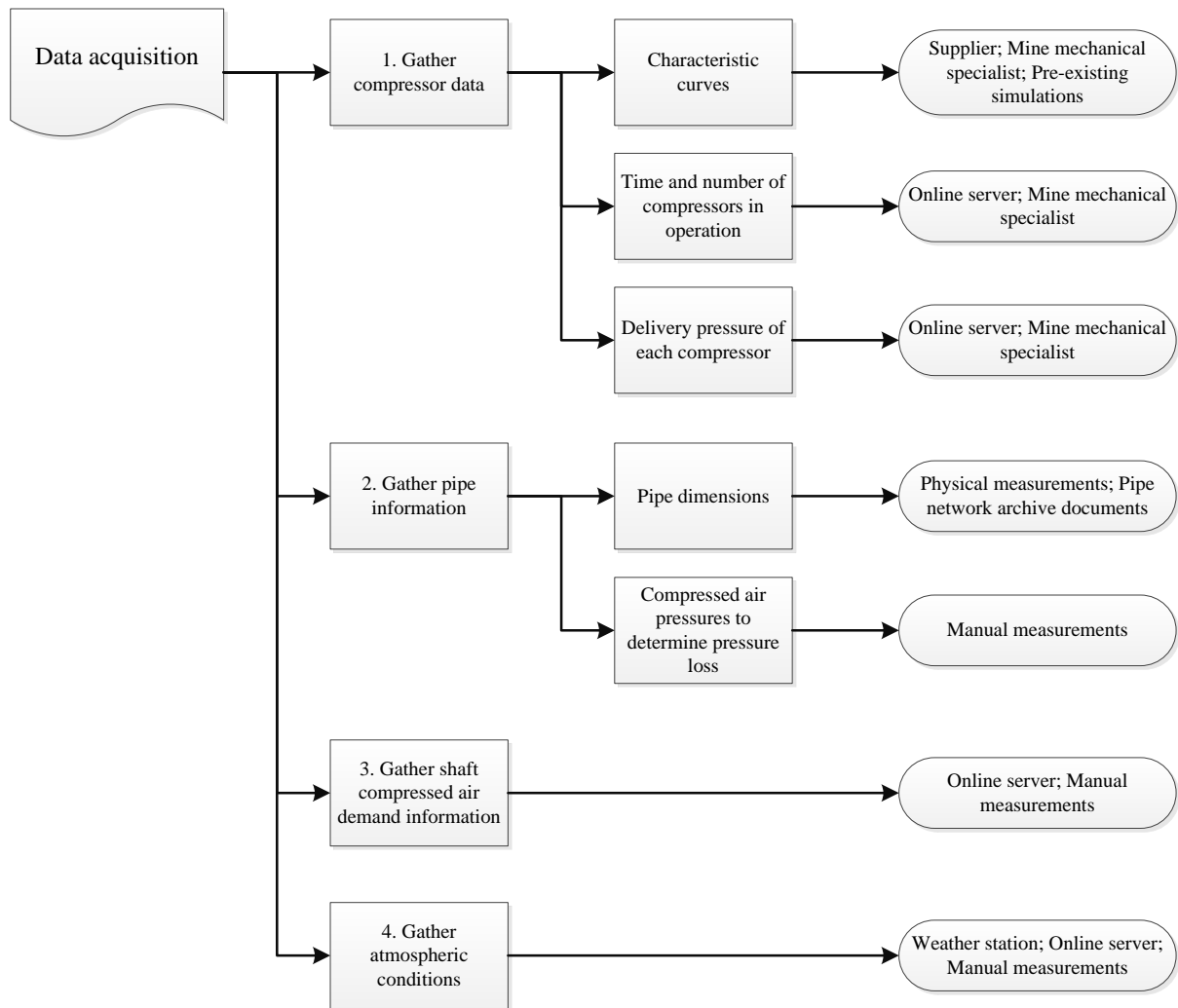


Figure 6: Data acquisition procedure

It is essential that all necessary data and information be obtained before creating a simulation model. Table 9 summarises the various components along with key features within each component that are explicitly required for PTB simulation purposes.

Table 9: PTB simulation data requirements

Component	Key features
Compressors	<ul style="list-style-type: none"> ○ Characteristics curve ○ Efficiencies ○ Running status ○ Delivery pressure
Pipes	<ul style="list-style-type: none"> ○ Airflow ○ Pressure ○ Valve fraction ○ Temperature ○ Volume ○ Heat transfer coefficient ○ Heat transfer area ○ Hydraulic diameter ○ Pipe flow area ○ Pipe length ○ Surface roughness
Air nodes	<ul style="list-style-type: none"> ○ Pressure ○ Temperature ○ Elevation ○ Volume ○ Heat transfer area ○ Relative humidity
Pressures	<ul style="list-style-type: none"> ○ Shaft pressure ○ Delivery pressure
Airflow	<ul style="list-style-type: none"> ○ Flow supply ○ Flow demand ○ Pressure
Atmosphere	<ul style="list-style-type: none"> ○ Temperature ○ Pressure ○ Relative humidity ○ Elevation

Evaluating data quality is equally as important as the components' key features. Data is often missing or is mismeasured due to faulty equipment. It is, therefore, important to evaluate multiple parameters to ensure the measured data coincides with simulation data. Crucial parameters include the supplied flow, supplied pressure and power usage. At least two of the three parameters must have accurate information to ensure that the third parameter has accurate simulation results.

Figure 7 illustrates the running status of all the compressors of Mine-A on 23 August 2017. It is evident from Figure 7 that there is no missing or interrupted data for the given period. The data can therefore be used without manipulating it to an estimated value. Sound data quality yields accurate power consumption calculations, resulting in accurate annual running cost estimations.

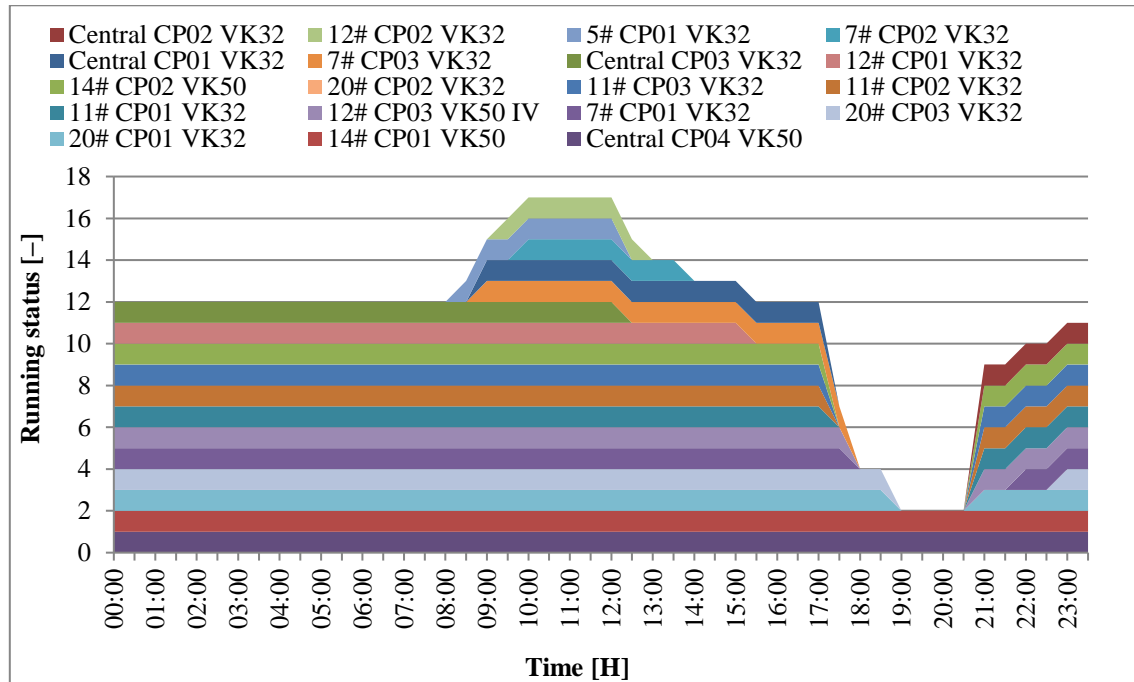


Figure 7: Quality compressor running statuses data

3.2.5 Summary

Figure 8 summarises the method used to develop the simulation models within this study.

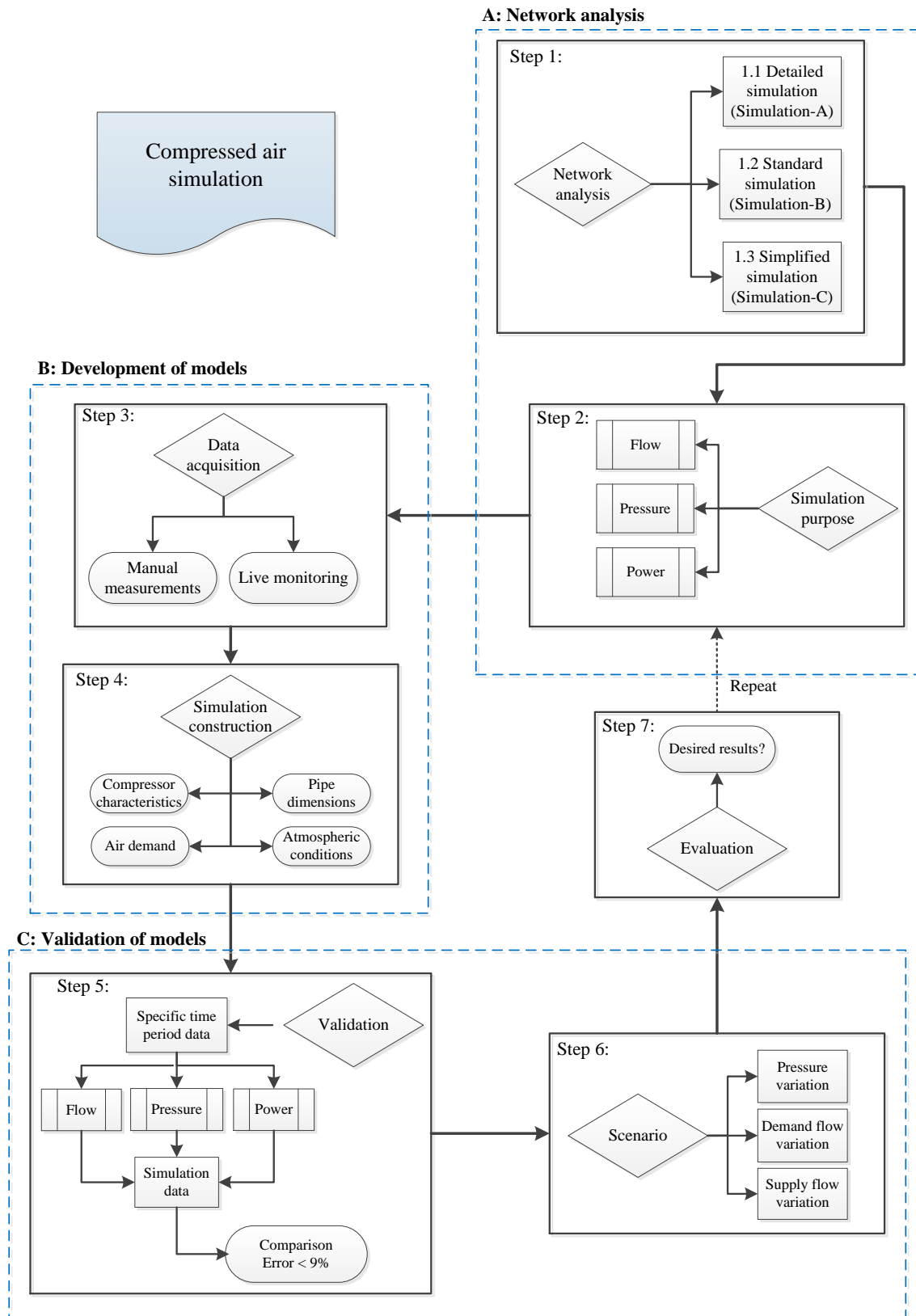


Figure 8: Method used to develop compressed air simulations

3.3 Development of models

3.3.1 Preamble

This section describes the development of the three simulation models for Mine-A. These models are developed, each with decreasing complexity, to determine the accuracy of less complex simulation models. All three simulations are compared with actual data to validate and ensure their accuracy. These simulation models are used to compare the information seen in Table 10.

Table 10: Simulation comparison parameters

Description	Units
Power consumption	MW
Supply airflow	kg/s
Supply pressure	kPa

The simulation models of Mine-A are created using PTB. As discussed in Chapter 2, PTB is a simulation program capable of simulating the compressed air system of Mine-A. A pre-existing AFT Arrow simulation model of Mine-A is used to obtain the necessary information to develop the simulations. It should be noted that having the correct data available can drastically reduce simulation setup time. Data however, is not always available and simulation setup time will vary because of this.

3.3.2 Development of Mine-A's compressed air network simulation

This section discusses how each of the three simulation models was created using PTB. The required data discussed in the previous section is shown and incorporated into the simulation models. This section uses the method developed in this chapter to create a compressed air simulation model of Mine-A.

Mine-A has a large and complex compressed air network. Table 11 summarises the surface compressed air reticulation network. Table 11 indicates fundamental component quantities as well as specific component dimensions. Figure 40 in Appendix D displays a schematic layout of the compressed air reticulation network of Mine-A.

Table 11: Mine-A compressed air network summary

Description	Value
Compressor houses count	7
Compressor count	19
Total pipe length	30.9 km
Number of shafts	12
Hourly average power consumption	39.1 MW
Annual electricity cost	R255.2 million

The schematic layout of the surface compressed air network illustrated in Figure 40 in Appendix D was used to understand Mine-A better. The layout was derived from the pre-existing simulation model. The layout indicates the name and location of the compressor houses, the number of compressors, and the distances between each of the compressor houses and shafts.

Because Mine-A's is so complex, a significant amount of data is required to simulate the system. Larger simulation models also result in longer simulation running times. These time factors all add up to longer times required for the simulation development procedure. Actual mine data for a given period must be obtained for comparison with simulated values. The gathered data is processed into hourly average values. The hourly average values are then compared with their simulated equivalent values.

As discussed earlier, the simulation model of Mine-A comprises the surface compressed air network only. The data required to simulate the network accurately is therefore mostly available. This data is used to determine the hourly averages for the power consumption, supplied airflow and surface supply pressure.

The information summarised in Table 12 was obtained from Mine-A's surface instrumentation. Data for 23 August 2017 was processed into hourly average values. Thereafter, these values were compared with the baseline simulation models.

Table 12: Description of required simulation data

No.	Data required	Description
1	Compressor specification	The design of each compressor used by Mine-A
2	Compressor power consumption	Annual power usage consumed by Mine-A to determine electricity costs
3	Compressor supply pressure	The surface pressure maintained by the compressors to supply adequate air to underground
4	Compressor supply flow	The air mass flow that is supplied by the compressors
5	Mining airflow demand	The air mass flow consumed by all mining operations

The data given in Table 12 was incorporated into the three simulation models. With the available information, three baseline simulation models, each a simplified version of the preceding model, were created to compare with the actual data of Mine-A.

a) Compressor specifications (A)

A cut-out section of the simulation software AFT Arrow, seen in Figure 41 of Appendix E, was used to specify components. The input data of the components used in the AFT Arrow simulation is illustrated in Figure 42 in Appendix E. These input values were used to characterise the components of the three PTB simulation models. The process of using the input data to characterise the simulation model components is shown in Figure 9.

Figure 9 indicates the compressor data obtained from the pre-existing AFT Arrow simulation model. The compressor data was processed into airflow (y-axis) versus pressure ratios (x-axis). The data was then used to characterise the three simulation model compressors.

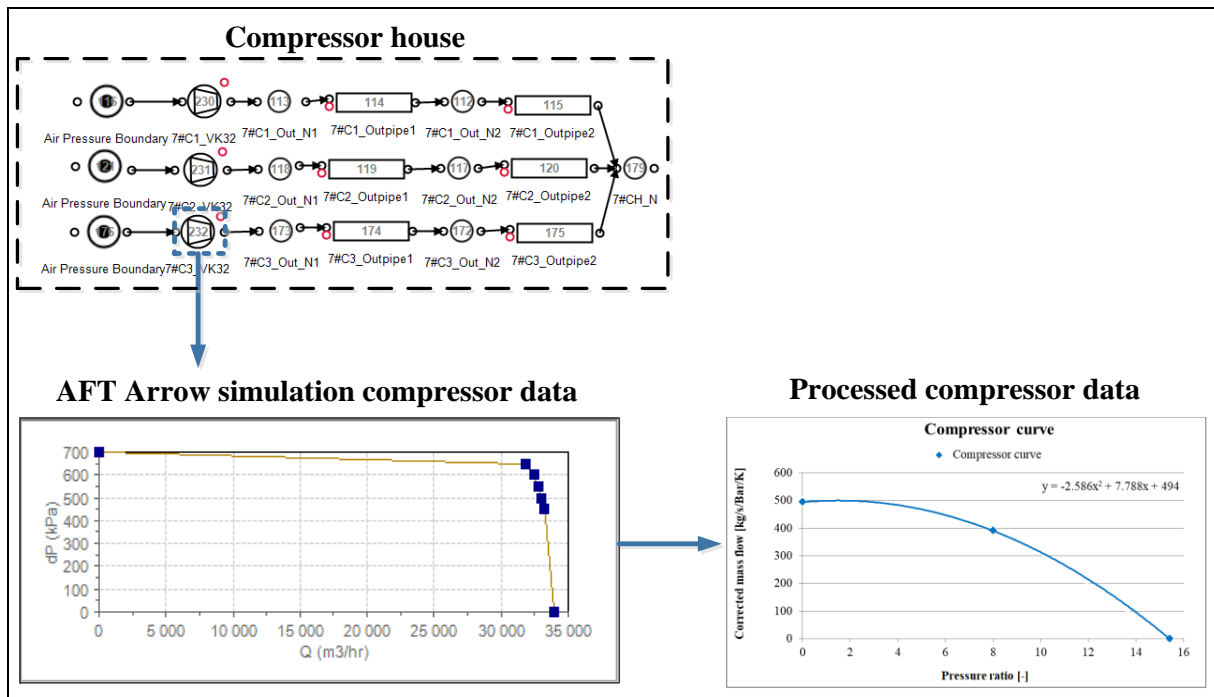


Figure 9: Compressor specification illustration

b) Compressor specifications (B)

It was possible to obtain the characteristics curve of these compressors by applying a quadratic function using three operating points as illustrated in Figure 10.

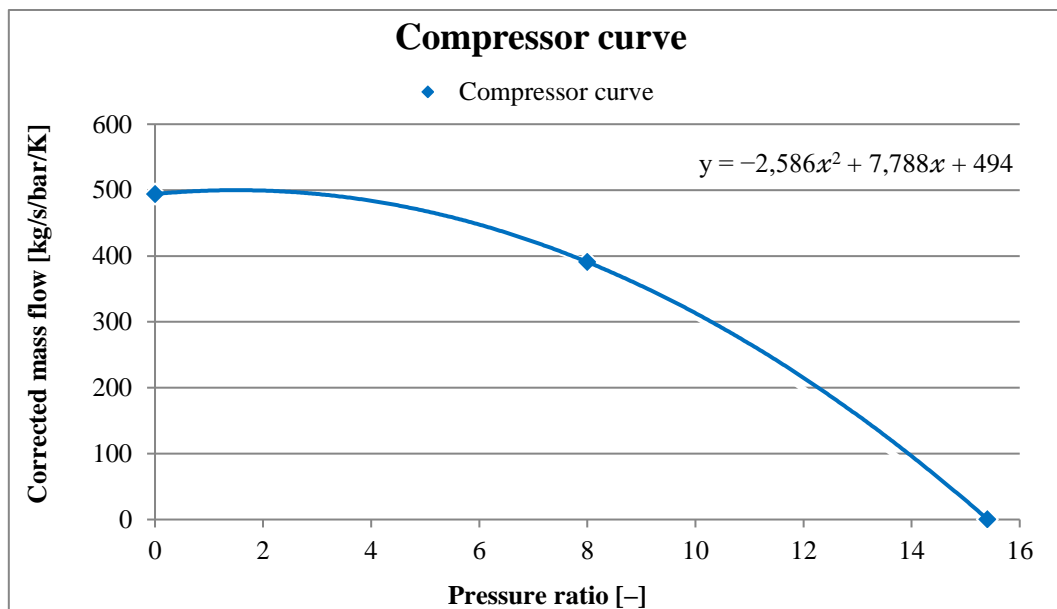


Figure 10: Quadratic function for compressor characteristics curve (adapted from [59])

The quadratic function, seen in Figure 10, allows the characteristic curve of a compressor to be determined when only one data point is available. Thus, it is possible to estimate the remaining two points by means of calculation.

c) Mine-A: Compressor specifications

Two compressor types are used in the surface compressed air network of Mine-A, namely, the VK32 and VK50 compressors. The VK32 compressor is the smaller one of the two, delivering a maximum airflow of 9.43 m³/s at 0 kPa discharge pressure. The VK50 delivers a maximum airflow rate of 14.22 m³/s at 0 kPa discharge pressure. Each compressor is calibrated individually, and the correct number of each type of compressor is placed in the various compressor houses of the simulation model.

The compressor data for the volumetric flows at given discharge pressures was available. The simulation, however, required the corrected flow values. Therefore, the corrected flow values were calculated for each simulation model. Thereafter, the corrected flow values were incorporated into the simulation models.

The following calculations were done to calculate the corrected flow values of both compressors [60].

Equation 8: Corrected flow calculation

$$\dot{m}_c = \frac{(\dot{m}\sqrt{\theta_t})}{\delta_t}$$

With:

Equation 9: Mass flow calculation

$$\dot{m} = V\rho = V\left(\frac{P}{RT}\right)$$

Equation 10: Temperature ratio calculation

$$\theta_t = \frac{T_{Tot}}{T_{ref}}$$

Equation 11: Pressure ratio calculation

$$\delta_t = \frac{P_{Tot}}{P_{ref}}$$

Substituting Equation 9, Equation 10, and Equation 11 into Equation 8 yielded the detailed corrected flow equation, namely, Equation 12.

Equation 12: Corrected flow detailed equation

$$\therefore \dot{m}_c = \frac{\left(V \left(\frac{P}{RT_{Tot}} \right) \cdot \sqrt{\frac{T_{Tot}}{T_{ref}}} \right)}{\frac{P_{Tot}}{P_{ref}}}$$

Where:

- \dot{m}_c = Corrected flow [kg/s/bar/K]
 V = Volumetric airflow rate [m³/s]
 P = Air pressure [kPa]
 R = Universal gas constant [kJ/kg·K]
 T_{Tot} = Total temperature [K]
 T_{ref} = Reference temperature [K]
 P_{Tot} = Total pressure [kPa]
 P_{ref} = Reference pressure [kPa]

d) Pipe dimensions

The pre-existing simulation and aerial images were used to determine the exact pipe dimensions for the surface compressed air network of Mine-A. The pre-existing simulation model of Mine-A had all the necessary pipe diameters required for Simulation-A. However, certain pipe lengths were not available within the pre-existing simulation model. An aerial image of the surface compressed air network was used to determine the pipe lengths. Manual measurements and calculations had to be done to determine the pipe lengths as accurately as possible.

The data available from the pre-existing simulation model is illustrated in Figure 11. This data was used alongside the manual measurements to specify the pipe dimensions as accurately as possible.

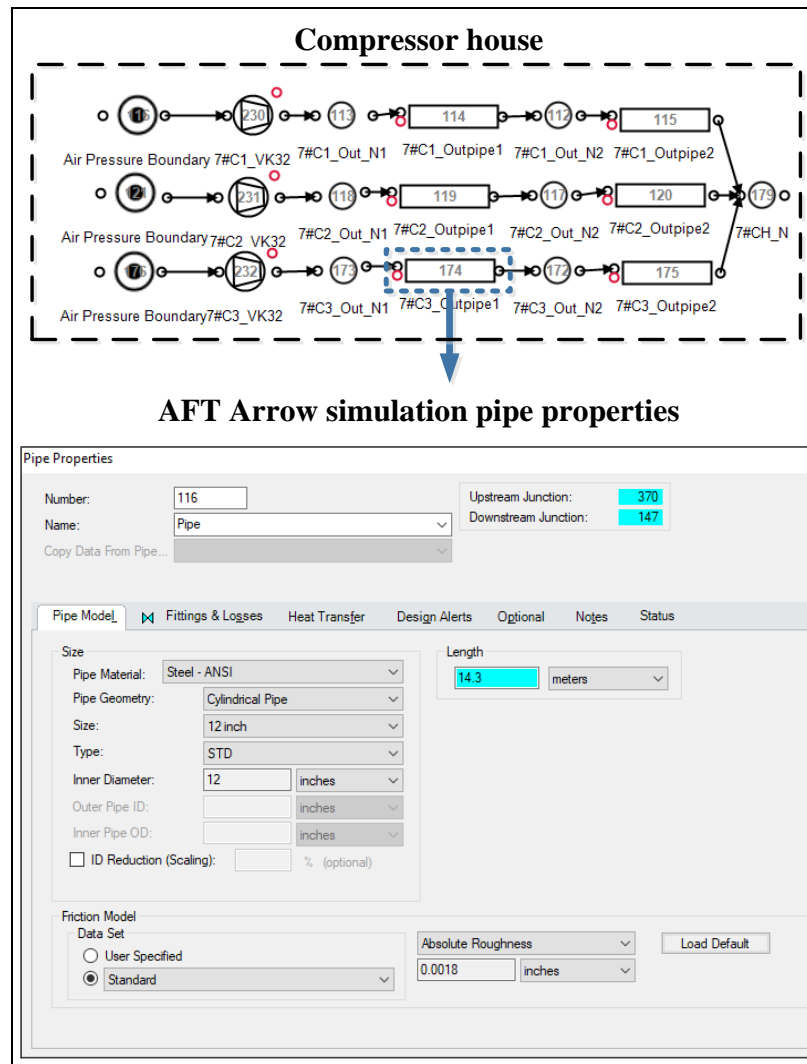


Figure 11: Available pipe dimensions

e) Compressed air demand

The compressed air demand of all the shafts feeding off the surface compressed air network was obtained through mine server data. This variable, however, remained constant as the simulation models were simplified.

f) Compressor efficiency

The efficiencies of each compressor can be calculated theoretically but depend on good data quality to ensure that no errors are shown in the simulation results. For this study, efficiencies were assumed during calibration until the desired power output was achieved. Assumptions during simulation development allow for faster calibration.

g) Assumptions

Ideally, actual atmospheric conditions should be obtained to ensure an accurate simulation development. However, the atmospheric conditions for this study were unavailable and assumed values were used based on elevation and winter temperatures.

- Atmospheric pressure: 87 kPa
- Atmospheric temperature: 20°C
- Universal gas constant: 0.287 kJ/kg·K

h) Simulated models of Mine-A surface compressed air network

- Simulation-A
 - The total number of compressors was simulated along with the precise design specification for each compressor.
 - Actual pipe diameters and lengths were used to simulate each section of the compressed air pipe network.
- Simulation-B
 - The total number of compressors was simulated along with the precise design specification for each compressor. The compressors were identical to Simulation-A.
 - Average pipe diameters and lengths were used for individual sections between shafts and compressor houses.
- Simulation-C
 - All identical compressors within each compressor house were simulated as one large compressor component.
 - Average pipe diameters and lengths were used for the individual sections between shafts and compressor houses.

By simplifying the simulation models, the number of components used in the simulation process could be reduced. Simulation-A had 261 components, Simulation-B had 220, and Simulation-C had 157. A detailed description of the total components is given in Chapter 4. These components are illustrated in Table 30.

3.3.2.1 Simulation-A model development

a) Compressor specification

VK32 compressor:

The designed flow rates at a given set point for a single VK32 compressor used in Simulation-A are shown in Table 34 (Appendix F). The data in Table 34 was used in combination with the assumptions made earlier to determine the corrected flow rates for Simulation-A's VK32 compressors. Calculations were done by substituting the data into Equation 12. By doing so, the corrected flow values in Table 35 (Appendix F) were calculated. As seen in Table 35, the airflow rate increases as the pressure ratio over the compressor decreases. The changes in airflow rates versus the pressure ratio for Simulation-A are illustrated in Figure 12 below.

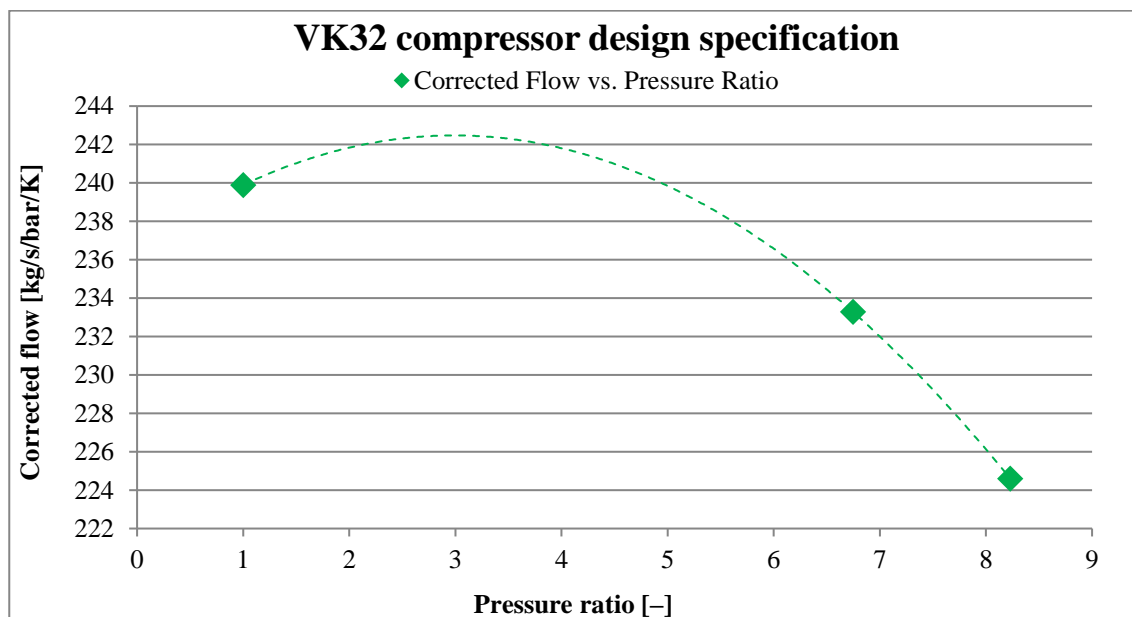


Figure 12: VK32 design specification – Simulation-A

As seen in Figure 12, the corrected flow value of a single VK32 compressor depreciated substantially as the pressure difference over the compressor increased. These compressors were simulated individually and in parallel as they would run on Mine-A. The optimal design point of the compressor was not required for Simulation-A as the actual conditions of Mine-A were merely replicated.

VK50 compressor:

The designed flow rates at a given set point for Simulation-A are shown in Table 36 (Appendix F). Using the data in Table 36, the corrected flows were calculated similarly to the VK32 compressor. By doing so, the corrected flow values in Table 37 in Appendix F were calculated. As seen in Table 37, the airflow rate of the VK50 compressor increased more than the VK32 compressor as the pressure ratio over the compressor decreased. The changes in airflow rates versus the pressure ratio for the VK50 compressor of Simulation-A are visually illustrated in Figure 13 below.

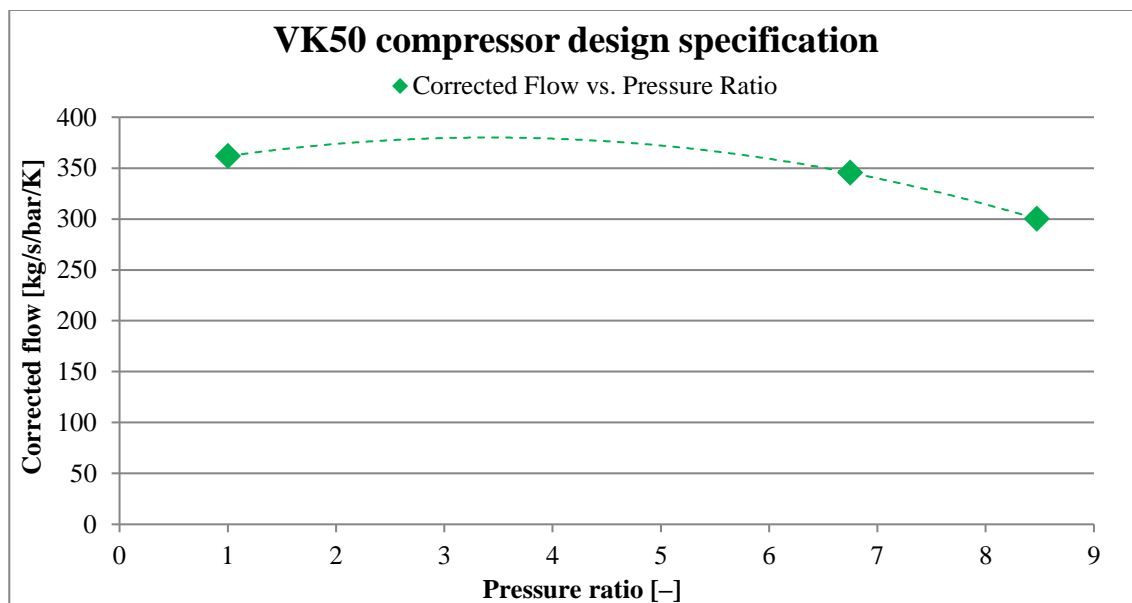


Figure 13: VK50 design specification – Simulation-A

As seen in Figure 13, the VK50 compressor was able to deliver higher volumes of airflow rates at similar pressure ratios. For Simulation-A, the VK50 compressors were also simulated individually and in parallel as they would operate on Mine-A. The compressors running in parallel resulted in higher airflow rates at given pressure ratios over all of the compressors.

b) Pipe dimensions

i. Pipe length

As discussed previously, the pipe lengths for Simulation-A were obtained through a previous simulation and physical measurements. These measurements were taken on an aerial map of the surface compressed air network. The pipe lengths for Simulation-A have been determined as accurately as possible.

ii. Pipe diameter

As discussed previously, the diameters of each pipe obtained were from the pre-existing simulation model of Mine-A. For Simulation-A, each pipe was used and specified. The pipe details mean that no average pipe diameters were calculated for different sections of the compressed air network.

iii. Surface roughness

The surface roughness where compressed air is in contact with the pipes was obtained directly from the pre-existing simulation model of Mine-A.

3.3.2.2 Simulation-B model development

a) Compressor specification

The compressor specifications of Simulation-B were identical to that of Simulation-A, which was discussed previously.

b) Pipe dimensions

i. Pipe length

The pipe lengths discussed in Simulation-A's section were used to calculate an average pipe length for individual sections of the compressed air network. The total pipe length from one compressor house to the shaft was used instead of the exact length per section.

ii. Pipe diameter

The pipe diameters used for Simulation-A were used to calculate an average diameter for all the sections of pipe. Similar to the pipe length calculations, the diameters of all the sections from a compressor house to a shaft were used to determine the average diameter of that section. The average diameter sections reduced the total number of simulation model components while still considering all the necessary dimensions.

iii. Surface roughness

The surface roughness where compressed air is in contact with the pipes was obtained directly from the pre-existing simulation model of Mine-A. The average surface roughness was calculated per section to use in Simulation-B.

3.3.2.3 Simulation-C model development

a) Compressor specification

VK32 compressor:

Simulation-C used the specifications of a single VK32 compressor to define multiple compressors as one. This means that two compressors running in parallel are specified as one compressor with a higher volumetric airflow rate. The result is that the volumetric airflows are multiplied by the number of compressors as seen in Table 38 (Appendix F).

The volumetric airflow rates were used similarly in Equation 12 to determine the corrected flow values used in the simulation model. The calculation results are shown in Table 39 (Appendix F). As seen in Table 39, the airflow rates were far higher than those of Simulation-A and Simulation-B because one component needed to deliver the same amount of airflow than two or three components did previously. Figure 14 and Figure 15 below illustrate this.

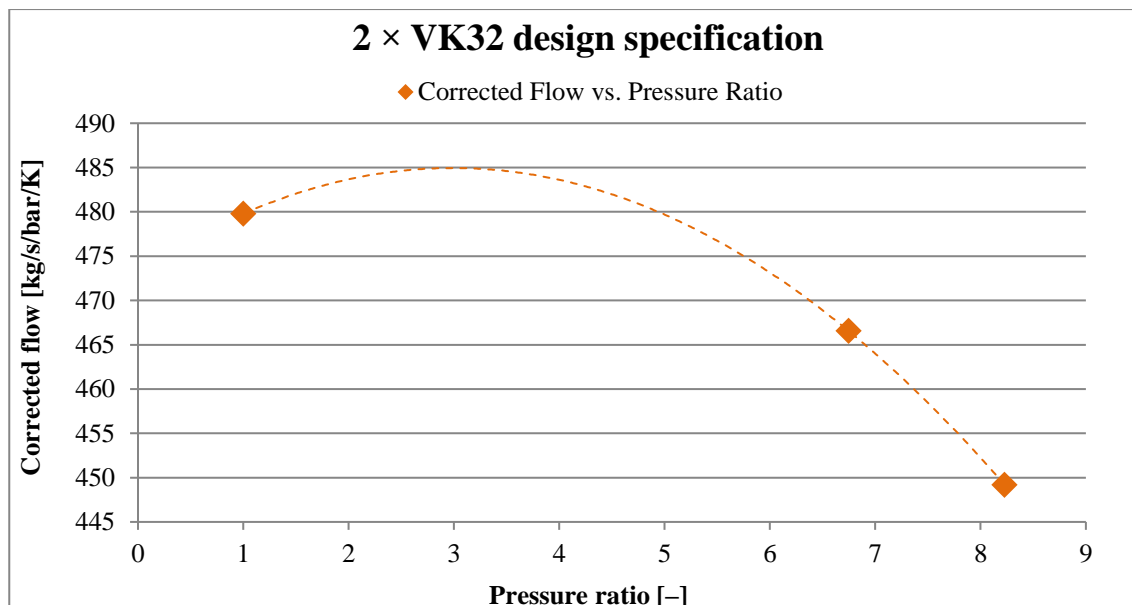


Figure 14: 2 x VK32 design specification – Simulation-C

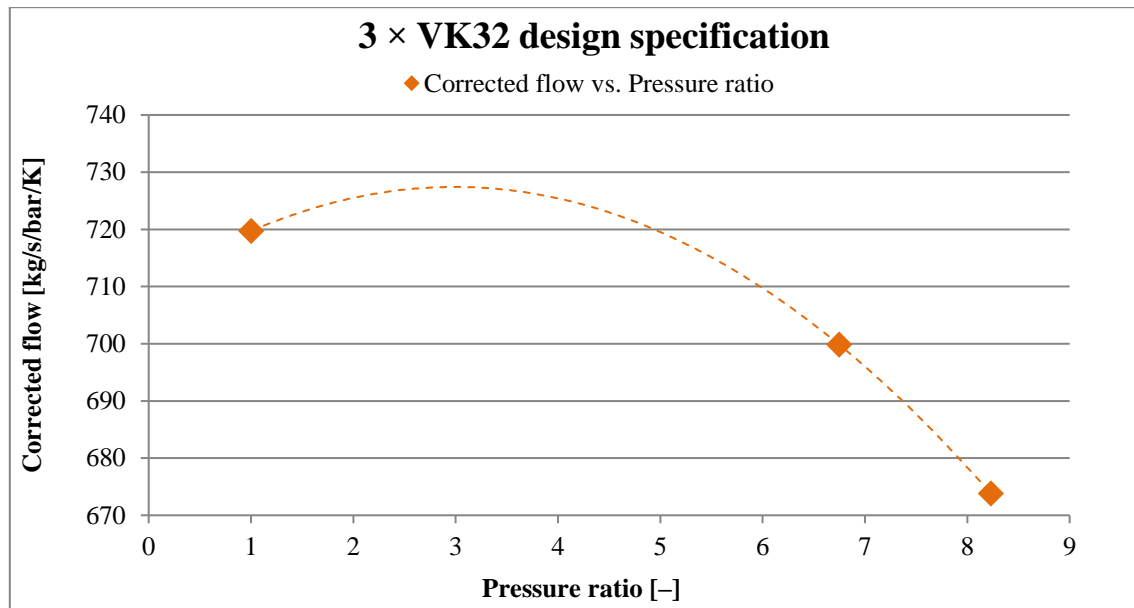


Figure 15: 3 x VK32 design specification – Simulation-C

As seen in both Figure 14 and Figure 15, the corrected flow values of multiple VK32 compressors simulated as one delivered far higher flow rates at the same pressure difference than a single VK32 compressor.

VK50 compressor:

Simulation-C used the specifications of a single VK50 compressor to define multiple compressors as one. Identical to the VK32, multiple compressors running in parallel were specified as one compressor with a higher volumetric airflow rate. This is seen in Table 40 (Appendix F). The calculated corrected flow values are shown in Table 41 (also found in Appendix F).

As seen in Table 41, the airflow rates were far higher than that of Simulation-A and Simulation-B because one component delivered the same amount of airflow than two or three components did previously. Figure 16 and Figure 17 illustrate this.

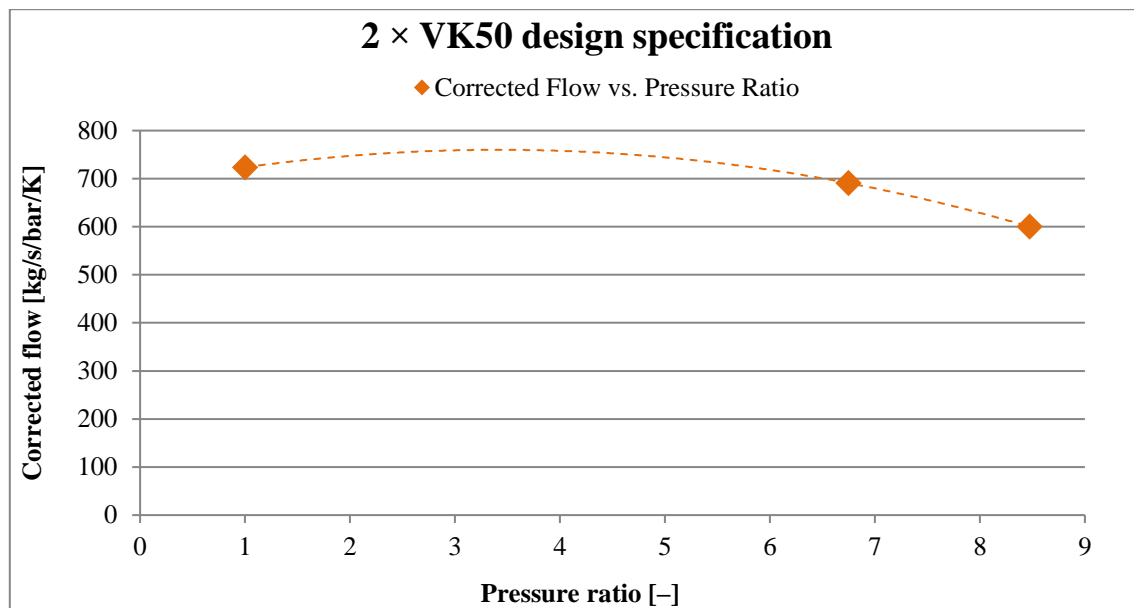


Figure 16: 2 × VK50 design specification – Simulation-C

As seen in Figure 16, the corrected flow values of two VK50 compressors simulated as one delivered doubled the flow rate of one VK50 compressor at the same pressure ratio.

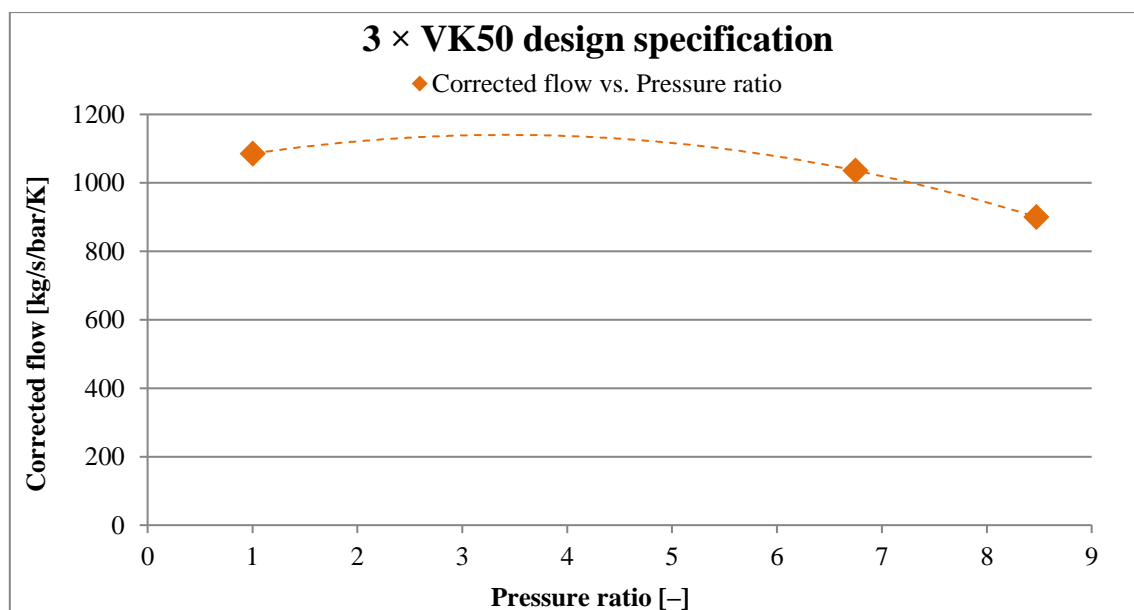


Figure 17: 3 × VK50 design specification – Simulation-C

As seen in Figure 17, the corrected flow values of three VK50 compressors simulated as one delivered three times the flow rates at the same pressure ratio. The result is that the same conditions on Mine-A could be replicated using far fewer components in the simulation model.

b) Pipe dimensions**i. Pipe length**

The average pipe lengths discussed for Simulation-B were used in the same manner for Simulation-C.

ii. Pipe diameter

The average pipe diameters discussed for Simulation-B were used in the same manner for Simulation-C.

iii. Surface roughness

The surface roughness was used in the same manner as for Simulation-B discussed previously.

3.4 Validation of models

3.4.1 Preamble

Experimental verification is the typical traditional approach used to validate the accuracy of simulation models [28]. Physical measurements were, however, taken throughout the mine compressed air network to ensure high-level accuracy results when validating simulations within this dissertation.

Three baseline simulation models, each a simplified version of the preceding model, were created to replicate the surface compressed air network of Mine-A. This followed after the need was identified to simplify simulation models. This was done to determine their accuracies in the event of limited data and information on the compressed air network of mines. Additionally, the purpose is to minimise the complexity and study the impact thereof. Screenshots of the three simulation models are shown in Figure 43, Figure 44, and Figure 45 of Appendix G.

The baseline simulation models are compared with actual compressor data obtained directly from Mine-A's servers. The selected server data is that of 23 August 2017. Multiple days worth of data could, however, not be used because of data disruptions. A single day with the best data quality was therefore selected. The data of 23 August 2017 includes the following:

- Daily supplied airflow
- Daily supply pressure
- Daily power usage

The data was used to compare the corresponding parameters of the three simulation models. It was found that the daily supplied flow and daily power usage for the three baseline simulation models were simulated to within 4.87% of the actual data. Simulation-A had the lowest difference at 2.88%, resulting in a 97.12% accurate simulation model.

The daily supplied pressure had data interruptions for the corresponding period (23 August 2017). Therefore, an accurate pressure comparison regarding the baseline simulation models could not be made. However, because both the daily power usage and supply flow were within 2.88% accuracy, it could be assumed that Simulation-A's supply pressure was within 2.88% accuracy as well. This assumption applies to Simulation-B and Simulation-C as well.

3.4.2 Baseline simulation validation

a) Simulation-A validation

Simulation-A was created using PTB. The simulation model yielded the following results when compared with actual mine data of 23 August 2017. A 24-hour profile of 23 August 2017 was plotted for both the actual and Simulation-A surface compressed air parameters. The data is compared in Figure 18 to Figure 20 below.

i. Daily supplied airflow

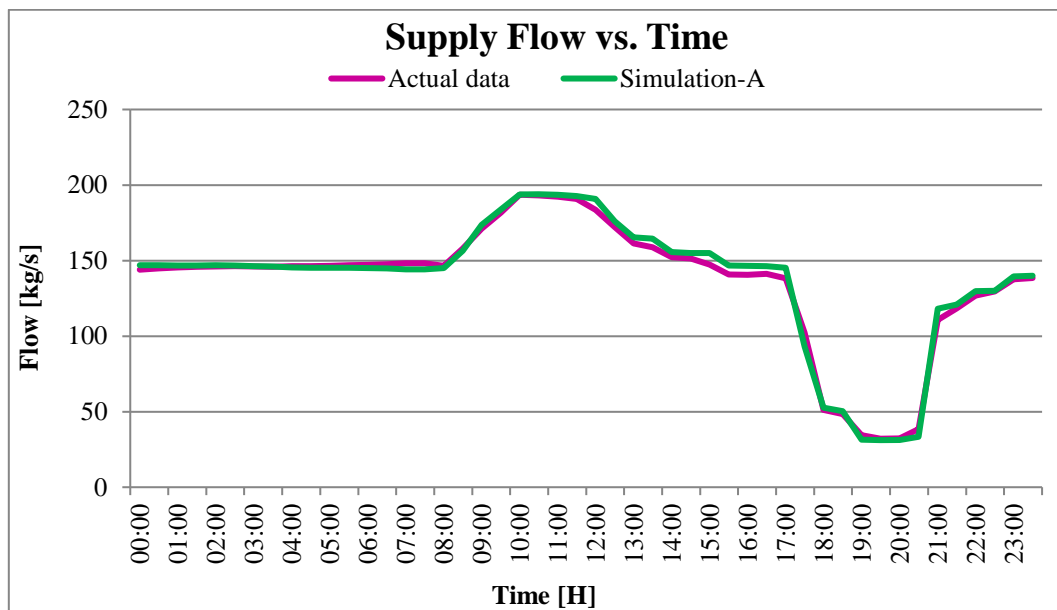


Figure 18: Simulation-A validation – supply flow

As seen in Figure 18, the simulation data represented by the green line followed a consistent trend with the actual mine data, represented by the pink line. The MAE percentage difference, discussed in Chapter 2, was 2.56%. This resulted in a 97.44% simulation accuracy when comparing the supplied flow of Simulation-A with the actual data of Mine-A.

ii. *Daily power usage*

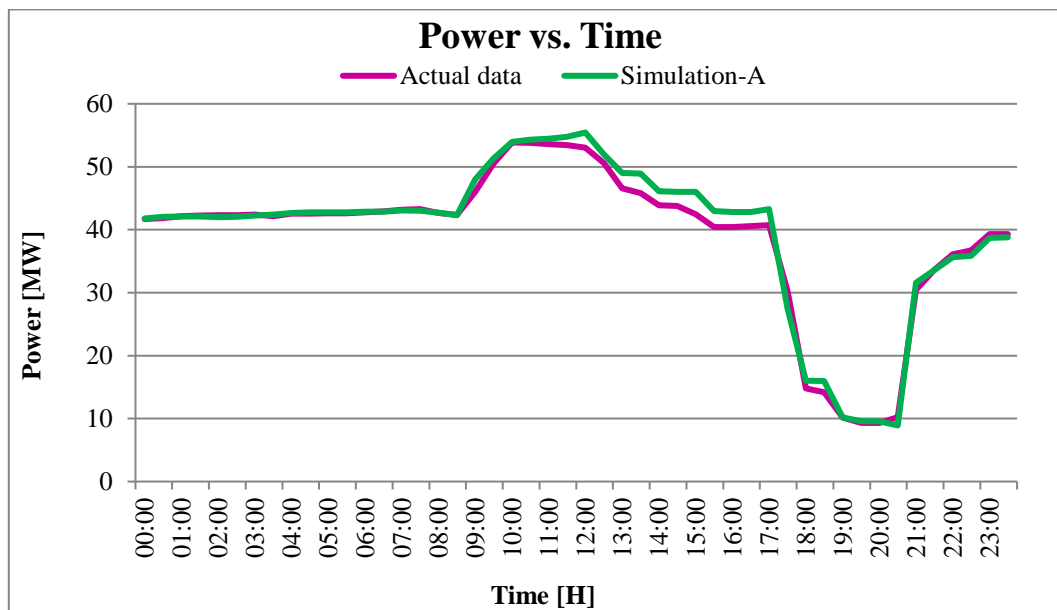


Figure 19: Simulation-A validation – power usage

As seen in Figure 19, the simulation data again followed a consistent trend with the actual mine data. The calculated MAE percentage difference was 2.88%. This resulted in a 97.12% simulation accuracy when comparing the power usage of Simulation-A with the actual usage of Mine-A.

iii. *Daily supply pressure*

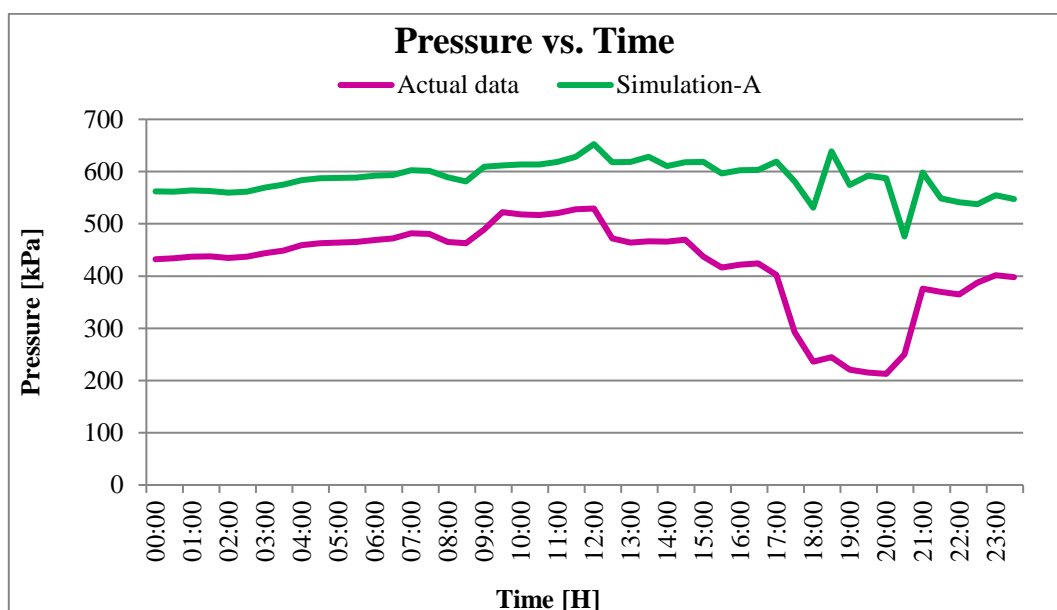


Figure 20: Simulation-A validation – supply pressure

In Figure 20, the simulation data follows a similar trend to that of the actual data. However, because of the data interruptions discussed earlier, the average supply pressure of the actual data is lower than it indeed is. The consistent trend between the two data sets and the accuracies of the supply- and power usage allow for the assumption that the pressure is also accurate to within 2.88% difference. This is because two of the three parameters are within range. The simulation components are specified according to component design and therefore have to result in the same pressure outputs.

b) Simulation-B validation

Figure 46 to Figure 48 (Appendix H) illustrate the same comparisons with actual data for Simulation-B (represented by the blue lines) as for Simulation-A. Data from 23 August 2017 was used to plot the 24-hour profiles of the previously mentioned comparisons.

i. Daily supplied airflow

As seen in Figure 46, Simulation-B data follows a consistent trend with actual data. The calculated MAE difference between the two simulation models is 4.50%, resulting in 95.50% accuracy.

ii. Daily power usage

As seen in Figure 47, Simulation-B data again follows a consistent trend when compared with actual data. The calculated MAE difference between the two simulation models is 2.92%, resulting in a 97.08% accuracy.

iii. Daily supply pressure

As seen in Figure 48, the two simulation models follow a similar trend. However, due to the data interruptions discussed earlier, the percentage difference does not reflect actual values. A percentage difference of 4.50% is therefore assumed as explained in the previous section.

c) Simulation-C validation

Figure 49 to Figure 51 (Appendix H) illustrate the same comparisons with actual data for Simulation-C (represented by the orange lines) as for Simulation-A. Data from 23 August 2017 was used to plot the 24-hour profiles of the previously mentioned comparisons.

i. Daily supplied airflow

As seen in Figure 49, Simulation-C data continues to follow a consistent trend when compared with actual data. The MAE percentage difference, however, slightly increases to 4.87%. The result is a simulation accuracy of 95.13%.

ii. Daily power usage

As seen in Figure 50, Simulation-C data again follows a consistent trend with actual data. The MAE percentage difference for the power usage is 4.37%, resulting in a simulation accuracy of 95.63%.

iii. Daily supply pressure

As seen in Figure 51, data loss causes a more significant percentage difference between the data sets than genuinely reflected in the data. However, as discussed previously, the MAE percentage difference can be assumed to be a value of 4.87%.

3.4.3 Simulation evaluation

After each simulation model is developed, the percentage error between the model and actual data must be evaluated. As stated in Chapter 2, an acceptable error is 9% or less. If any of the developed models have an error greater than 9%, the model should be re-evaluated and calibrated until the desired accuracy is achieved.

After evaluating Simulation-A, Simulation-B and Simulation-C, it is clear that all model comparisons give an error less than the required 9%. It can therefore be concluded that all simulation models have successfully been validated as accurate representations of Mine-A.

3.5 Summary

A method was developed in this chapter to create compressed air simulations of varying complexity. The method was applied to a case study, Mine-A, to determine the effect that simulation complexity has on simulation accuracy. Three simulation models, namely, Simulation-A, Simulation-B and Simulation-C were developed.

Simulation-A is used when most of a mine's compressed air network data is available. In this study, Simulation-A was calibrated to within 2.88% difference when compared with actual mine data. Table 13 displays the percentage differences of the three compared variables.

Table 13: Simulation-A accuracy comparison

Simulation model	Supplied airflow % difference	Supply pressure % difference	Power usage % difference
Simulation-A	2.56	2.88*	2.88

*Assumed

Simulation-B is used when either the pipe section specifications or airflow demand is not available in detail. This means that individual compressor details are available, but not pipe specifications or compressed airflow. Table 14 displays the calculated percentage differences of the compared variables.

Table 14: Simulation-B accuracy comparison

Simulation model	Supplied airflow % difference	Supply pressure % difference	Power usage % difference
Simulation-B	4.50	4.50*	2.92

*Assumed

Simulation-C is used under similar conditions to that of Simulation-B. Simulation-C, however, uses compressor house average power consumption and total supplied airflow instead of individual compressor data. Table 15 displays the calculated percentage differences of the compared variables.

Table 15: Simulation-C accuracy comparison

Simulation model	Supplied airflow % difference	Supply pressure % difference	Power usage % difference
Simulation-C	4.87	4.87*	4.37

*Assumed

Table 13, Table 14 and Table 15 show that all the simulation models have successfully been calibrated to replicate Mine-A. The highest percentage difference of 4.87% is that of Simulation-C. This, however, results in a minimum simulation accuracy of 95.13%. The information gathered from this study shows that all three simulation models have successfully been validated as accurate representations of the compressed air network of Mine-A.

With the validation of all three simulation models, it can be concluded that the method developed in this chapter can be used to create compressed air simulations. It can also be concluded that the developed method is able to create various degrees of complex simulation models accurately. One can therefore assume that a simulation accuracy of less than 5% can still be expected, even with limited data.

Chapter 4 Results



9

“You cannot teach a man anything, you can only help him discover it in himself” – Galileo

⁹ Adapted from Mapio [Online]. Available: <https://mapio.net/pic/p-67199139/> [Accessed: 04 August 2018].

4.1 Introduction

Simulation-A developed in Chapter 3 has a percentage difference of only 2.88% when compared with actual data. Because of the small error, Simulation-A is used as the benchmark simulation to represent Mine-A in this chapter. All comparisons are made using Simulation-A, which represents Mine-A.

The three simulation models developed in Chapter 3 vary in accuracy when compared with actual data. The direct impact of simplifying the models needs to be investigated. This chapter investigates the direct impact of simplifying a compressed air simulation model.

After the simulation models are validated as accurate representations of Mine-A, various scenarios need to be implemented. The scenarios are used to determine the effect that various changes to the system will have on the accuracy of the developed models. The scenarios are used to ensure that each simulation model remains valid.

An accuracy comparison between the compressor house outputs is investigated. This is done to investigate the accuracy of each component used to simulate the compressed air network.

The time and financial impact of reducing the simulation complexity are investigated. This is done to determine the reduction in project cost and time spent on simulation development.

Finally, the method developed in Chapter 3 is implemented on a different case study, namely, Mine-B. The case study is done to verify that the developed method can be used to identify the accuracy of other compressed air simulations.

.

4.2 Impact of the simulation complexity

4.2.1 Preamble

The simulation models were validated in the previous chapter after comparing the outputs of the three simulation models with actual mine data. This section discusses the direct impact that simplifying the simulation models has on the accuracies of the results. In this section, Simulation-B and Simulation-C developed in Chapter 3 are compared with Simulation-A. The comparison results identify the direct impact of simplifying the simulation models. The financial impact accompanied by the time spent to create each simulation model is also discussed.

4.2.2 Simulation accuracy

This section discusses the direct impact that simulation complexity has on simulation accuracy. Comparison accuracies depend on equipment calibration. Also, components do not operate at design specification, but are simulated as if they do. This can result in small comparison errors. Simulation-B and Simulation-C are compared with Simulation-A. Comparisons are made between the supply flow, power usage and supply pressure.

4.2.2.1 Simulation-A and Simulation-B baseline comparison

Figure 21 to Figure 23 compare the supply flows, power usage and supply pressure between Simulation-B and Simulation-A.

a) Daily supplied airflow

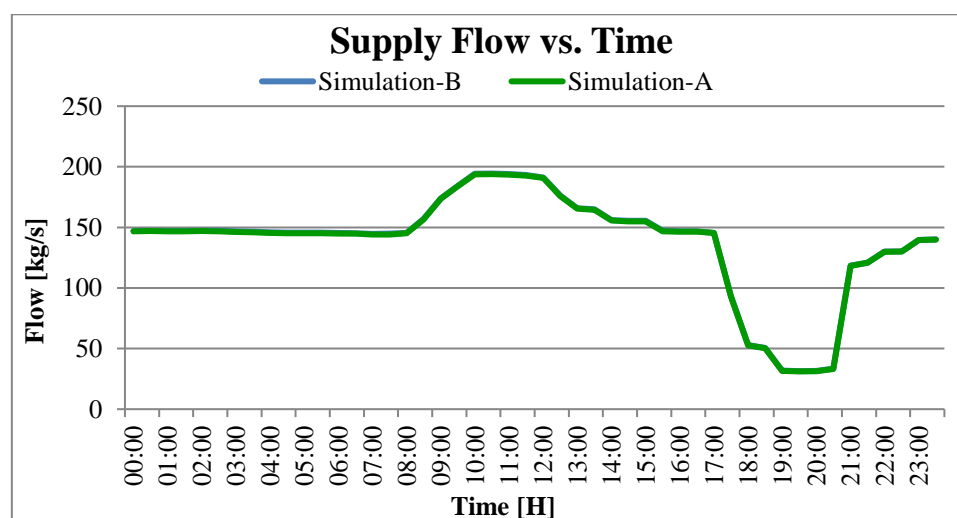


Figure 21: Simulation-B accuracy comparison – supply flow

As seen in Figure 21, Simulation-B data (represented by the near-invisible blue line) consistently follows a near-perfect trend that matches that of Simulation-A. The MAE percentage difference and total accuracy between the two data sets are tabulated in Table 16.

b) Daily power usage

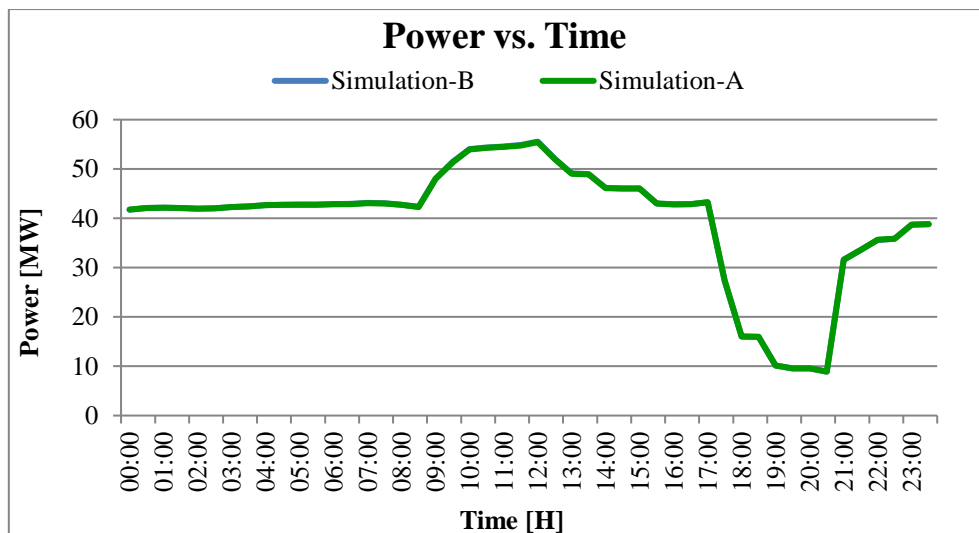


Figure 22: Simulation-B accuracy comparison – power usage

As seen in Figure 22, Simulation-B data again follows a near-perfect trend with Simulation-A. The MAE percentage difference and total accuracy between the two data sets are tabulated in Table 16.

c) Daily supply pressure

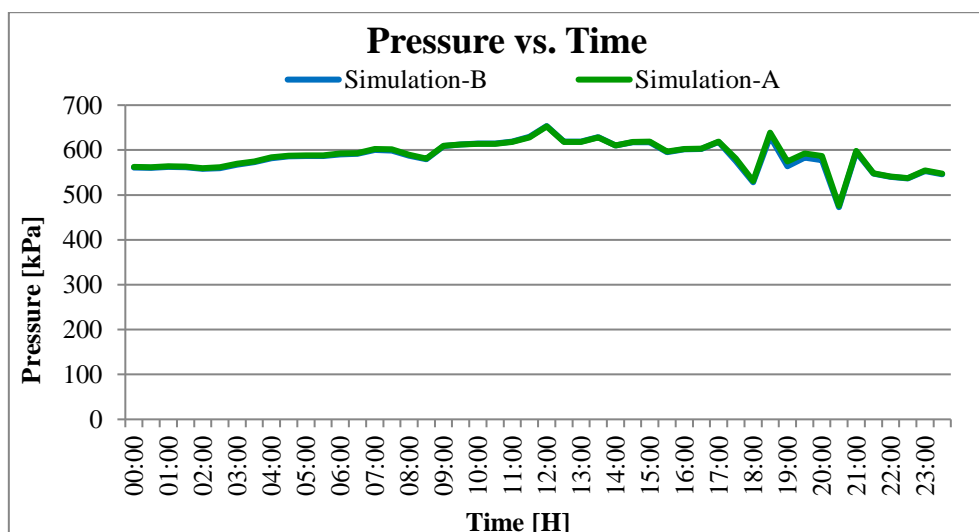


Figure 23: Simulation-B accuracy comparison – supply pressure

As seen in Figure 23, the two simulation models again follow a near identical trend. The MAE percentage difference and total accuracy between the two data sets are tabulated in Table 16.

Table 16: Simulation-B accuracy analysis

Description	Error [%]	Accuracy [%]
Supply flow vs. time	0.26	99.74
Power vs. time	0.10	99.90
Pressure vs. time	0.37	99.63

As seen in Table 16, Simulation-B has a maximum difference of only 0.37% when compared with Simulation-A. It can therefore be concluded that reducing a simulation model to Simulation-B has almost no effect on the accuracy of that model.

4.2.2.2 Simulation-A and Simulation-C baseline comparison

The same comparisons apply for Simulation-C as for Simulation-B. Figure 24 to Figure 26 illustrate these comparisons.

a) Daily supplied airflow

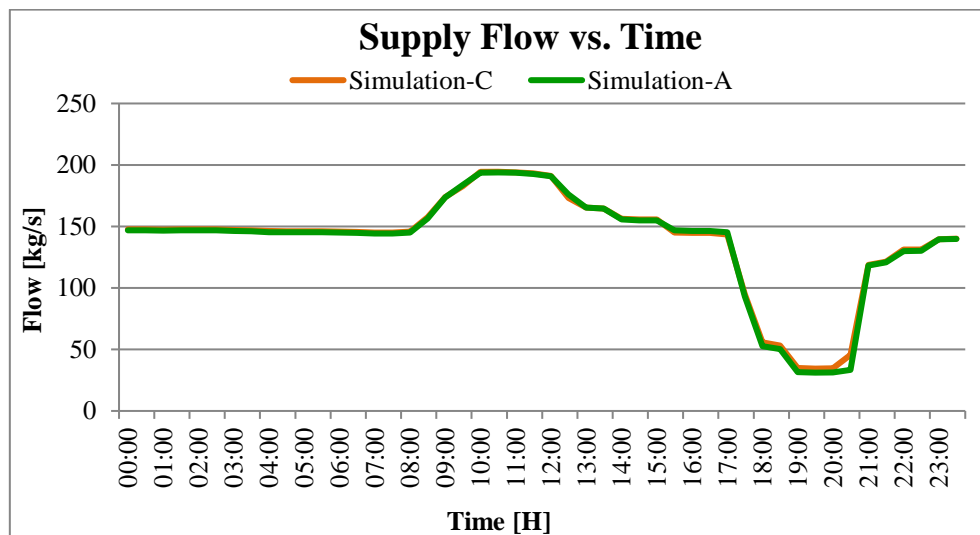


Figure 24: Simulation-C accuracy comparison – supply flow

As seen in Figure 24, Simulation-C data represented by the orange line consistently follows a trend that matches that of Simulation-A. The MAE percentage difference and total accuracy between the two data sets are tabulated in Table 17.

b) Daily power usage

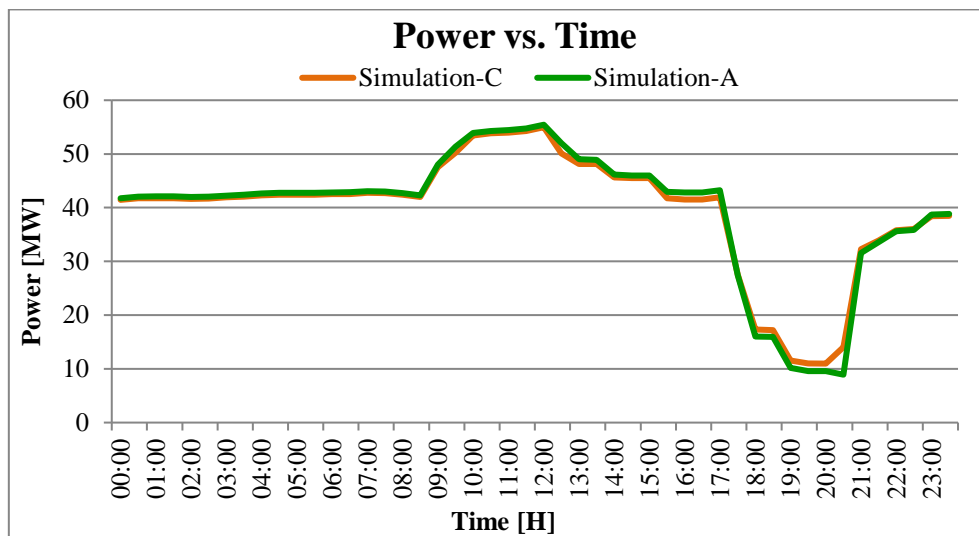


Figure 25: Simulation-C accuracy comparison – power usage

As seen in Figure 25, Simulation-C data again follows a consistent trend with Simulation-A. The MAE percentage difference and total accuracy between the two data sets are tabulated in Table 17.

c) Daily supply pressure

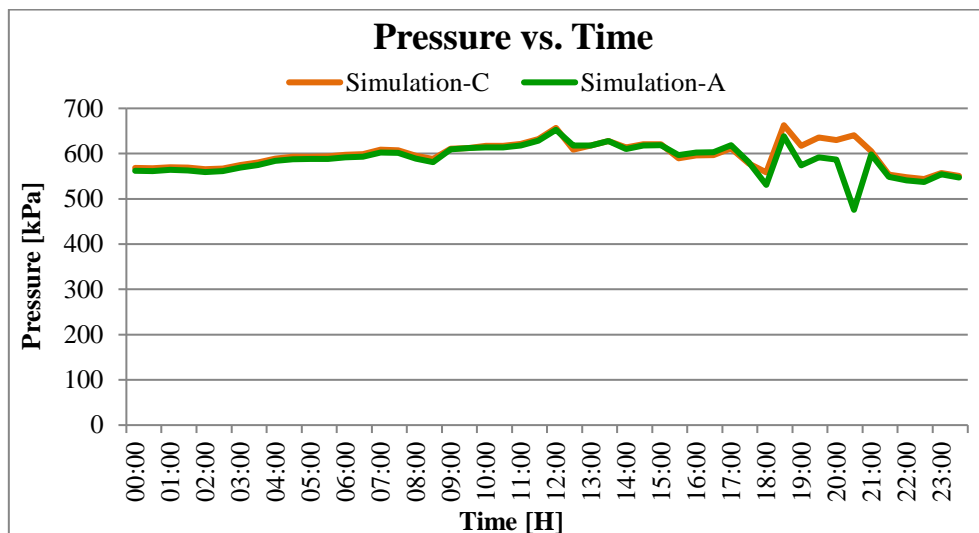


Figure 26: Simulation-C accuracy comparison – supply pressure

As seen in Figure 26, the two simulation models again follow a consistent comparison trend. The MAE percentage difference and total accuracy between the two data sets are tabulated in Table 17.

Table 17: Simulation-C accuracy analysis

Description	Error [%]	Accuracy [%]
Supply flow vs. time	1.92	98.08
Power vs. time	2.90	97.10
Pressure vs. time	1.86	98.14

As seen in Table 17, the maximum error of Simulation-C is only 2.90% when compared with Simulation-A. A total accuracy comparison of 97.10% was obtained. It can therefore be concluded that reducing the number of simulation components has a minimal effect on the accuracy of a compressed air simulation model.

4.3 Variation of probability parameters

4.3.1 Preamble

In this section, the variation of single parameters is brought forth to the three simulation models. This section compares the simulation models with the baseline simulation model after changes have been made to the parameters.

Each parameter described in this section is increased and decreased by 20%. This simulates the accuracy of all simulation models in the event of changes made to the compressed air network.

4.3.2 Simulated scenarios

The baselines for all three simulation models are validated as accurate representations of Mine-A in the preceding section. With these simulation models, one is able to impose various scenarios to determine the effect that changes would have on the accuracy of the simulation models. Descriptions of the various scenarios implemented on the simulation models of Mine-A as well as the reasons for these specific scenarios are discussed in this section.

a) Single probability parameters

Each simulation model underwent various scenarios in which one parameter was changed at a time. This was done to investigate the impact of that specific parameter on the simulation model. Table 18 lists the single probability parameters that were varied in all the simulation models.

Table 18: Single probability parameter variations

Scenario no.	Parameter
i	Supply pressure variation
ii	Airflow demand variation
iii	Pipe dimension variation

- i. By increasing or decreasing the supply pressure requirement, the compressors were forced to increase or decrease the amount of air supplied. This was done to simulate the effect of mines requiring an increase in supply pressure due to a lack of pressure underground. The change had an adverse effect on the power usage of the compressors as well as supplied flow with which to compare accuracies.

- ii. By increasing or decreasing the flow demand of all the shafts, the compressor was forced to maintain a supply pressure. This was done to mimic occurrences on a mine when the drilling shift is active and more air is demanded. The change in compressed airflow caused the supply pressure to fluctuate at the compressor discharge. This, in turn, caused the compressor power usage to increase or decrease to maintain a particular supply pressure.
- iii. By changing pipe dimensions, the changes that can occur regularly on mines as the mine network changes were simulated. It is therefore vital to be able to determine the effect changes to the pipe network will have on the accuracy of a simulation model.

b) Multiple probability parameters

The fourth and final simulation scenario is a combination of all parameters seen in Table 18. This is to determine the accuracy of all the simulation models under extreme circumstances. The motivation for the specific parameters remains the same as discussed previously.

4.3.3 Single probability parameter variation

As discussed previously, all parameters below were increased and decreased by 20%. Changes are made to a single parameter at a time. The simulation results are then compared with Simulation-A's results. The same conditions are applied to all simulation models, and comparisons are made based on the corresponding simulation scenario results. Table 19 to Table 26 indicate the percentage error comparisons between the simulated scenario and the corresponding Simulation-A scenario.

4.3.3.1 Flow demand

The compressed air flow demand was increased to simulate the effect of an expanding compressed air network. The more a network expands, the more compressed air is required. The compressed air flow demand was also decreased. The decrease in compressed air simulated the effect of the blasting shift when the compressed air rock drills are not in use.

Table 19 and Table 20 compare the result of increasing and decreasing the compressed air flow demand of the shafts in the compressed air network by 20%.

Table 19: Flow demand variation results – Simulation-B

Simulation-B	Baseline comparison error [%]	Increased flow comparison error [%]	Difference – increased flow [%]	Decreased flow comparison error [%]	Difference – decreased flow [%]
Flow	0.26	0.25	–0.01	0.27	+0.01
Power	0.10	0.20	+0.10	0.12	+0.02
Pressure	0.37	0.60	+0.23	0.23	–0.14

Table 19 indicates that neither an increase nor a decrease in compressed air flow demand had a considerable effect on the simulation accuracy. The simulation accuracy of Simulation-B decreased by a maximum of only 0.23% after increasing the compressed air flow demand.

Table 20: Flow demand variation results – Simulation-C

Simulation-C	Baseline comparison error [%]	Increased flow comparison error [%]	Difference – increased flow [%]	Decreased flow comparison error [%]	Difference – decreased flow [%]
Flow	1.92	2.06	+0.14	1.71	–0.21
Power	2.90	3.13	+0.23	2.68	–0.22
Pressure	1.86	1.90	+0.04	1.74	–0.12

Table 20 indicates that the percentage difference of Simulation-C increased by a maximum of only 0.23% after increasing the compressed air flow demand. However, after decreasing the compressed air flow demand, the simulation accuracy increased by a maximum of 0.22% and a minimum of 0.12%.

4.3.3.2 Compressor set points

Mines regularly adjust compressor set points to supply adequate compressed air pressures to the rock drills during the drilling shift. The set points are increased during drilling shifts and decreased during blasting shifts. The simulation compressor set points were increased and decreased to mimic these changes. However, the simulation model compressors were calibrated to deliver maximum flow. To increase the delivery pressure by 20%, a new baseline was therefore created for the increased supply pressure scenario.

Table 21 and Table 22 compare the result of increasing and decreasing the compressor set points of all compressors in the compressed air network by 20%.

Table 21: Compressor set point variation results – Simulation-B

Simulation-B	Baseline comparison error [%]	Increased set point comparison error [%]	Difference – increased set point [%]	Decreased set point comparison error [%]	Difference – decreased set point [%]
Flow	0.26	0.33	+0.07	0.46	+0.20
Power	0.10	0.19	+0.09	0.64	+0.54
Pressure	0.37	0.46	+0.09	0.13	–0.24

Table 21 indicates that the simulation accuracy for Simulation-B decreased by a maximum of only 0.54% when compared with the results of Simulation-A.

Table 22: Compressor set point variation results – Simulation-C

Simulation-C	Baseline comparison error [%]	Increased set point comparison error [%]	Difference – increased set point [%]	Decreased set point comparison error [%]	Difference – decreased set point [%]
Flow	1.92	1.72	–0.20	0.58	–1.34
Power	2.90	2.60	–0.30	1.84	–1.06
Pressure	1.86	1.67	–0.19	0.58	–1.28

Table 22 indicates that the simulation accuracy for Simulation-C increased by a maximum of 1.34% and a minimum of 0.19% when compared with Simulation-A.

4.3.3.3 Pipe dimensions

Although changes to pipe dimensions are not as frequent as previous parameters, they are still possible. Therefore, Table 23 and Table 24 compare the results of increasing and decreasing the pipe diameter of all pipe sections in the compressed air network by 20%.

Table 23: Pipe dimension variation results – Simulation-B

Simulation-B	Baseline comparison error [%]	Increased diameter comparison error [%]	Difference – increased diameter [%]	Decreased diameter comparison error [%]	Difference – decreased diameter [%]
Flow	0.26	0.13	–0.13	0.62	+0.36
Power	0.10	0.05	–0.05	0.15	+0.05
Pressure	0.37	0.19	–0.18	0.82	+0.45

Table 23 indicates that the simulation accuracy of Simulation-B increased by a maximum of 0.18% and a minimum of 0.05% when pipe diameter was increased. However, the simulation accuracy was decreased by a maximum of 0.45% when pipe diameter was decreased.

Table 24: Pipe dimension variation results – Simulation-C

Simulation-C	Baseline comparison error [%]	Increased diameter comparison error [%]	Difference – increased diameter [%]	Decreased diameter comparison error [%]	Difference – decreased diameter [%]
Flow	1.92	1.86	−0.06	2.07	+0.15
Power	2.90	2.99	+0.09	2.76	−0.14
Pressure	1.86	1.87	+0.01	1.87	+0.01

Table 24 indicates that the simulation accuracy of Simulation-C is decreased by a maximum of only 0.15% when compared with Simulation-A.

4.3.4 Multiple probability parameter variations

All the parameters that were varied in the previous section are now combined within this section. Changes are made simultaneously to all three parameters to determine the impact specific changes to parameters will have on the simulation model accuracies. The simulation results are then compared with those of Simulation-A that underwent the same parameter settings changes. The same conditions are applied to all simulation models, and comparisons are made to the corresponding Simulation-A scenario results.

Table 25 and Table 26 compare the result of increasing and decreasing multiple parameters in the compressed air network simultaneously by 20%.

Table 25: Multiple parameter variation results – Simulation-B

Simulation-B	Baseline comparison error [%]	Increased parameters comparison error [%]	Difference – increased parameters [%]	Decreased parameters comparison error [%]	Difference – decreased parameters [%]
Flow	0.26	0.12	−0.14	0.61	+0.35
Power	0.10	0.11	+0.01	0.29	+0.19
Pressure	0.37	0.30	−0.07	0.49	+0.12

Table 25 indicates that the simulation accuracy of Simulation-B decreased by a maximum of only 0.35% when compared with Simulation-A results.

Table 26: Multiple parameter variation results – Simulation-C

Simulation-C	Baseline comparison error [%]	Increased parameters comparison error [%]	Difference – increased parameters [%]	Decreased parameters comparison error [%]	Difference – decreased parameters [%]
Flow	1.92	2.01	+0.09	1.88	−0.04
Power	2.90	3.19	+0.29	2.52	−0.38
Pressure	1.86	1.93	+0.07	1.80	−0.06

Table 26 indicates that the simulation accuracy of Simulation-C decreased by a maximum of only 0.29% when compared with Simulation-A results.

4.4 Analyses of simulation accuracy

4.4.1 Preamble

This section analyses all the simulation model compressor houses. This is to determine the effect of various changes to the parameters, which were discussed previously, on various outputs. All simulations are compared with Simulation-A since it is an accurate representation of the compressed air network of Mine-A, as proven previously.

This section analyses the various compressor outputs of Simulation-B and Simulation-C and compares them with the outputs of Simulation-A. The supplied flow, power usage and supply pressure of each compressor in the various compressor houses are compared individually. This is done after the increase and decrease of 20% are implemented to the various parameters discussed in the previous section.

The comparisons identify the main contributors to the inaccuracies between the two simulation models in the total output comparisons. Descriptions of the compressor houses are given in the compressed air schematic layout seen in Figure 40 of Appendix D. All simulation comparisons discussed in this section are illustrated in Figure 52 to Figure 99 (Appendix I).

4.4.2 Simulation analysis

The simulated results are analysed to determine the accuracy of each individual compressor house contributing to the overall accuracy. The error of each compressor house is, therefore, investigated. A detailed analysis of the accuracies of the compressor houses is given in Appendix J.

Table 27 and Table 28 display the maximum simulated error for a single compressor house between the three developed models. The average error between all the compressor houses is also indicated. The inaccuracies are determined using the simulated scenarios discussed in Section 4.3.

Table 27: Simulation-B – Parameter variation accuracy comparison

Simulation-B	Maximum error [%]	Average error [%]
Flow demand variation	3.19	1.96
Supply pressure variation	248.77	33.76
Pipe dimension variation	4.11	1.92
Multiple parameter variation	3.02	1.65

As seen in Table 27, varying parameters such as flow demand, pipe diameters and multiple parameters results in a maximum average error of only 1.96%. Varying the supply pressure, however, results in an average error of 33.76%.

The reason for this, as discussed in Appendix J, is because of interconnecting pipes supplying compressed air from other compressor houses. The supply pressure of one compressor house is influenced because it receives a pressure increase from another. This is evident from the corresponding decreased supply pressure error of only 0.85% as seen in Table 44 of Appendix J.

Table 28: Simulation-C – Parameter variation accuracy comparison

Simulation-C	Maximum error [%]	Average error [%]
Flow demand variation	30.43	1.56
Supply pressure variation	48.03	1.68
Pipe dimension variation	30.31	1.71
Multiple parameter variation	30.61	1.74

As seen in Table 28, the maximum error of all the parameters is 48.03%. This again is caused by the interconnecting pipes allowing compressed air from one compressor house to another. The average error, therefore, only results in a maximum error of 1.74%.

4.4.3 Simulation comparison analysis

Upon investigating the simulations, it was found that the percentage errors for Simulation-B and Simulation-C were within acceptable range. There were, however, individual components that differed with higher percentage errors. The compressor houses that caused the increase in percentage difference were consistent throughout the scenarios.

The higher percentage error of Simulation-B, when compared with Simulation-C, can be attributed to the way PTB calculates the simulation response. Larger compressors used in Simulation-C distribute air differently than those of Simulation-B. It is, therefore, important to compare the average simulation errors.

a) Simulation-B: Highest percentage errors

Throughout all the simulation scenarios, the compressor house CH14# resulted in the highest error for all scenarios. This is, however, if the percentage error of the outlying results of compressor CH7# is neglected. The percentage error of compressor house CH14# can be attributed to the VK50 compressor used in CH14#.

As discussed in the previous chapter, the VK50 compressor is the higher rated compressor of the two types used. The higher rated compressor delivers higher flow rates at similar pressures than the VK32 compressor. This results in higher or lower flow rates than expected if the compressor is marginally calibrated incorrectly.

It is evident from the results that the sensitivity of the higher rated compressor is higher than that of the smaller compressor. The compressor sensitivity, however, does not influence the simulation accuracies enough to have an impact on the simulation outputs as the maximum average error is only 1.96%.

b) Simulation-C: Highest percentage errors

The outlying results of the supply pressure variation are again neglected from the high percentage error analysis as discussed earlier. As described in Appendix J, the high percentage errors achieved on Simulation-C's compressor houses are a result of the low flow rates of compressor house CHCentral#.

CHCentral# contributes 3.84% of the total flow of the compressed air network of Mine-A. It is evident in the simulation comparison that, if the average flow rate of CHCentral# differs by only 1 kg/s, the result for the compressor house is an error of over 30%. Thus, it is essential to compare the entire network. Doing so results in a maximum average percentage difference of only 1.74%.

4.4.4 Time and financial impact of simulation complexity

a) Financial impact

The time it takes to create a simulation is an important factor in the industry. It determines how quickly the simulation model can be used to make any financial or energy savings. It is, therefore, essential to understand the impact of the time it takes to create more detailed simulation models instead of simplified versions. Table 29 indicates the time spent on travel, data gathering, development and calibration of the simulation models used in this study. The financial impact is calculated according to productive work hours at an engineering consultation tariff of R800 per hour.

Table 29: Financial impact of simulation complexity

Simulation model	Time [H]	Engineering tariff [R/h]*	Total cost [R]
Simulation-A	168	800	134 400
Simulation-B	118	800	94 400
Simulation-C	64	800	51 200

*Consultation tariffs may vary

Table 29 displays how the cost of creating a simulation model decreases drastically as the simulation complexity decreases. The time it takes to create a simplified simulation model (Simulation-C) is less than half the times it takes to create a detailed simulation model (Simulation-A). In this study, the cost to create a simplified simulation model is R51 200 instead of R134 400, as for a detailed simulation model. This results in a financial saving of R83 200 for the simulation of Mine-A.

b) Impact on simulation time

Table 30 displays the total number of components used in the three compressed air simulation models. As seen in Table 30, Simulation-A has 261 different components. Simulation-C has 157 different components, which is 104 fewer components than Simulation-A.

Table 30: Simulation component count comparison

Description	Simulation-A	Simulation-B	Simulation-C
Compressor	19	19	10
Air pipe	97	74	55
Air demand	9	9	9
Air nodes	86	73	54
Flow controller (proportional and integral)	19	19	10
Air pressure boundary	31	26	19
Total	261	220	157

Simulation time is also a determining factor. The more complex the simulation, the longer it takes. Simulation time is highly dependent on the size of the simulation model, as well as the simulation software that has been selected. Table 31 displays how fast the simplified versions (i.e. Simulation-B and Simulation-C) of Simulation-A can simulate relative to Simulation-A.

Table 31: Impact of simulation complexity on simulation speed

Simulation model	Time [s]	Percentage faster [%]
Simulation-A	37	—
Simulation-B	28	24.3
Simulation-C	19	48.6

Table 31 displays how the simulation time is reduced as the simulation model complexity is reduced. Simulation-B resulted in a 24.3% faster simulation time. Simulation-C resulted in a 48.6% faster simulation time.

4.5 Verification of simulation accuracy

4.5.1 Preamble

In previous sections of this chapter, detailed results comparisons were analysed to determine simulation differences based on individual component outputs. The components of the initial simulation model used to develop the method of this study were compared. To verify the method, it must be implemented on a different case study.

This section applies the developed method to a different mine, Mine-B. The method will be used to predict the expected simulation accuracy based on the available data of Mine-B.

4.5.2 Simulation development

The method developed in Chapter 3 is used to develop the simulation model of Mine-B. Table 32 displays a summary of the developed method used to create the simulation model.

Table 32: Summary of simulation development method

Phase	Description
A	Network analysis
B	Development of models
C	Validation of models

a) Network analysis

The compressed air network of Mine-B was investigated to obtain knowledge of the system. Figure 27 illustrates a layout of Mine-B along with the total number of compressors and pipe section details.

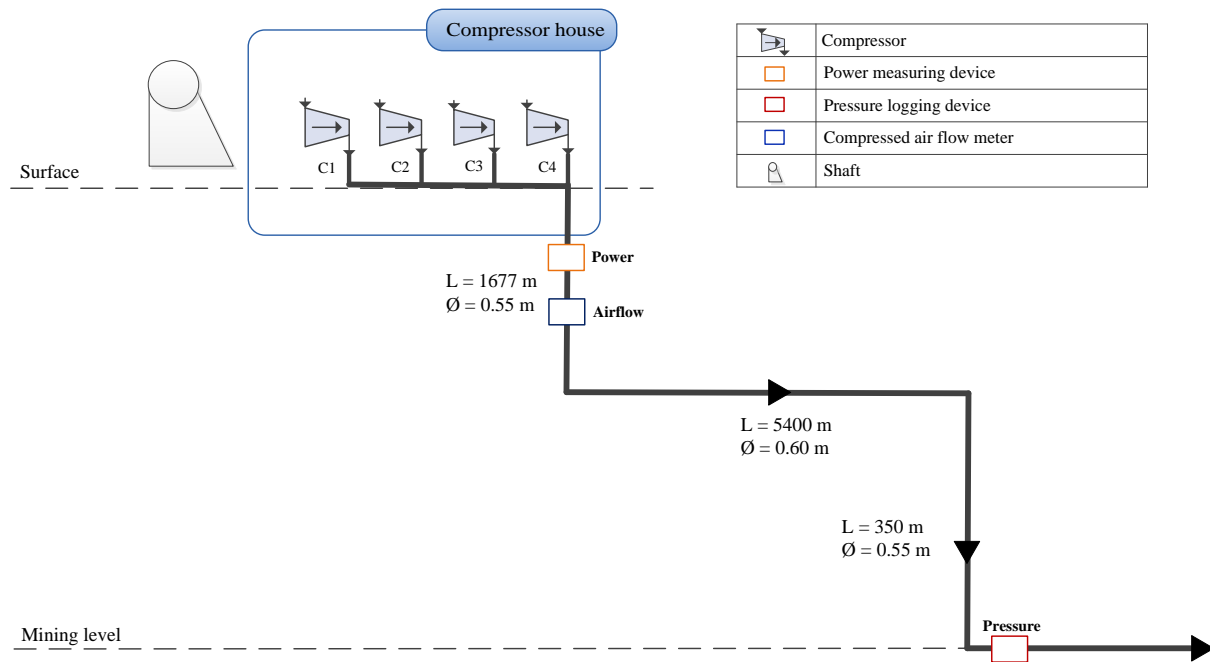


Figure 27: Mine-B compressed air layout

Upon investigating the installed instrumentation of Mine-B, it is evident that there is a shortage of monitoring devices. The compressor house is monitored by one power and one airflow measuring device. The delivery pressure is also measured at the intake of the underground mining level.

Following the method developed in Chapter 3, the type of simulation model one is able to create is determined. Using this method allows the expected simulation accuracy to be predicted. The method discussed is followed as shown in Figure 28.

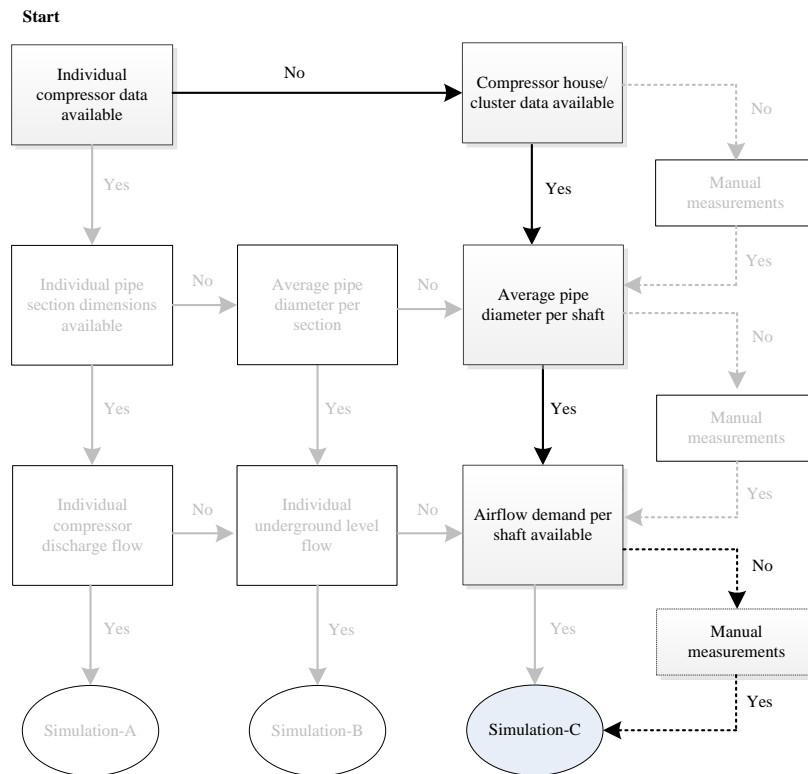


Figure 28: Mine-B simulation identification

As indicated by the process followed in Figure 28, the simulation model to be created is Simulation-C. This simulation model uses the least amount of input data. Therefore, the layout can be simplified as illustrated in Figure 29. The simulation model, as predicted in Chapter 3, is expected to achieve a simulation accuracy of roughly 4.87% when compared with actual data.

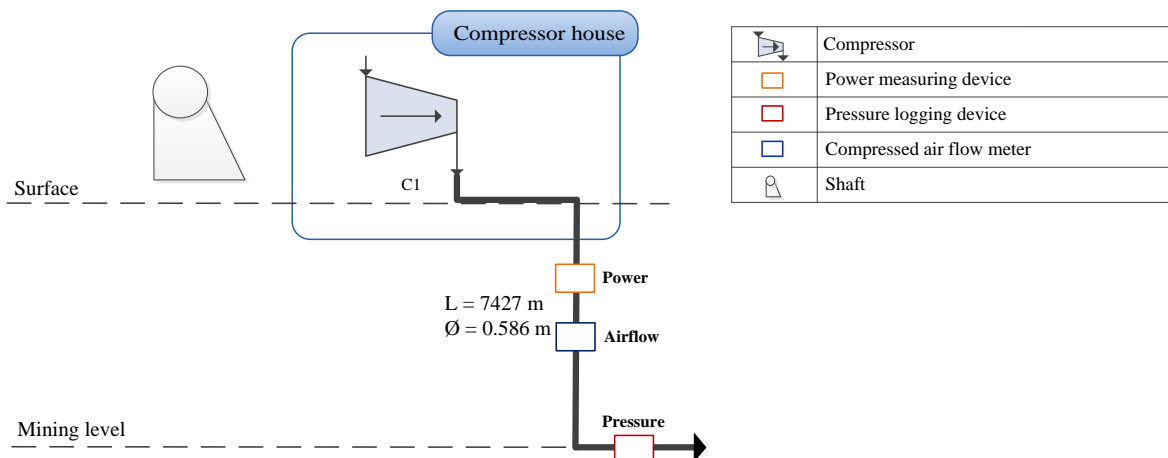


Figure 29: Mine-B simplified compressed air layout

The purpose of the simulation model is to achieve the desired mining level pressure while ensuring that the power usage and airflow match that of Mine-B.

b) Development of models

The necessary data for simulating Mine-B was obtained directly from the online server of Mine-B. Data for a 24-hour period was obtained for 7 May 2018. Data for the power usage, compressor flow and mining level pressure was obtained. Details of the 24-hour time raw data points are illustrated in Table 50 (Appendix K).

The data, along with the layout seen in Figure 29, was used to create the simulation model of Mine-B. The simulation model, illustrated in Figure 30, was set to deliver the required mining level pressure to the end users.

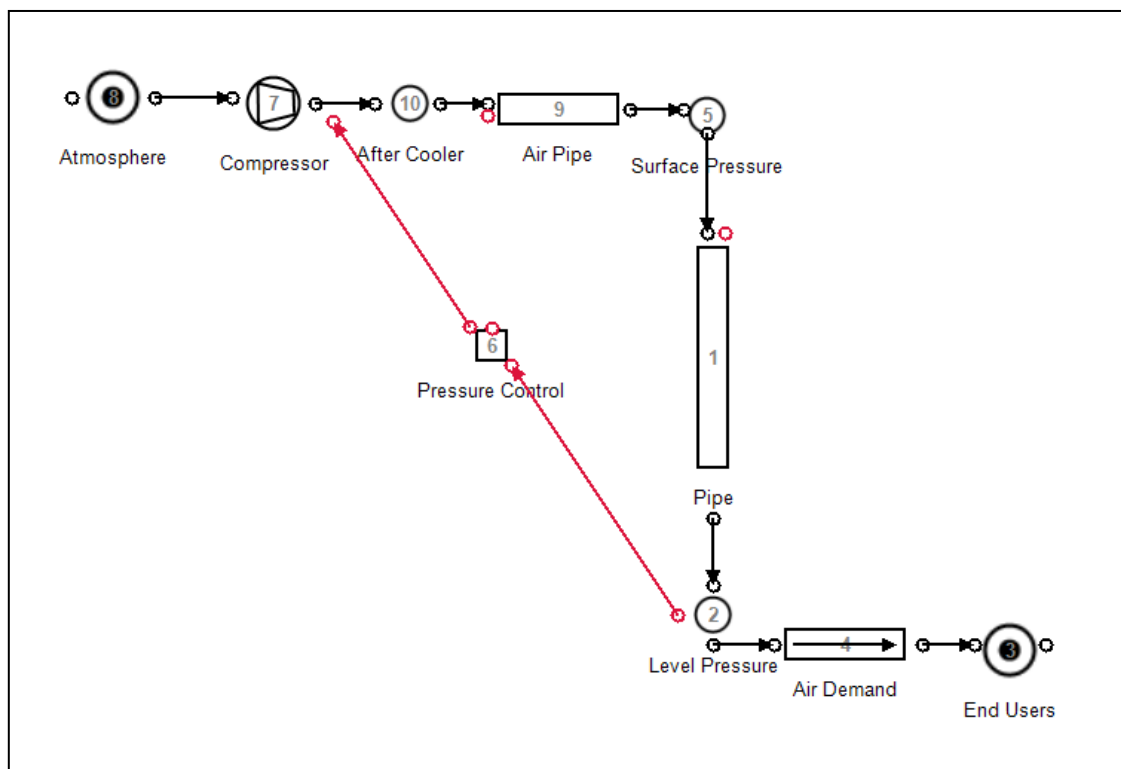


Figure 30: Mine-B simulation model

c) Validation of model

To validate the simulation model of Mine-B, a 24-hour profile comparison for data of 7 May 2018 is made. Comparisons are made between the power usage, compressed air flow, and mining level pressure. Figure 31, Figure 32, and Figure 33 display the comparison between actual data and simulated data. The 24-hour simulated and actual data are illustrated in Table 51, Table 52, and Table 53 in Appendix K.

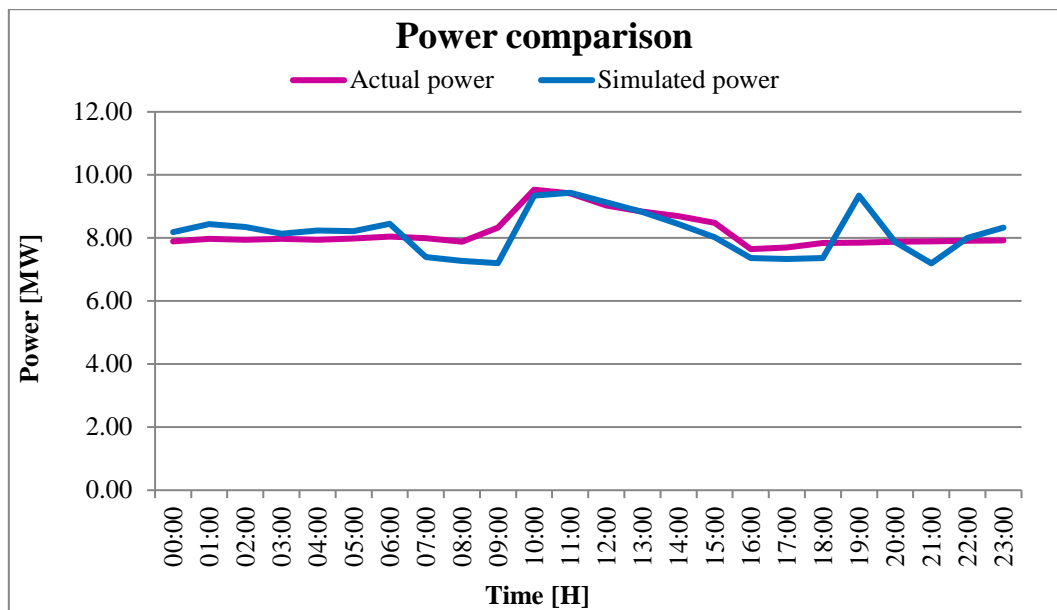


Figure 31: Mine-B power usage comparison

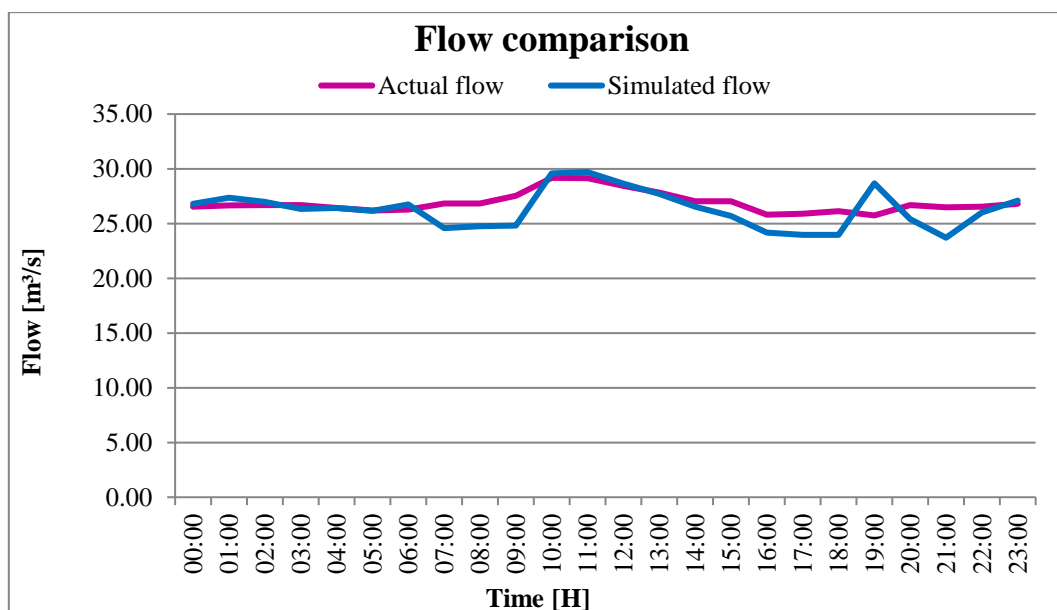


Figure 32: Mine-B compressor flow comparison

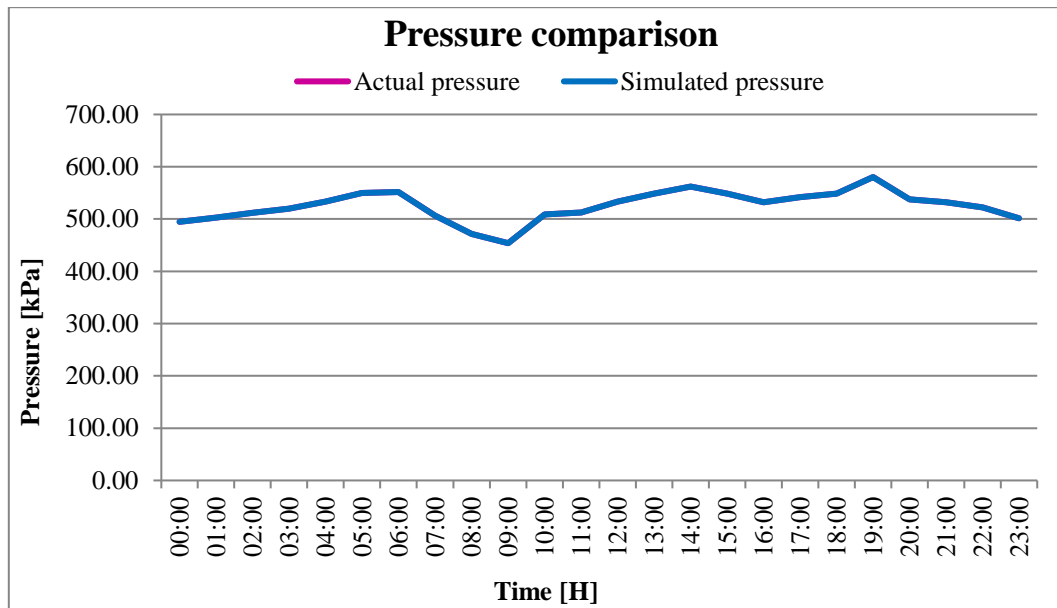


Figure 33: Mine-B level pressure comparison

The power usage and compressed air flow comparisons, as seen in Figure 31 and Figure 32 respectively, follow a consistent trend with actual data. Figure 33 shows that the mining level pressure, as instructed by PTB, was replicated perfectly to represent the pressure conditions underground. The percentage errors between the simulated values and actual data, given in Appendix K, are summarised in Table 33.

Table 33: Mine-B validation comparison

Parameter	Percentage error [%]
Power usage	4.94
Compressor flow	4.24
Level pressure	0

The percentage errors seen in Table 33 are well below the recommended 9% as previously determined. The current errors are a result of the lack of mine data available as proven in the method development. Thus, the simulation model has successfully been calibrated to represent the compressed air network of Mine-B accurately.

Table 33 shows that the maximum percentage error is 4.94%. The method developed in Chapter 3 determined that Simulation-C type models can expect an error of 4.87%. This results in a 99.93% accuracy between the developed error prediction for Mine-A and the case study error of Mine-B. The comparisons in this section, therefore, verify the method developed in Chapter 3.

4.6 Summary

The impact on simulation accuracy after simplifying a highly detailed simulation model was investigated. The baseline model of Simulation-B was calibrated to within 99.63% accuracy when compared with Simulation-A. Simulation-C was calibrated to within 97.10% accuracy when compared with Simulation-A. From the high simulation accuracies, it was concluded that simplifying a detailed simulation model has a minimal effect on the accuracy of the baseline simulation models.

An analysis was conducted to ensure that the simplified baseline simulation models could be used to predict outcomes of various system changes accurately. The compressed air flow demand, compressor power usage and compressor supply pressure were varied and compared. It was found that the maximum decrease in simulation accuracy was only 0.54% for simplified versions of Simulation-A. Thus, both Simulation-B and Simulation-C were able to accurately determine the effect of various changes to the compressed air network.

Upon investigation of the individual compressor house outputs, it was found that the delivery flow varied for individual compressors within the simulation model. This, however, was a result of the simulation model being set to deliver or maintain a delivery pressure within an interconnecting pipe network. One compressor house could, therefore, supply compressed air to another during the implementation of various scenarios, resulting in higher than expected percentage errors. The total flow, total power, and total average supply pressure, however, remained within high percentage accuracies as discussed previously.

By simplifying the simulation models, the time spent developing the models could be reduced drastically. The simulation running time was also reduced by 48.6%. A reduction in time reduces the cost of creating these simulation models. Reducing the simulation complexity does not compromise the accuracy of the models. Simplified simulations are therefore ideal to use for mine compressed air systems.

The method developed in Chapter 3 was implemented on a different case study: Mine-B. The method identified Mine-B as a mine with limited monitoring instrumentation, resulting in Simulation-C model being used. The developed method predicted the simulation accuracy to be 4.87%. The actual accuracy of Mine-B was 4.94%. This resulted in a 99.93% accuracy between the developed method and the implementation thereof on Mine-B. The high accuracy between the two case studies verifies the accuracy of the developed method.

Chapter 5 Conclusion



10

“If I have seen further, it is by standing on the shoulders of giants” – Isaac Newton

¹⁰ Adapted from Daily Mail [Online]. Available: <http://www.dailymail.co.uk/wires/ap/article-3600913/South-Africa-Miners-lung-disease-prepare-lawsuit.html> [Accessed: 04 August 2018].

5.1 Study limitations

This study focused on the compressed air distribution of an interconnected surface compressed air network. The surface network is vast in size and complicated. It is, therefore, easy to make dimension errors when determining the simulation input values. This can lead to inaccuracies when comparing simulated data with actual data.

Monitoring systems in the mining industry regularly make data logging errors. This, in turn, creates missing or unreliable data. When simulating a compressed air network, it is essential that data sets be complete and trustworthy. Within this study, the data of both the compressed air flow and power usage was of good quality. The compressed air pressures at various times, however, had missing and irregular data.

5.2 Recommendations

This study indicated the accuracy of a simulation model when data availability was limited. It also indicated that, when creating a simulation model using limited data, it could be done in a reduced amount of time. It is recommended that further research be done on the exact amount of time saved creating simplified simulation models. This will serve as an indication of how much time can be saved by creating simplified rather than detailed simulations.

This study discussed the amount of time spent creating simulation models of a surface compressed air network. The amount of time spent creating these simulation models was limited to one case study. Thus, the financial impact that this has on an engineering firm cannot be determined accurately. It is therefore recommended that the direct financial impact of simplified simulation models be investigated further.

5.3 Conclusion

As stated in the scope of work, the impact simulation complexity has on simulation accuracy was successfully analysed.

Comprehensive literature surveys were done to investigate the best approach to create compressed air simulation models. Strengths and shortcomings from various past research were identified. The shortcomings created the need to develop a detailed process applicable to this study. The strengths of past compressed air simulation studies were used to develop the simulation process within this study. A process was successfully developed to create compressed air simulation models.

The process was used to develop three compressed air simulation models successfully. Data from Mine-A was used to create a highly complex compressed air simulation model. After the complex simulation was created, the model was simplified by reducing the number of simulation components. The components were reduced to represent a mine with limited data available. The three simulation models, therefore, each vary in complexity. The variation in complexity was used to determine the accuracy of the models when data availability varied.

A method was successfully developed that enabled the type of simulation model to be identified. The method identified the complexity of a simulation based on the total available data. The three simulation models, labelled Simulation-A, Simulation-B, and Simulation-C, were identified in the method. Each succeeding simulation was a simplified version of the preceding simulation model. The three developed models each represented one of the three identified simulation types. The three simulation types, therefore, had an accuracy variation because of the variation in simulation complexity.

The developed method was able to identify the expected accuracy of the three simulation types successfully. This was done by using the results of the three developed simulation models. The maximum errors of the simulation power consumption, supply flow and supply pressure were investigated. It was found that the maximum error for Simulation-A was 2.88%, for Simulation-B 4.50%, and for Simulation-C 4.87%. It could, therefore, be concluded that an accurate compressed air simulation model can be calibrated with limited available data.

Simulation-A was regarded as an accurate representation of Mine-A. Scenarios could be implemented on all three simulation types (Simulation-A, Simulation-B and Simulation-C). The results of the simplified models (Simulation-B and Simulation-C) were compared with the results of Simulation-A. The comparison between the simplified models and Simulation-A resulted in a maximum error increase of only 3.19%. It could, therefore, be concluded that simplified models can undergo various system changes without compromising on simulation accuracy.

Finally, the method developed to identify the simulation type (Simulation-A, Simulation-B and Simulation-C) was implemented on a different case study, namely, Mine-B. The method identified the simulation type as a Simulation-C type model. The expected simulation accuracy for a Simulation-C type model, as obtained from Mine-A, was 4.87%. After following the process to develop compressed air simulation models, an error of 4.94% was achieved when compared with actual mine data. It could be concluded that the method can accurately determine the type and expected accuracy of compressed air simulation models. It could further be concluded that simplified models can simulate compressed air systems accurately.

The simplified compressed air simulations for both case studies indicated that less complex models can simulate mine compressed air systems accurately. It could, therefore, be concluded that simulation accuracy is not surrendered when simplified simulation models are developed.

Chapter 6 References

- [1] J. H. Marais, “An integrated approach to optimise energy consumption of mine compressed air systems,” Ph.D. Eng. thesis, North-West University, Potchefstroom, South Africa, 2012.
- [2] B. G. Pollet, I. Staffell, and K. Adamson, “Current energy landscape in the Republic of South Africa,” *International Journal of Hydrogen Energy*, vol. 40, no. 46, pp. 16685–16701, October 2015.
- [3] D. Struhs, “Towards an energy efficient mining sector,” 2010. [Online]. Available: http://www.eskom.co.za/sites/idm/Documents/121040ESKD_Mining_Brochure_paths.pdf. [Accessed: 27 April 2018].
- [4] P. Eret, “A cost-effective compressed air generation for manufacturing using modified microturbines,” *Applied Thermal Engineering*, vol. 107, pp. 311–319, June 2016.
- [5] G. P. Heyns, “Challenges faced during implementation of a compressed air energy savings project on a gold mine,” M. Eng. dissertation, North-West University, Potchefstroom, South Africa, 2014.
- [6] R. Saidur, N. A. Rahim, and M. Hasanuzzaman, “A review on compressed-air energy use and energy savings,” *Renewable and Sustainable Energy Reviews*, vol. 14, no. 4, pp. 1135–1153, 2010.
- [7] J. I. G. Bredenkamp, A. J. Schutte, and J. F. van Rensburg, “Challenges faced during implementation of a compressed air energy savings project on a gold mine,” in *Proceedings of the 12th Conference on the Industrial and Commercial Use of Energy (ICUE)*, Cape Town, South Africa, 2015.

- [8] R. Boehm and J. Franke, "Demand-side-management by flexible generation of compressed air," *The 50th CIRP Conference on Manufacturing Systems*, vol. 63, pp. 195–200, 2017.
- [9] C. Guo et al., "Performance analysis of compressed air energy storage systems considering dynamic characteristics of compressed air storage," *Energy*, vol. 135, pp. 876–888, 2017.
- [10] G. Popovics and L. Monostori, "An approach to determine simulation model complexity," *Changeable, Agile, Reconfigurable and Virtual Production*, vol. 52, pp. 257–261, 2016.
- [11] J. I. G. Bredenkamp, "Reconfiguring mining compressed air networks for cost savings," M. Eng. dissertation, North-West University, Potchefstroom, South Africa, 2014.
- [12] J. Jonker, "Automated mine compressed air control for sustainable savings," M. Eng. dissertation, North-West University, Potchefstroom, South Africa, 2016.
- [13] J. H. Marais, M. Kleingeld, and J. F. van Rensburg, "Simplification of mine compressed air systems," in *Proceedings of the 10th Conference on the Industrial and Commercial Use of Energy (ICUE)*, Cape Town, South Africa, 2013.
- [14] C. Cilliers, "Benchmarking electricity use of deep-level mines," Ph.D. Eng. thesis, North-West University, Potchefstroom, South Africa, 2015.
- [15] R. Joubert, "Cost and time effective DSM on mine compressed air systems," M. Eng. dissertation, North-West University, Potchefstroom, South Africa, 2010.
- [16] W. Booysen, "Reducing energy consumption on RSA mines through optimised compressor control," M. Eng. dissertation, North-West University, Potchefstroom, South Africa, 2010.
- [17] L. Meng, Y. D. Jiang, Y. Zhao, R. Shan, and Y. Song, "Probing into design of refuge chamber system in coal mine," *Procedia Engineering*, vol. 26, pp. 2334–2341, 2011.

- [18] B. Zhang, W. Zhao, W. Wang, and X. Zhang, "Pressure characteristics and dynamic response of coal mine refuge chamber with underground gas explosion," *Journal of Loss Prevention in the Process Industries*, vol. 30, no. 1, pp. 37–46, March 2014.
- [19] Z. Zhang, Y. Yuan, and K. Wang, "Effects of number and layout of air purification devices in mine refuge chamber," *Process Safety and Environmental Protection*, vol. 105, pp. 338–347, December 2016.
- [20] Y. Zhe, J. Longzhe, and W. Shu, "Study and analysis of human survival parameters in mine refuge station," *The Open Civil Engineering Journal*, vol. 9, no. 1, pp. 650–656, August 2015.
- [21] H. Shao, P. F. Li, and X. M. Shi, "Experimental study of the gas leakage and optimized supply of oxygen in coal mine refuge chamber," *Procedia Engineering*, vol. 211, pp. 599–605, 2018.
- [22] D. Rempel, A. Antonucci, A. Barr, M. R. Cooper, B. Martin, and R. L. Neitzel, "Pneumatic rock drill vs. electric rotary hammer drill: Productivity, vibration, dust, and noise when drilling into concrete," *Applied Ergonomics*, vol. 74, pp. 31–36, August 2018.
- [23] K. Wallace, B. Prosser, and J. D. Stinnette, "The practice of mine ventilation engineering," *International Journal of Mining Science and Technology*, vol. 25, no. 2, pp. 165–169, October 2014.
- [24] Republic of South Africa, "Mine health and safety act (no. 29 of 1996)," *Government Gazette*, vol. 372, no. 17242, 14 June 1996.
- [25] A. J. M. van Tonder, "Sustaining compressed air DSM project savings using an air leakage management system," in *Proceedings of the 8th Conference on the Industrial and Commercial Use of Energy (ICUE)*, Cape Town, South Africa, 2011.

- [26] R. Kuffel, P. Forsyth, and C. Peters, “The role and importance of real time digital simulation in the development and testing of power system control and protection equipment,” *International Federation of Automatic Control (IFAC) Conference Paper Archive*, vol. 49, no. 27, pp. 178–182, 2016.
- [27] G. E. du Plessis, D. C. Arndt, and E. H. Mathews, “The development and integrated simulation of a variable water flow energy saving strategy for deep-mine cooling systems,” *Sustainable Energy Technologies and Assessments*, vol. 10, pp. 71–78, March 2015.
- [28] J. Fan, R. Stewart, and T. Xu, “Simulation accuracy of crack-tip parameters with extended GP methods,” *Engineering Fracture Mechanics*, vol. 170, pp. 87–106, November 2016.
- [29] P. Maré, “Improved implementation strategies to sustain energy saving measures on mine cooling systems,” M. Eng. dissertation, North-West University, Potchefstroom, South Africa, 2014.
- [30] J. F. van Rensburg, M. F. Geyser, M. Kleingeld, and E. H. Mathews, “Developing Esco procedures for large telecommunication facilities using novel simulation techniques,” in *Proceedings of the 4th Conference on the Industrial and Commercial Use of Energy (ICUE)*, Cape Town, South Africa, 2007.
- [31] S. P. Upadhyay and H. Askari-Nasab, “Simulation and optimization approach for uncertainty-based short-term planning in open pit mines,” *International Journal of Mining Science and Technology*, vol. 28, no. 2, pp. 153–166, February 2017.
- [32] B. M. Friedenstein, “Simulating operational improvements on mine compressed air systems,” M. Eng. dissertation, North-West University, Potchefstroom, South Africa, 2017.
- [33] J. I. G. Bredenkamp, L. F. van der Zee, and J. F. van Rensburg, “Reconfiguring mining compressed air networks for cost savings,” in *Proceedings of the 11th Conference on the Industrial and Commercial Use of Energy (ICUE)*, Cape Town, South Africa, 2014.

- [34] A. M. Holman, G. P. Heyns, and R. Pelzer, “Benefits of improved performance monitoring of mine cooling systems,” in *Proceedings of the 11th Conference on the Industrial and Commercial Use of Energy (ICUE)*, Cape Town, South Africa, 2014.
- [35] O. Gölbaşı and N. Demirel, “A cost-effective simulation algorithm for inspection interval optimization: An application to mining equipment,” *Computers & Industrial Engineering*, vol. 113, pp. 525–540, September 2017.
- [36] B. Bartın, K. Ozbay, J. Gao, and A. Kurkcu, “Calibration and validation of large-scale traffic simulation networks: A case study,” *The 7th International Workshop on Agent-based Mobility, Traffic and Transportation Models, Methodologies and Applications*, vol. 130, no. 1, pp. 844–849, 2018.
- [37] H. Zou, C. Li, M. Tang, M. Wang, and C. Tian, “Online measuring method and dynamic characteristics of gas kinetic parameters of linear compressor,” *Measurement*, vol. 125, pp. 545–553, May 2018.
- [38] G. G. Jacobs and L. Liebenberg, “The influence of timed coolant injection on compressor efficiency,” *Sustainable Energy Technologies and Assessments*, vol. 18, pp. 175–189, October 2016.
- [39] R. E. Sonntag and C. Borgnakke. 2008. *Fundamentals of Thermodynamics*, 6th ed. Ann Arbor, MI: John Wiley & Sons.
- [40] H. P. R. Joubert, G. Bolt, and J. F. van Rensburg, “Energy savings on mining compressed air networks through dedicated process plant compressors,” in *Proceedings of the 9th Conference on the Industrial and Commercial Use of Energy (ICUE)*, Cape Town, South Africa, 2012.

- [41] A. Kneer, M. Wirtz, T. Laufer, B. Nestler, and S. Barbe, “Experimental investigations on pressure loss and heat transfer of two-phase carbon dioxide flow in a horizontal circular pipe of 0.4 mm diameter,” *International Journal of Heat and Mass Transfer*, vol. 119, pp. 828–840, November 2017.
- [42] T. Haktanir and M. Ardiçlioğlu, “Numerical modeling of Darcy–Weisbach friction factor and branching pipes problem,” *Advances in Engineering Software*, vol. 35, no. 12, pp. 773–779, August 2004.
- [43] K. Huang, J. W. Wan, C. X. Chen, Y. Q. Li, D. F. Mao, and M. Y. Zhang, “Experimental investigation on friction factor in pipes with large roughness,” *Experimental Thermal and Fluid Science*, vol. 50, pp. 147–153, June 2013.
- [44] E. Shashi Menon. 2005. Gas Pipeline Hydraulics, 2nd ed. Broken Sound Parkway, NY: Taylor & Francis.
- [45] J. Venter, “Development of a dynamic centrifugal compressor selector for large compressed air networks in the mining industry,” M. Eng. dissertation, North-West University, Potchefstroom, South Africa, 2012.
- [46] W. Bornman, J. Dirker, D. C. Arndt, and J. P. Meyer, “Integrated energy simulation of a deep level mine cooling system through a combination of forward and first-principle models applied to system-side parameters,” *Applied Thermal Engineering*, vol. 123, pp. 1166–1180, May 2017.
- [47] Y. Luo et al., “Building integrated photovoltaic thermoelectric wall system: Balancing simulation speed and accuracy,” in *Proceedings of the 8th International Conference on Applied Energy (ICAE)*, Beijing, China, 2016.

- [48] Y. Alomair, I. Ahmad, and A. Alghamdi, “A review of evaluation methods and techniques for simulation packages,” *The 2015 International Conference on Soft Computing and Software Engineering*, vol. 62, pp. 249–256, 2015.
- [49] A. J. M. van Tonder, “Automation of compressor networks through a dynamic control system,” Ph.D. Eng. dissertation, North-West University, Potchefstroom, South Africa, 2014.
- [50] J. H. Marais, E. H. Mathews, and R. Pelzer, “Analysing DSM opportunities on mine conveyor systems,” in *Proceedings of the 5th Conference on the Industrial and Commercial Use of Energy (ICUE)*, Cape Town, South Africa, 2008.
- [51] W. van Niekerk, “The value of simulation models for mine DSM projects,” M. Eng. dissertation, North-West University, Potchefstroom, South Africa, 2013.
- [52] M. Kleingeld and W. van Niekerk, “The value of simulation models for mine DSM projects,” in *Proceedings of the 10th Conference on the Industrial and Commercial Use of Energy (ICUE)*, Cape Town, South Africa, 2013.
- [53] F. Xiao, “Unified formulation for compressible and incompressible flows by using multi-integrated moments I: One-dimensional inviscid compressible flow,” *Journal of Computational Physics*, vol. 195, no. 2, pp. 629–654, October 2003.
- [54] W. Jiang, J. Khan, and R. A. Dougal, “Dynamic centrifugal compressor model for system simulation,” *Journal of Power Science*, vol. 158, no. 2, pp. 1333–1343, December 2005.
- [55] P. Maré, J. I. G. Bredenkamp, and J. H. Marais, “Evaluating compressed air operational improvements on a deep-level mine through simulations,” in *Proceedings of the 14th Conference on the Industrial and Commercial Use of Energy (ICUE)*, Cape Town, South Africa, 2017.

- [56] B. Pascoe, H. J. Groenewald, and M. Kleingeld, “Improving mine compressed air network efficiency through demand and supply control,” in *Proceedings of the 14th Conference on the Industrial and Commercial Use of Energy (ICUE)*, Cape Town, South Africa, 2017.
- [57] L. Frías-Paredes, F. Mallor, M. Gastón-Romeo, and T. León, “Dynamic mean absolute error as new measure for assessing forecasting errors,” *Energy Conversion and Management*, vol. 162, pp. 176–188, February 2018.
- [58] A. de Myttenaere, B. Golden, B. Le, and F. Rossi, “Mean absolute percentage error for regression models,” *Neurocomputing*, vol. 192, pp. 38–48, March 2016.
- [59] D. Arndt, “Process Toolbox thermal hydraulic simulation tool user manual,” pp. 1–198, HVAC International (Pty) Ltd, Pretoria, South Africa, 2016.
- [60] C. Beckey, R. Hartfield, and M. Carpenter “Compressor modelling for engine control and maintenance,” Air Force Flight Test Center (AFFTC), Palmdale, CA, July 2011.

Appendix A

Compressor fundamental calculations

Compressor fundamental calculations

Equation 13 calculates the electric motor power required to compress air [11].

Equation 13: Electric motor power required by centrifugal compressors

$$P_{motor} = \frac{P_{comp}}{\eta_{motor}}$$

Where:

P_{motor} = Electric motor power required [kW]

P_{comp} = Compressor power required [kW]

η_{motor} = Efficiency of electric motor [–]

Equation 14 calculates the power required by the compressors to compress air [11].

Equation 14: Compressor power required to compress air

$$P_{comp} = \dot{m}_{air} W_{comp}$$

Where:

P_{comp} = Compressor power required [kW]

\dot{m}_{air} = Air mass flow rate [kg/s]

W_{comp} = Mechanical energy required [kJ/kg]

Equation 15 calculates the mechanical energy required to compress air [11].

Equation 15: Mechanical energy required to compress air

$$W_{comp} = \frac{nRT_{in}}{\eta_{comp}(n-1)} \left(\left(\frac{p_2}{p_1} \right)^{\frac{n-1}{n}} - 1 \right)$$

Where:

W_{comp} = Mechanical energy required [kJ/kg]

n = Polytrophic constant [–]

R = Universal gas constant [kJ/kg·K]

T_{in} = Inlet air temperature [K]

η_{comp} = Efficiency of compressor [–]

p_2 = Discharge air pressure [kPa]

p_1 = Inlet air pressure [kPa]

Equation 16 illustrates how the polytrophic constant is calculated [11].

Equation 16: Polytrophic constant calculation

$$n = \frac{C_p}{C_v}$$

Where:

- n = Polytrophic constant [–]
 C_p = Specific heat at constant pressure [kJ/kg·K]
 C_v = Specific heat at constant volume [kJ/kg·K]

Equation 17 illustrates how the air mass flow rate is calculated from the volume flow rate [11].

Equation 17: Air mass flow rate calculation

$$\dot{m}_{air} = \rho_{air} Q_{air}$$

Where:

- \dot{m}_{air} = Air mass flow rate [kg/s]
 ρ_{air} = Density of air [kg/m³]
 Q_{air} = Air volume flow rate [m³/s]

Equation 18 illustrates how air density is calculated using ideal gas laws [11].

Equation 18: Density of compressed air calculation

$$\rho_{air} = \frac{p_{abs}}{RT}$$

Where:

- ρ_{air} = Density of air [kg/m³]
 p_{abs} = Absolute air pressure [kPa]
 R = Universal gas constant [kJ/kg·K]
 T = Temperature of compressed air [K]

Appendix B

Process Toolbox® description

Process Toolbox

Process Toolbox[®] (PTB) is a transient thermal-hydraulic system simulation and optimisation tool [59]. It is used to analyse and optimise various mining system performances as well as design new systems. Figure 34 displays the graphical user interface (GUI) of PTB along with various components used for compressed air simulation studies.

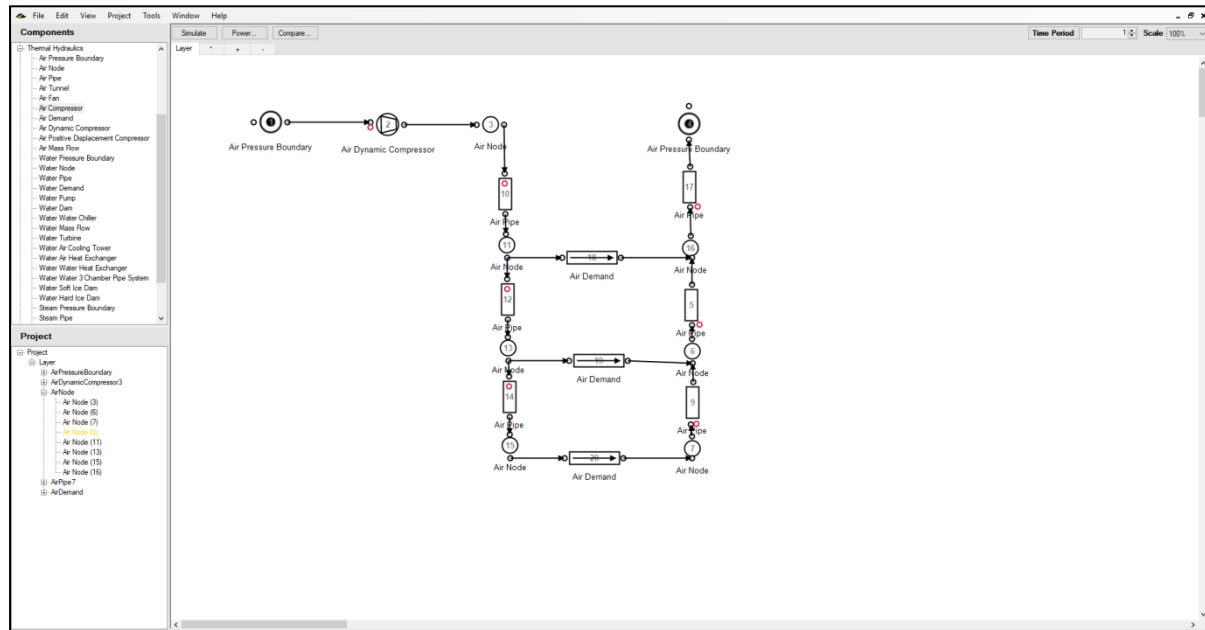


Figure 34: GUI of PTB

As seen in Figure 34, PTB allows the user to drag and drop various components into the GUI to replicate or design mining systems. Each component is connected to one another from the outlet of one component, into the inlet of the next.

After a system is created in PTB, each component can be characterised according to its design specification. By selecting a component, one can quickly characterise it. Various inputs for the different components are available to ensure accurate calibration is possible. After a component is selected, an input window appears as illustrated by the example seen in Figure 35.

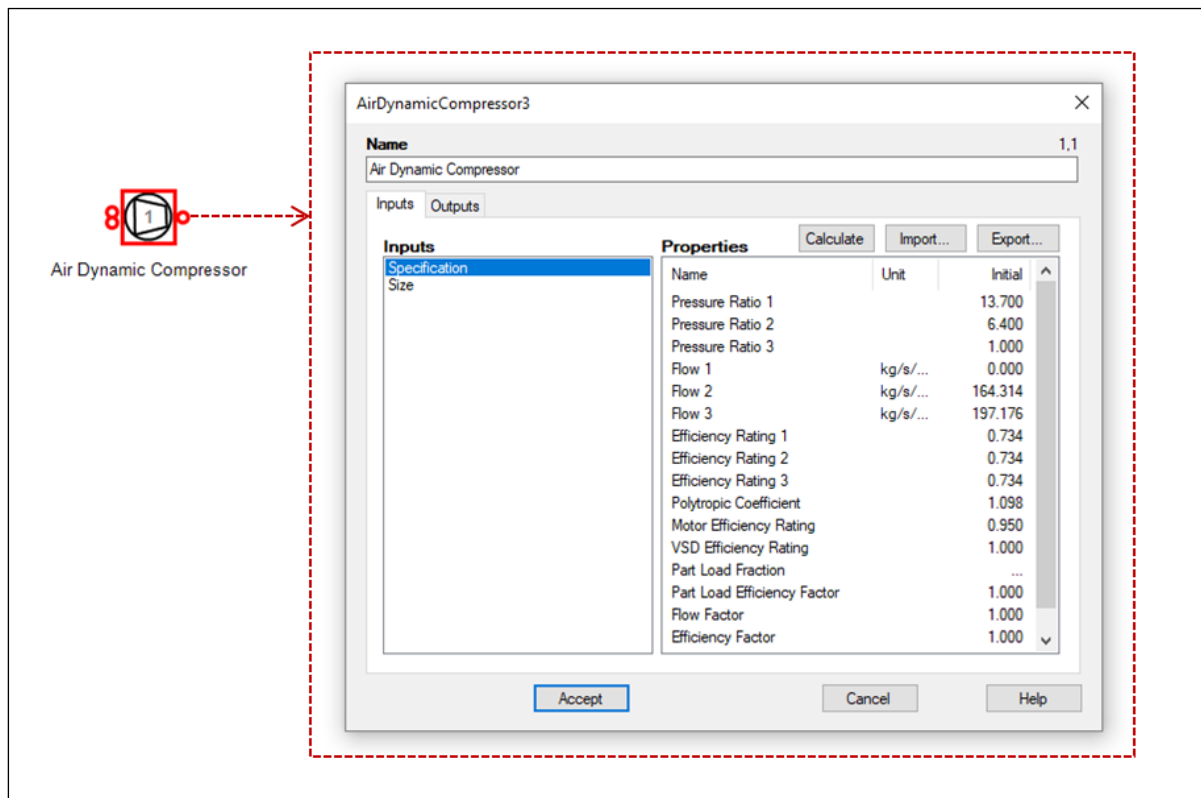


Figure 35: PTB compressor input window

As seen in Figure 35, one can set the compressor characteristic curve and various efficiencies to the compressor's design specification. This window is similar to other components where the different input values can be characterised by the various components.

PTB can accurately simulate a network after the simulation model is created and the various components are characterised. PTB mathematically calculates the system's response to the characterised components and delivers high accuracy outputs. Therefore, the decision is made to use PTB for all simulation purposes in this study.

Appendix C

Previous simulation development methods

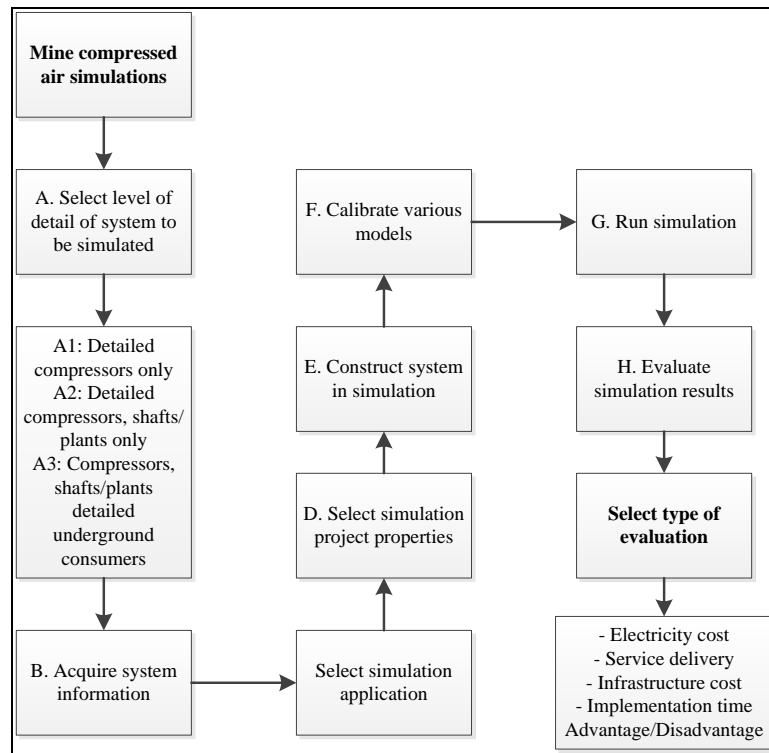


Figure 36: Simplified mine compressed air simulation method (adapted from [55])

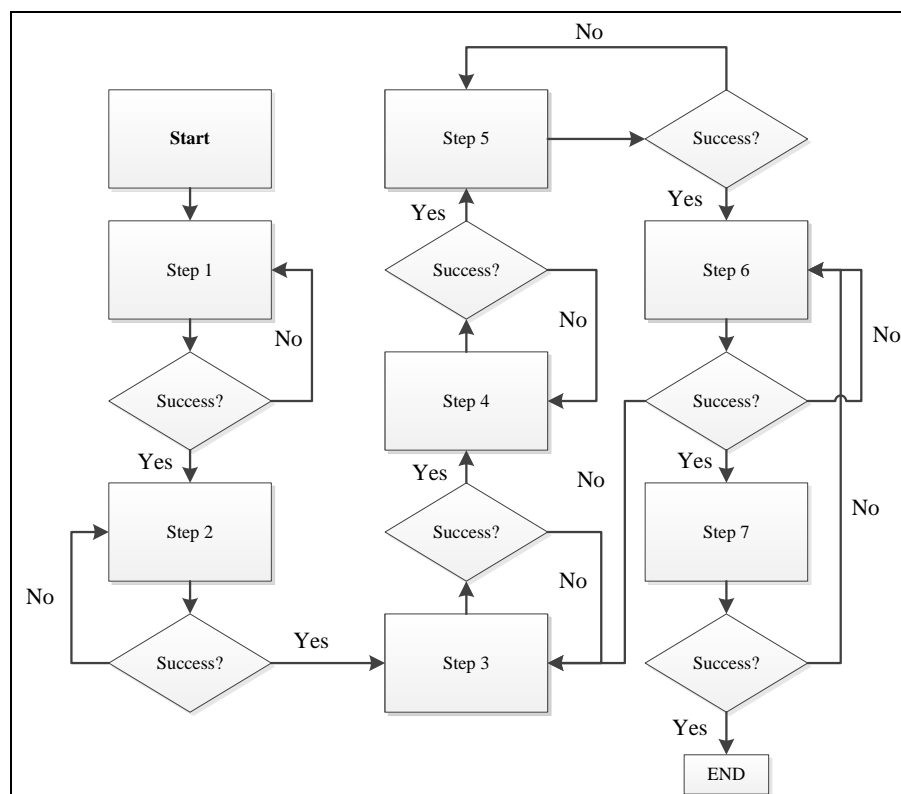


Figure 37: Compressed air ring simulation development (adapted from [56])

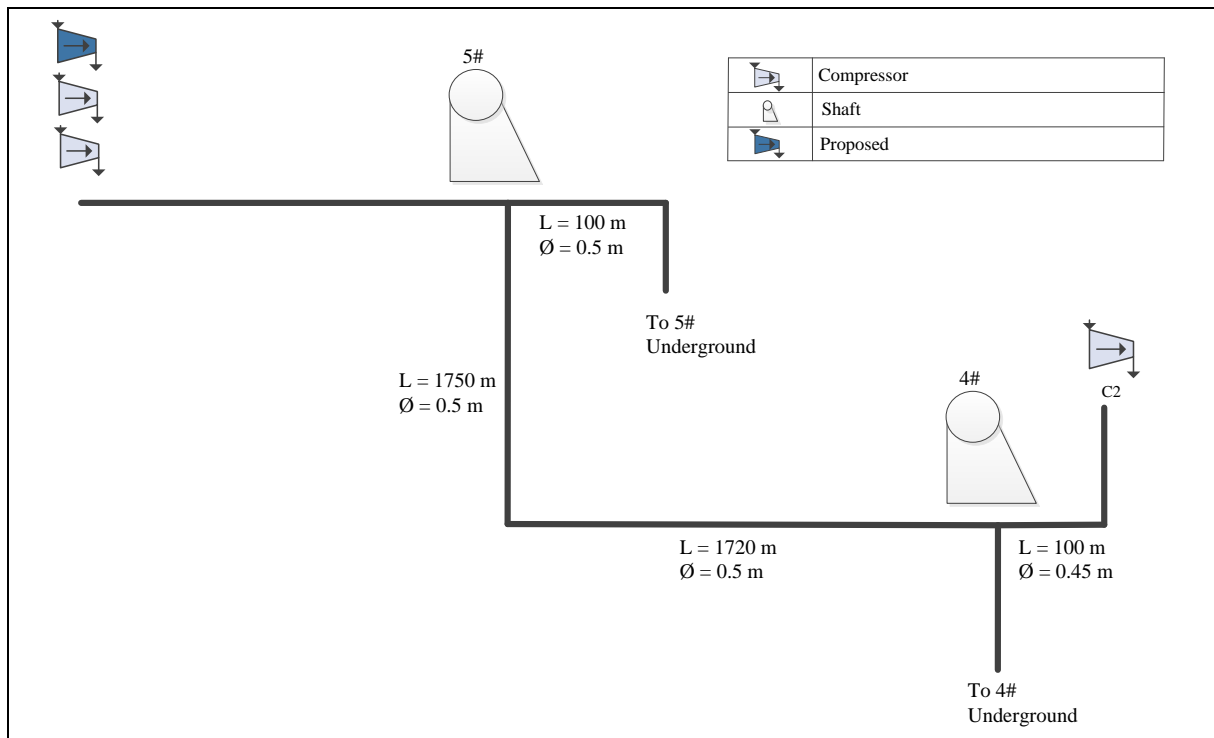


Figure 38: Illustration of compressor relocation simulation (adapted from [11])

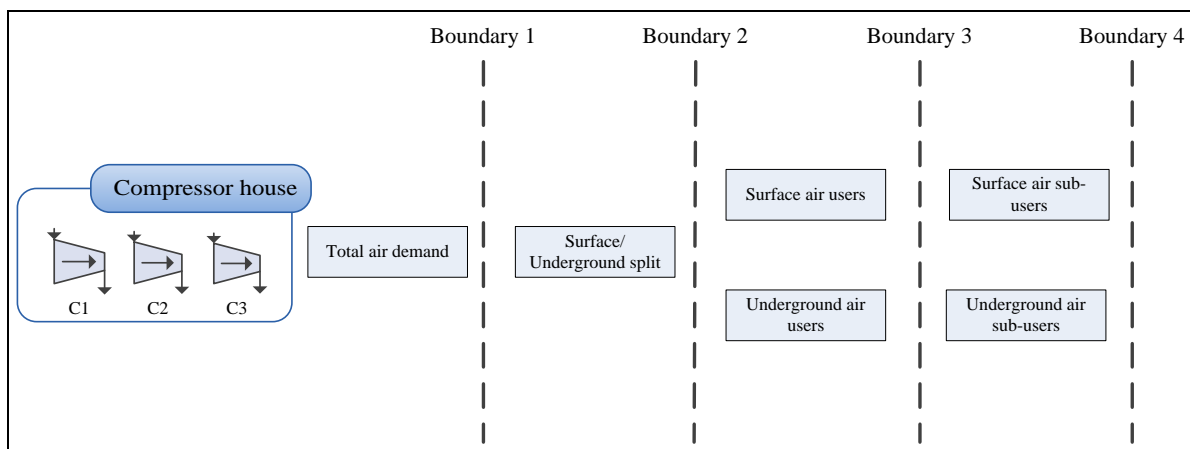


Figure 39: Simulation boundary condition selection (adapted from [32])

Appendix D

Schematic layout of Mine-A

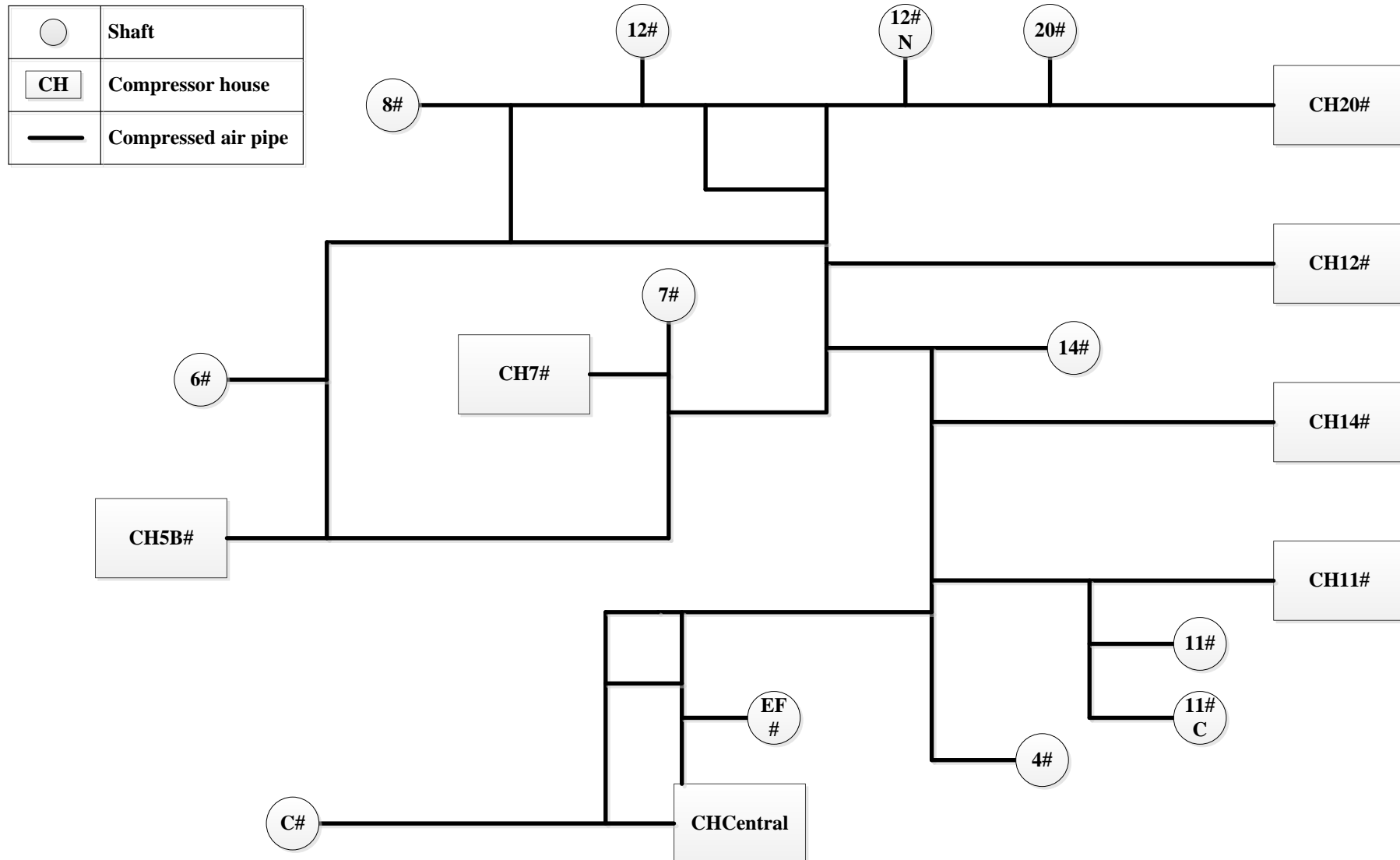


Figure 40: Schematic layout of Mine-A's compressed air network

Appendix E

AFT Arrow® simulation data

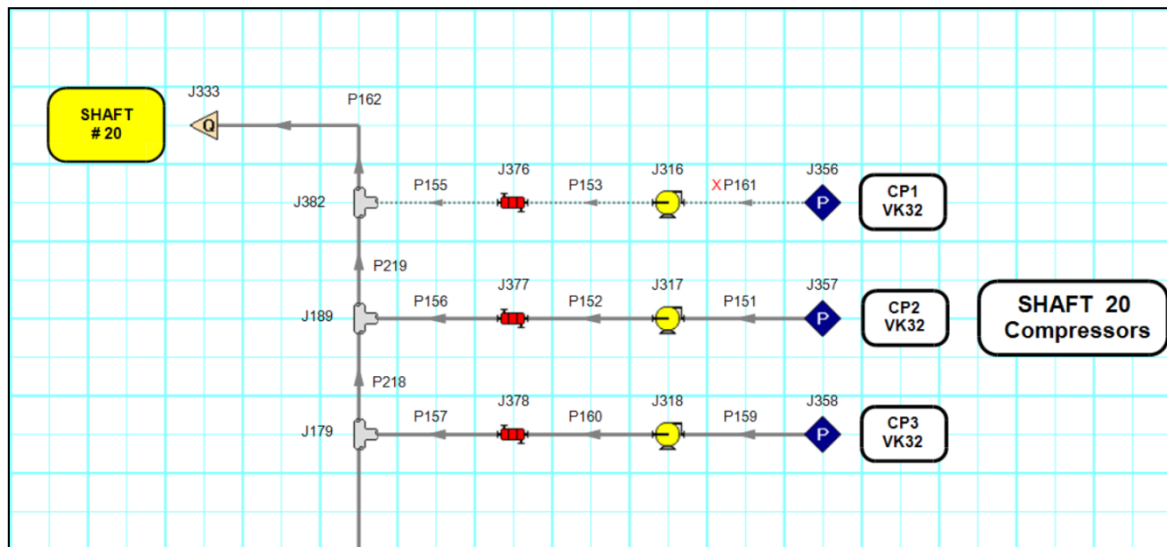


Figure 41: AFT Arrow[®] simulation section screenshot

Compressor/Fan Properties

Number: 316
Name: Shaft #20 - CP1 VK32
Database List:
Copy Data From Jct...

Upstream Pipe: 161
Downstream Pipe: 153
Elevation: 1 meters

READ-ONLY INFORMATION
Close
Jump...
Help

Compressor/Fan Model Variable Speed Optional Notes Status

Compressor/Fan Model
☒ Compressor/Fan Curve Enter Curve Data...
☐ Volumetric Flow Rate Fixed (at Inlet)
☐ Mass Flow Rate Fixed
☐ Head Rise Fixed
☐ Pressure Rise Fixed
 Added Pressure
☐ Stagnation ☒ Static

Compression Process Thermodynamics
☒ Adiabatic
☐ Polytropic Constant:
☐ Determine From Efficiency Data
 Efficiency data not required and will be ignored.
 Efficiency is effectively 100%.

Max X-Axis Value: 80000 Update Graph

Pressure Rise Efficiency Parameters and Constants

☒ Check Valve at Discharge (No Backflow Allowed)

Figure 42: AFT Arrow[®] compressor component input variables

Appendix F

Compressor corrected flow calculations

Table 34: VK32 design specifications

Point no.	Discharge pressure [kPa]	Volumetric airflow [m ³ /s]
1	628.86	8.83
2	500	9.17
3	0	9.43

Table 35: VK32 corrected flow values

Point no.	Pressure ratio	Corrected flow [kg/s/bar/K]
1	8.23	224.6
2	6.75	233.28
3	1	239.89

Table 36: VK50 design specifications

Point no.	Discharge pressure [kPa]	Volumetric airflow [m ³ /s]
1	650	11.80
2	500	13.57
3	0	14.22

Table 37: VK50 corrected flow values

Point no.	Pressure ratio	Corrected flow [kg/s/bar/K]
1	8.47	300.17
2	6.75	345.36
3	1	361.78

Table 38: Multiple VK32 design specifications

Point no.	Discharge pressure [kPa]	Volumetric airflow (2 compressors) [m ³ /s]	Volumetric airflow (3 compressors) [m ³ /s]
1	628.86	17.66	26.49
2	500	18.34	27.51
3	0	18.86	28.29

Table 39: Multiple VK32 corrected flow values

Point no.	Pressure ratio	Corrected flow (2 compressors) [kg/s/bar/K]	Corrected flow (3 compressors) [kg/s/bar/K]
1	8.23	499.20	673.81
2	6.75	466.56	699.84
3	1	479.79	719.68

Table 40: Multiple VK50 design specifications

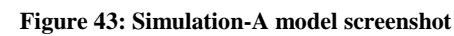
Point no.	Discharge pressure [kPa]	Volumetric airflow (2 compressors) [m ³ /s]	Volumetric airflow (3 compressors) [m ³ /s]
1	650	23.6	35.4
2	500	27.15	40.73
3	0	28.44	42.67

Table 41: Multiple VK50 corrected flow values

Point no.	Pressure ratio	Corrected flow (2 compressors) [kg/s/bar/K]	Corrected flow (3 compressors) [kg/s/bar/K]
1	8.47	600.33	900.50
2	6.75	690.72	1036.08
3	1	723.57	1085.35

Appendix G

PTB® simulation model screenshots



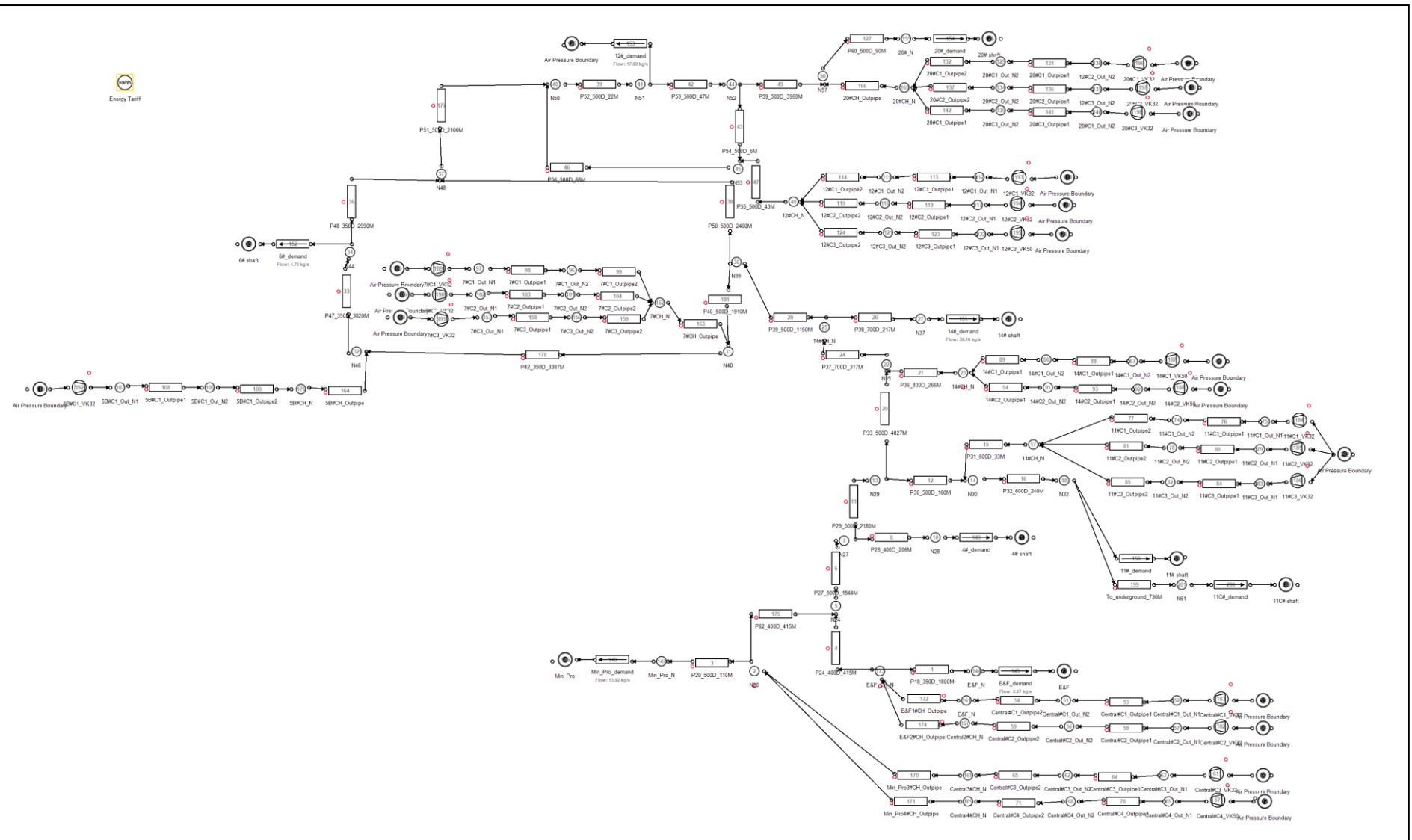


Figure 44: Simulation-B model screenshot

Trade-off between simulation accuracy and complexity for mine compressed air systems

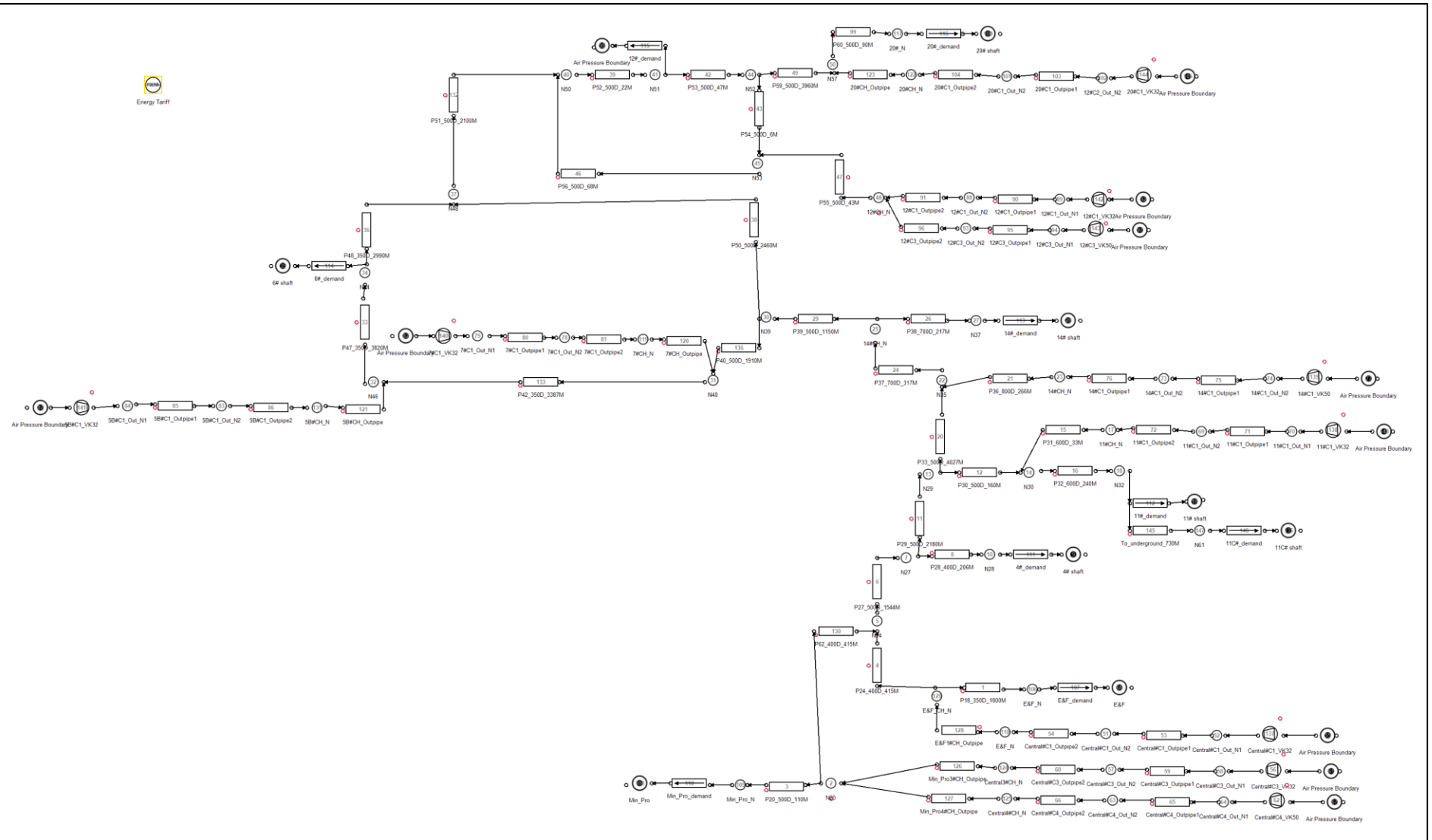


Figure 45: Simulation-C model screenshot

Appendix H

Simulation validation results comparison

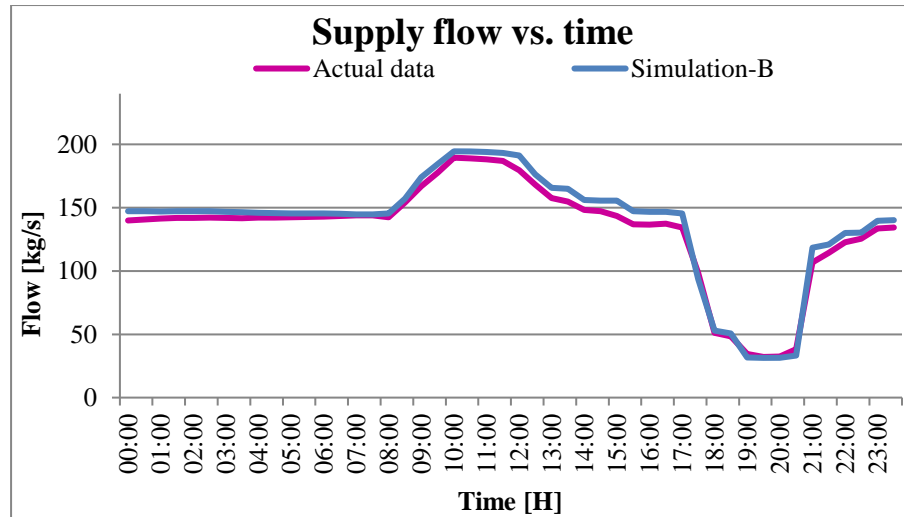


Figure 46: Simulation-B validation – supply flow

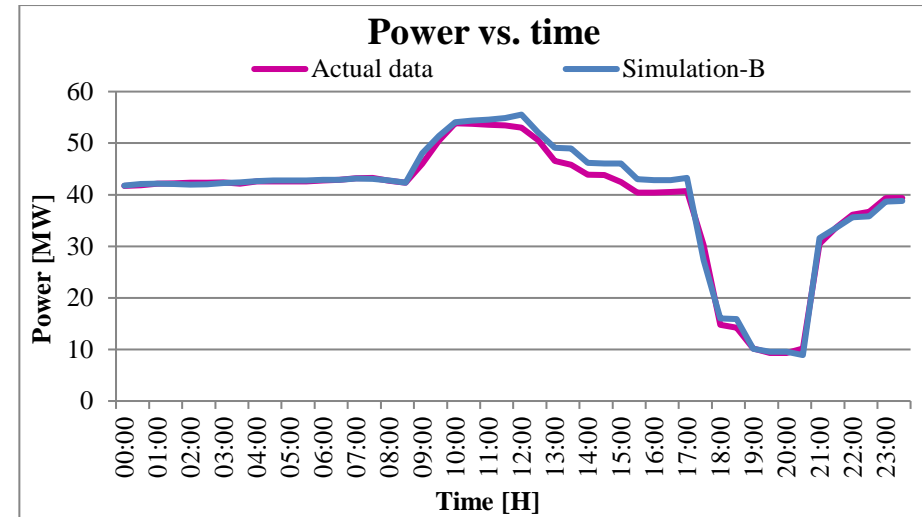


Figure 47: Simulation-B validation – power usage

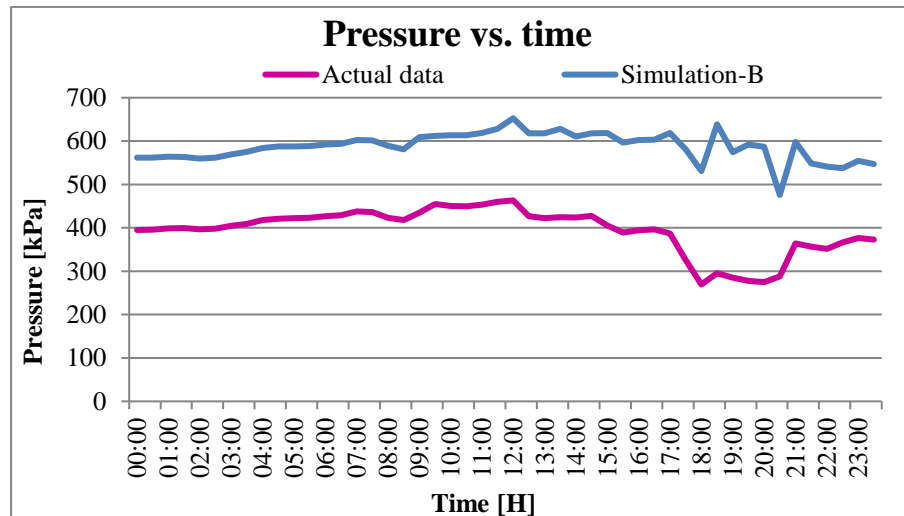


Figure 48: Simulation-B validation – supply pressure

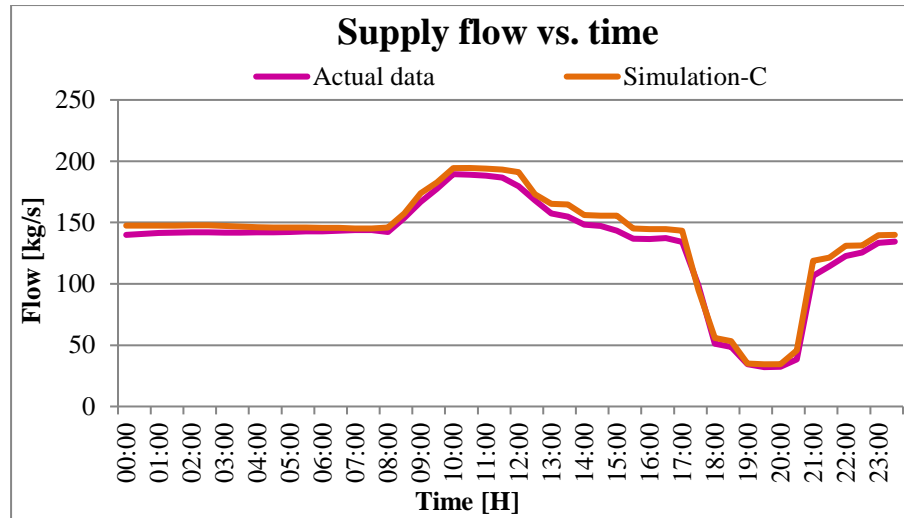


Figure 49: Simulation-C validation – supply flow

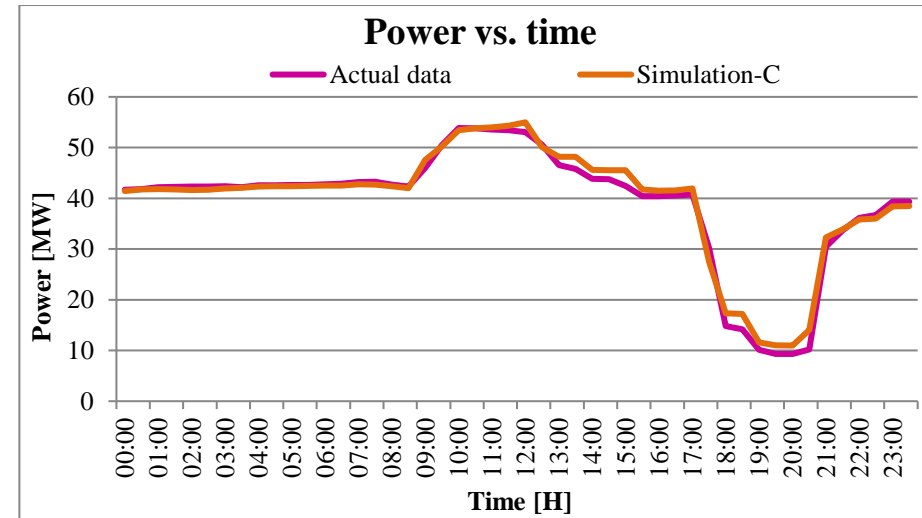


Figure 50: Simulation-C validation – power usage

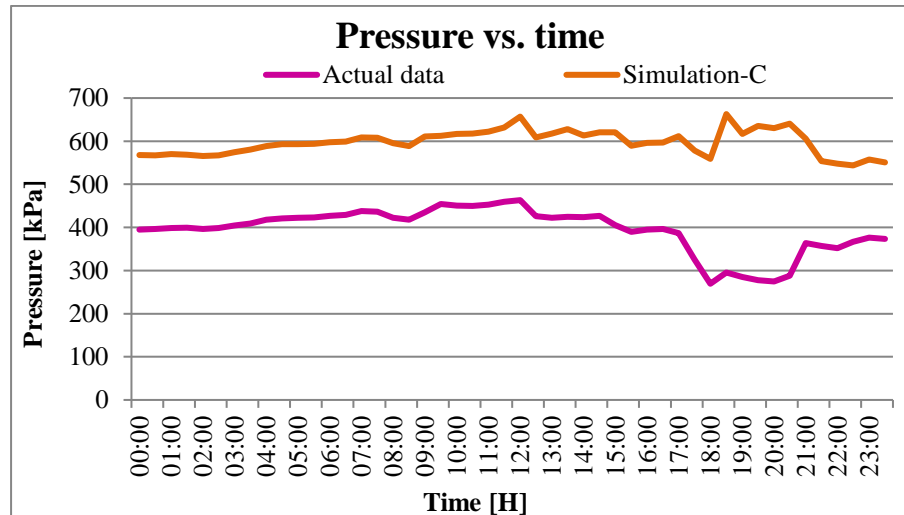


Figure 51: Simulation-C validation – supply pressure

Appendix I

Results comparison of simulated scenarios

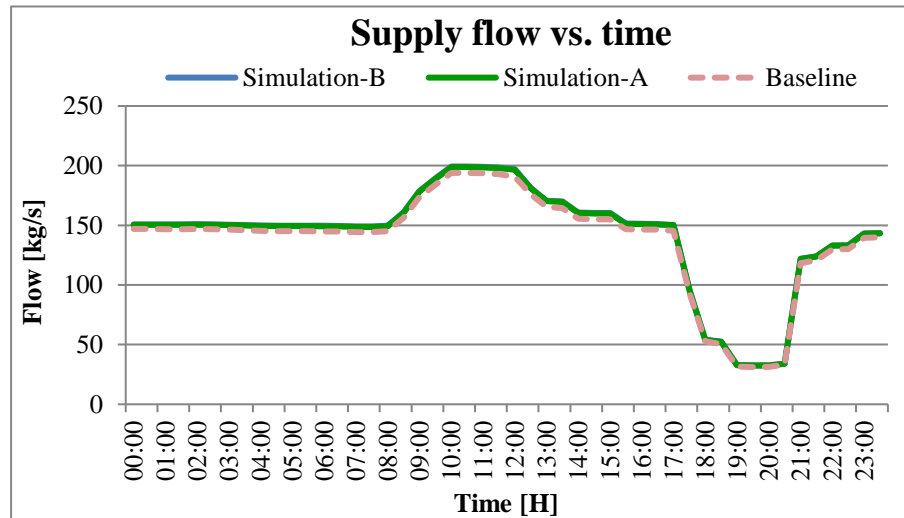


Figure 52: Supply flow increase comparison – Simulation-B – flow vs. time

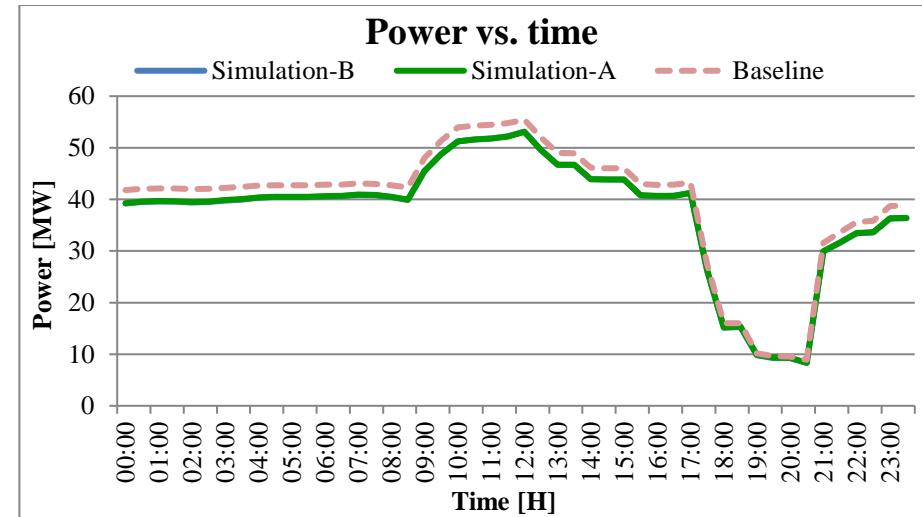


Figure 53: Supply flow increase comparison – Simulation-B – power vs. time

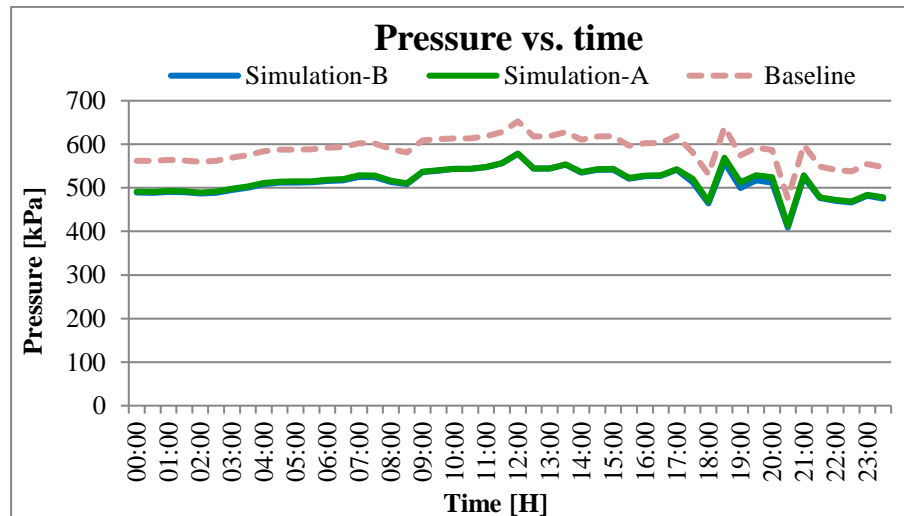


Figure 54: Supply flow increase comparison – Simulation-B – pressure vs. time

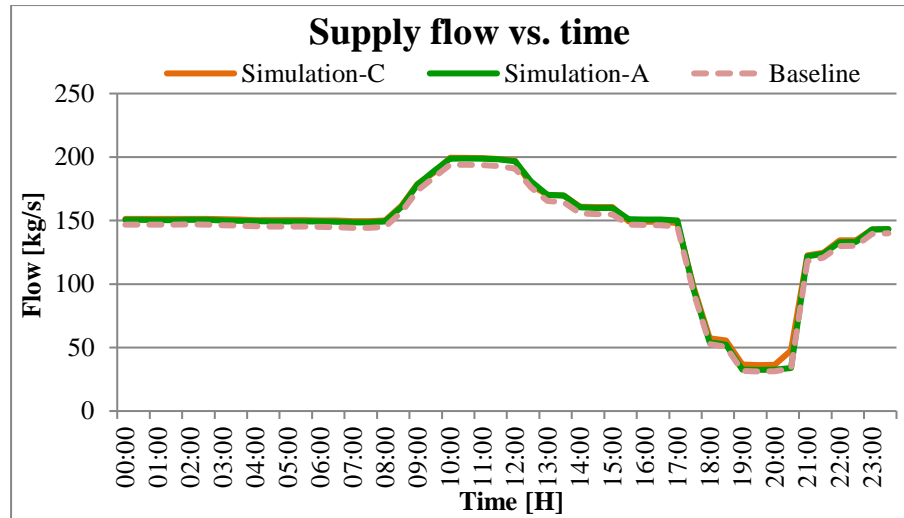


Figure 55: Supply flow increase comparison – Simulation-C – flow vs. time

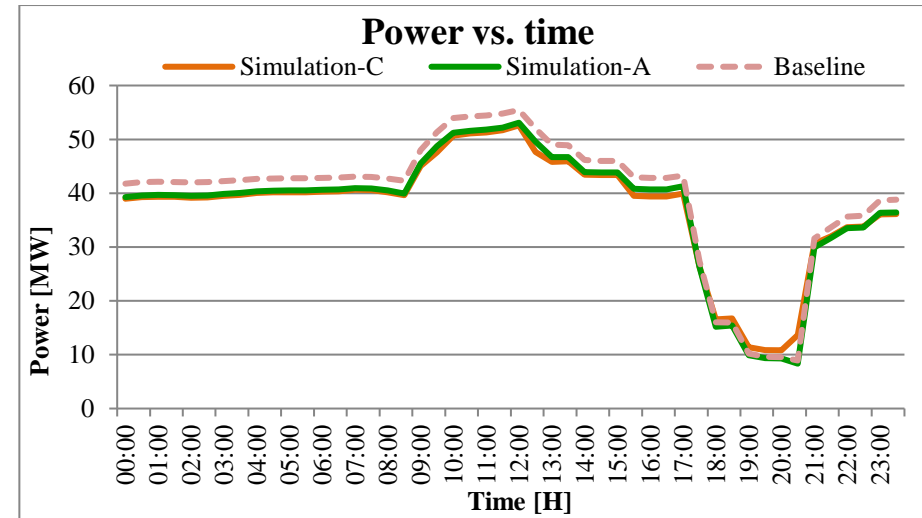


Figure 56: Supply flow increase comparison – Simulation-C – power vs. time

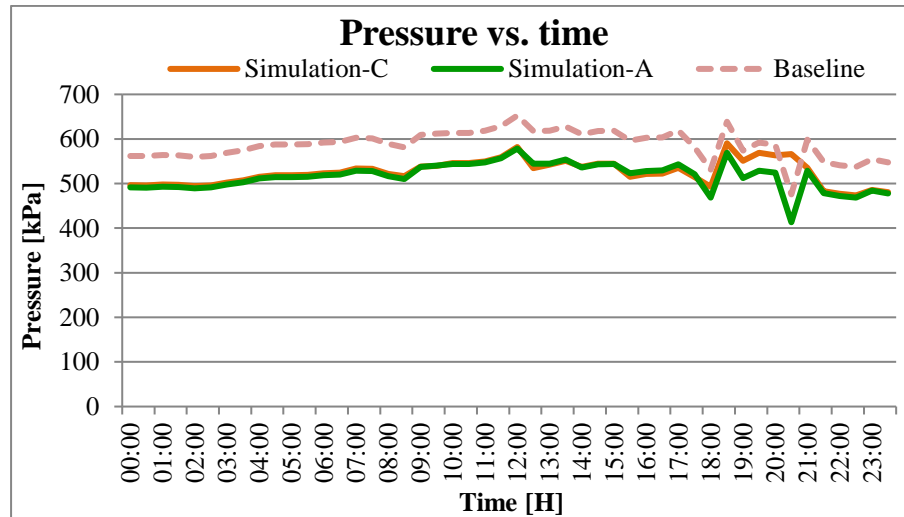


Figure 57: Supply flow increase comparison – Simulation-C – pressure vs. time

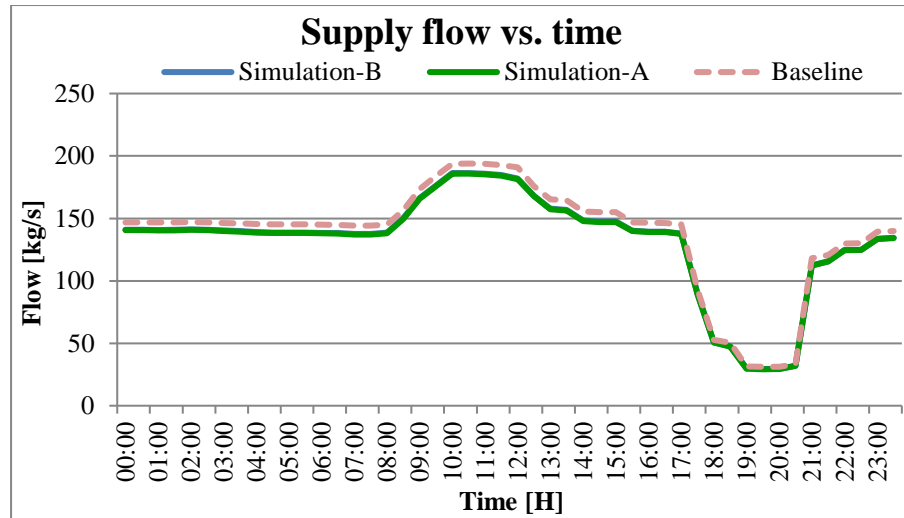


Figure 58: Supply flow decrease comparison – Simulation-B – flow vs. time

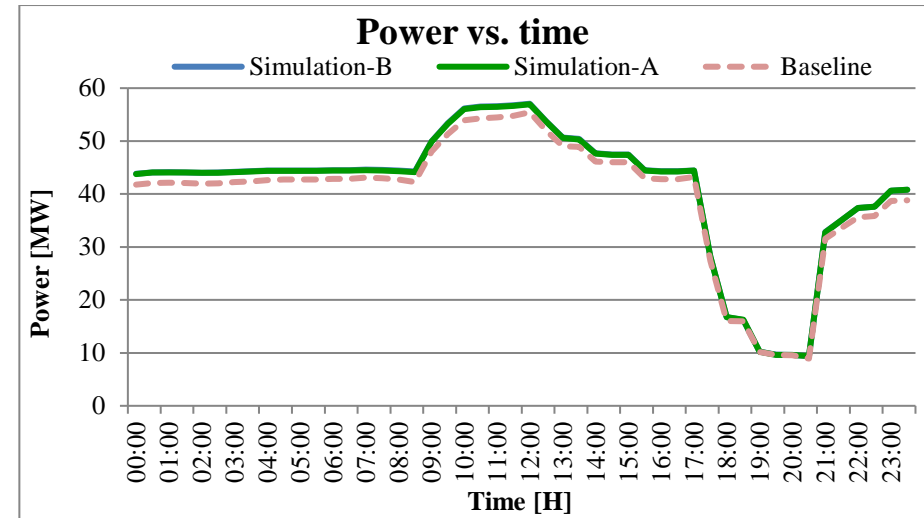


Figure 59: Supply flow decrease comparison – Simulation-B – power vs. time

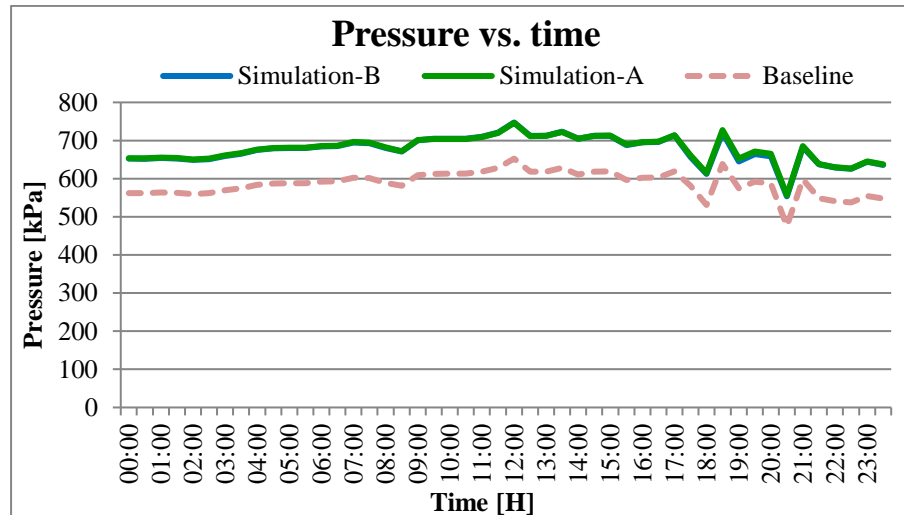


Figure 60: Supply flow decrease comparison – Simulation-B – pressure vs. time

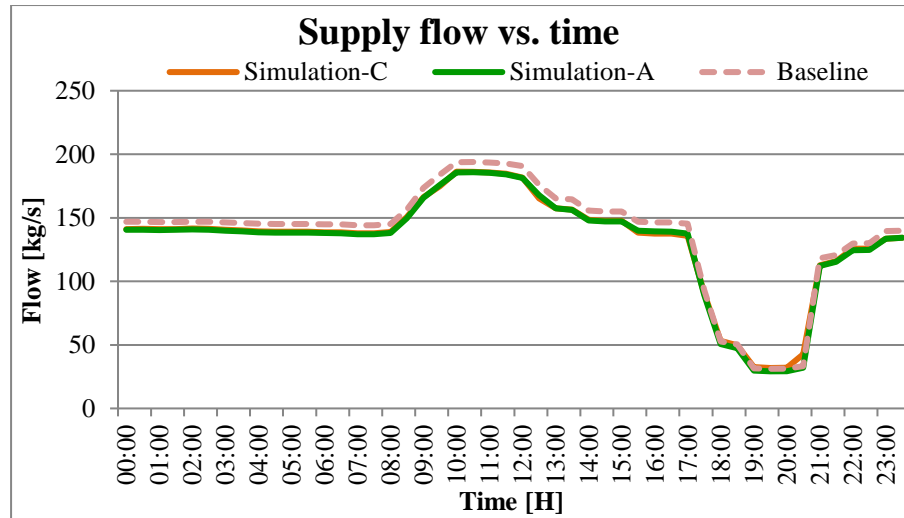


Figure 61: Supply flow decrease comparison – Simulation-C – flow vs. time

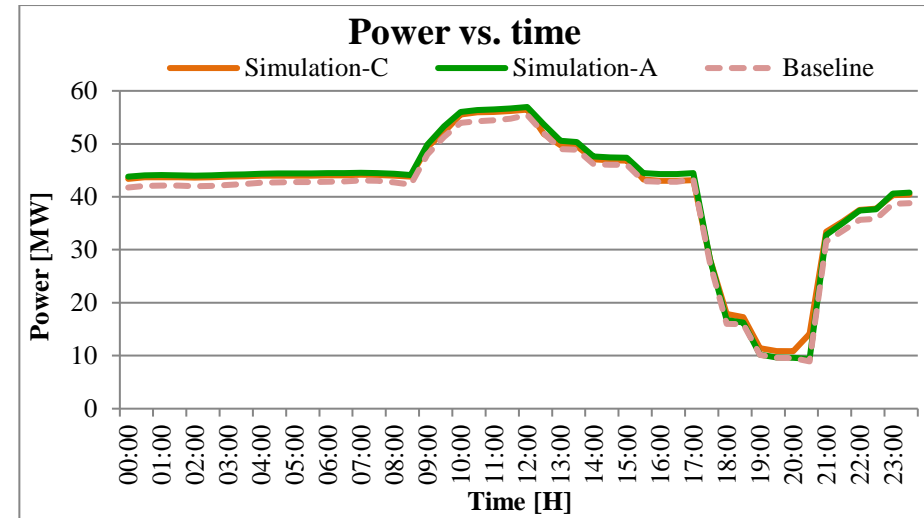


Figure 62: Supply flow decrease comparison – Simulation-C – power vs. time

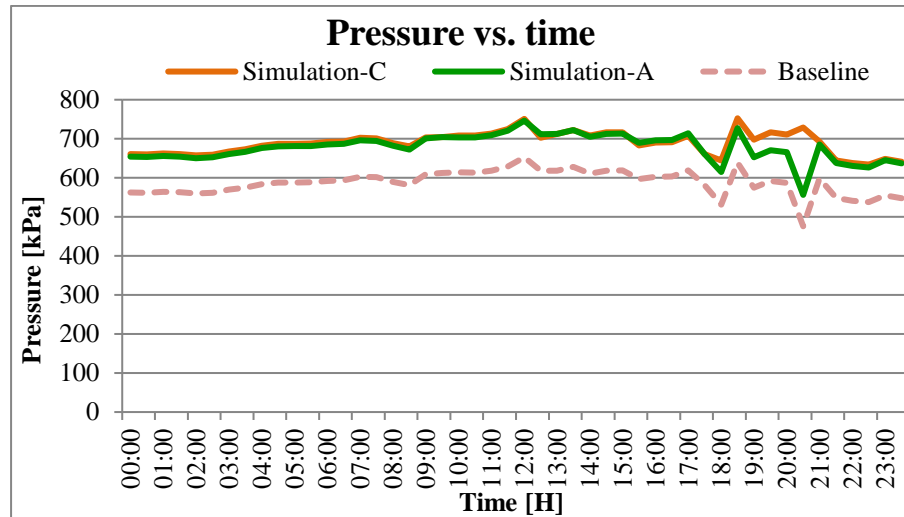


Figure 63: Supply flow decrease comparison – Simulation-C – pressure vs. time

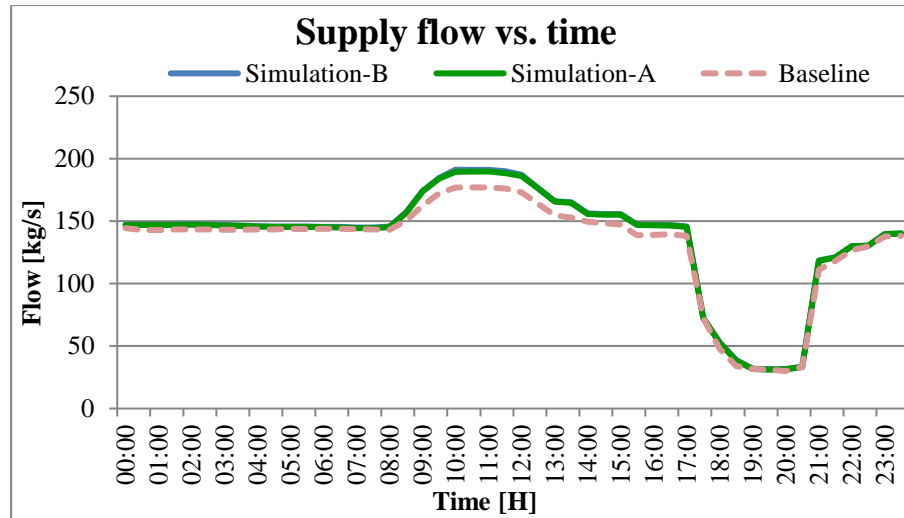


Figure 64: Supply pressure increase comparison – Simulation-B – flow vs. time

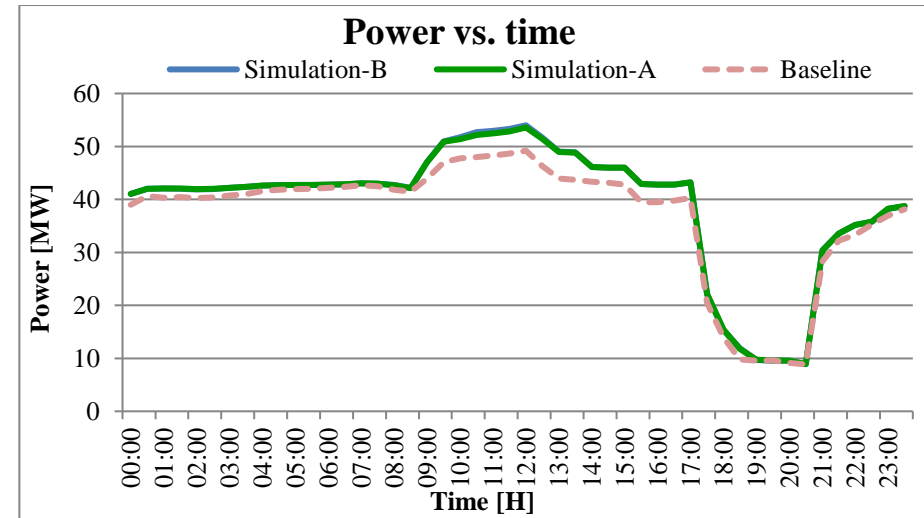


Figure 65: Supply pressure increase comparison – Simulation-B – power vs. time

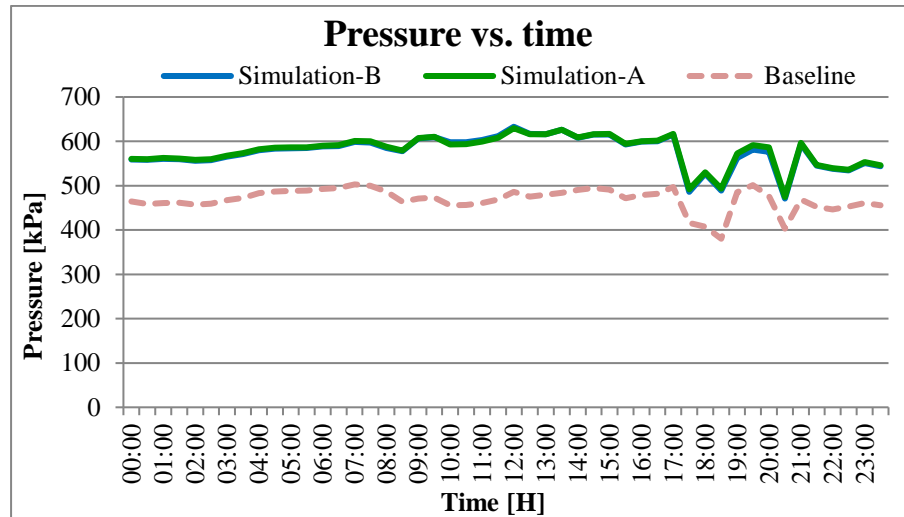


Figure 66: Supply pressure increase comparison – Simulation-B – pressure vs. time

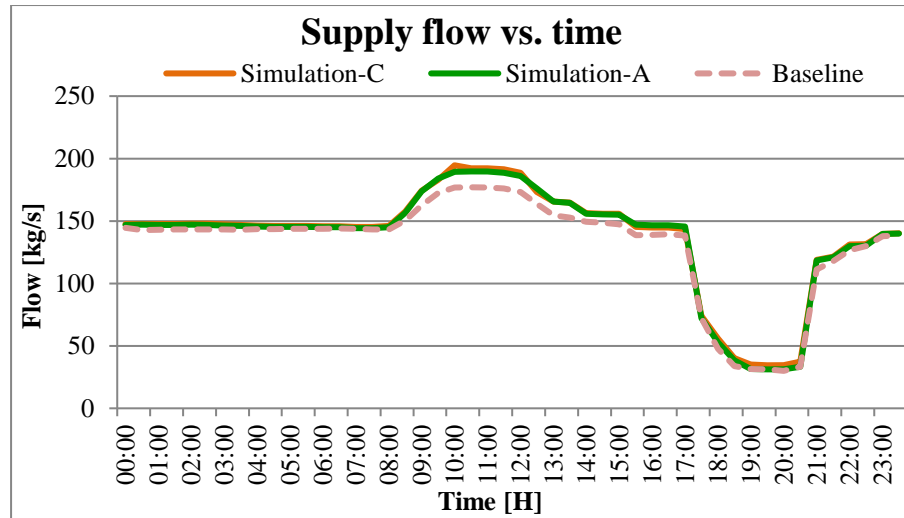


Figure 67: Supply pressure increase comparison – Simulation-C – flow vs. time

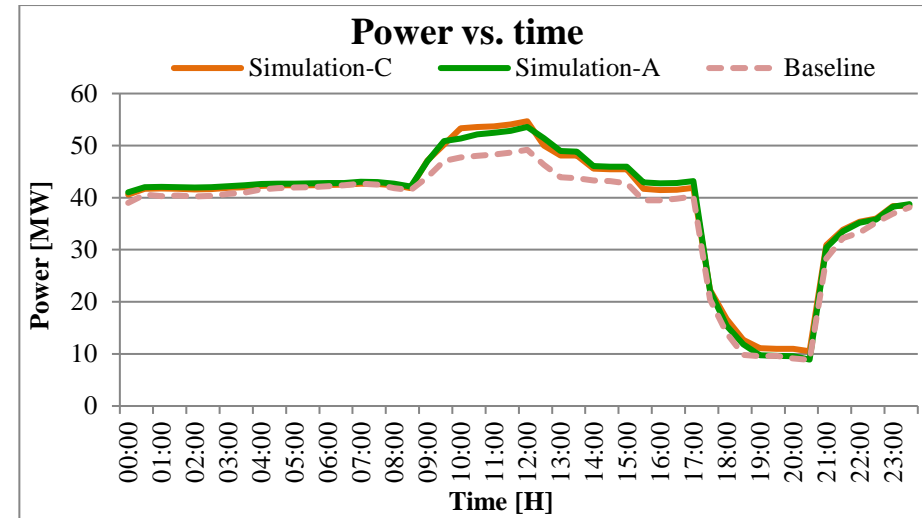


Figure 68: Supply pressure increase comparison – Simulation-C – power vs. time

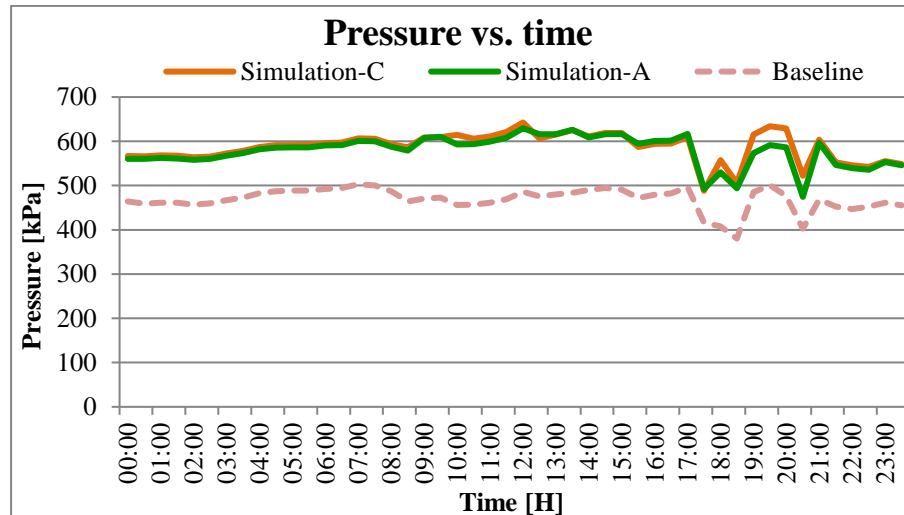


Figure 69: Supply pressure increase comparison – Simulation-C – pressure vs. time

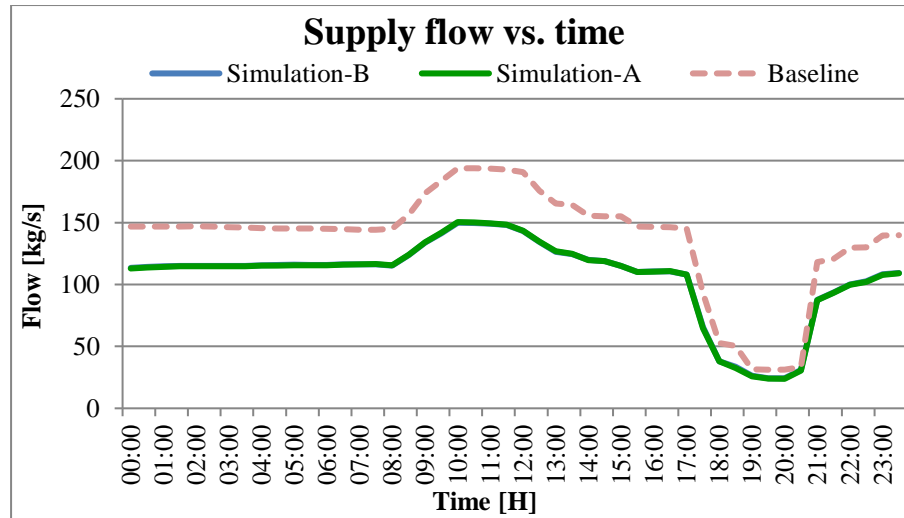


Figure 70: Supply pressure decrease comparison – Simulation-B – flow vs. time

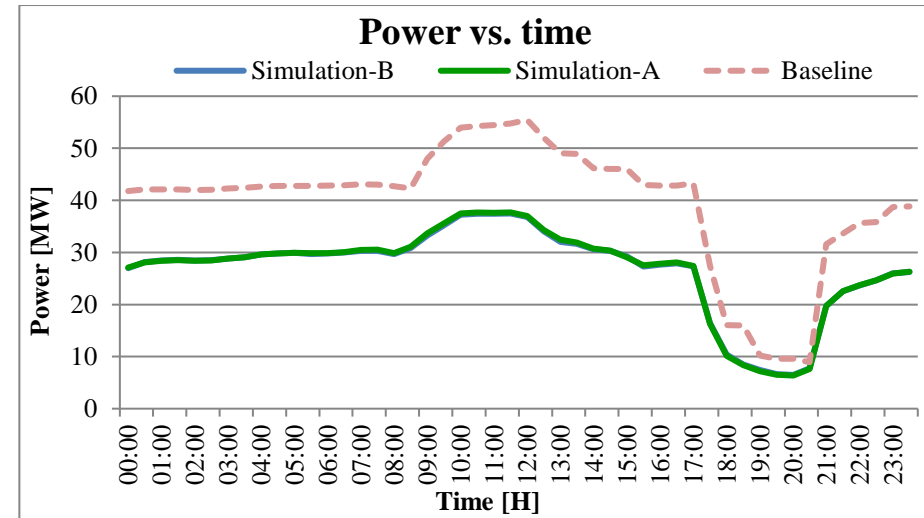


Figure 71: Supply pressure decrease comparison – Simulation-B – power vs. time

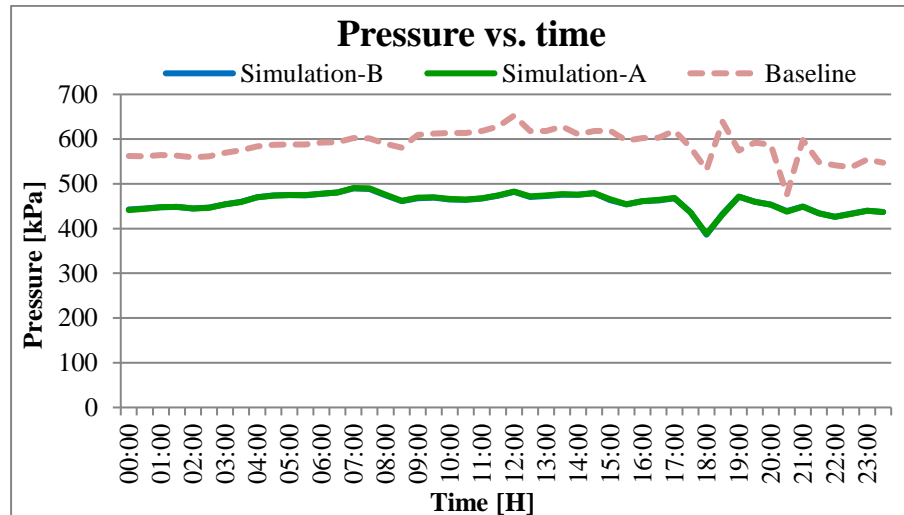


Figure 72: Supply pressure decrease comparison – Simulation-B – pressure vs. time

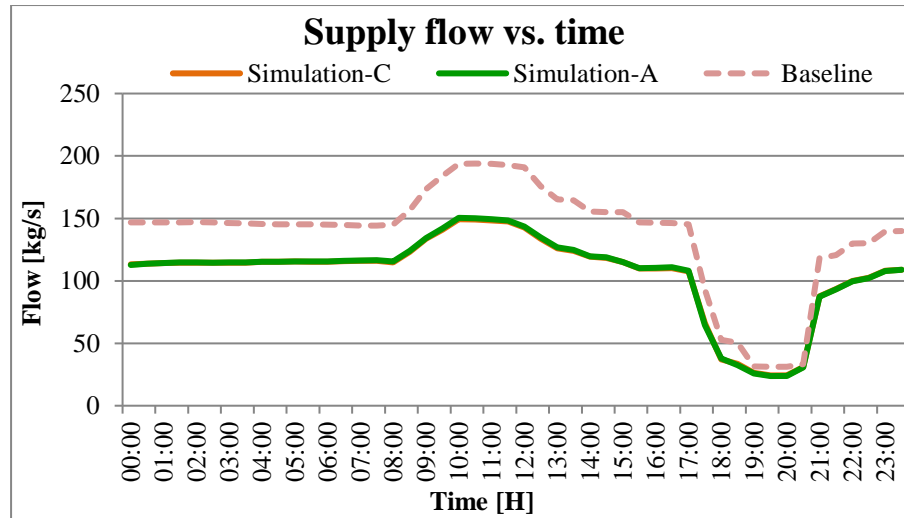


Figure 73: Supply pressure decrease comparison – Simulation-C – flow vs. time

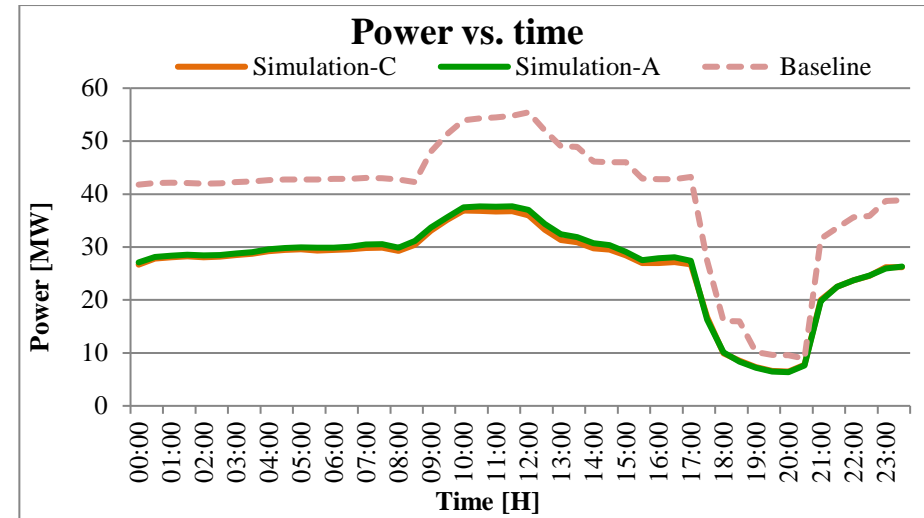


Figure 74: Supply pressure decrease comparison – Simulation-C – power vs. time

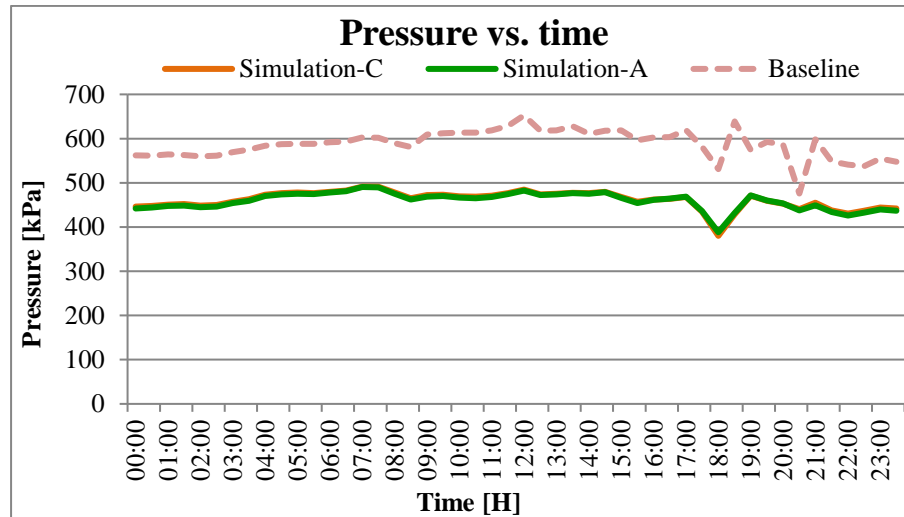


Figure 75: Supply pressure decrease comparison – Simulation-C – pressure vs. time

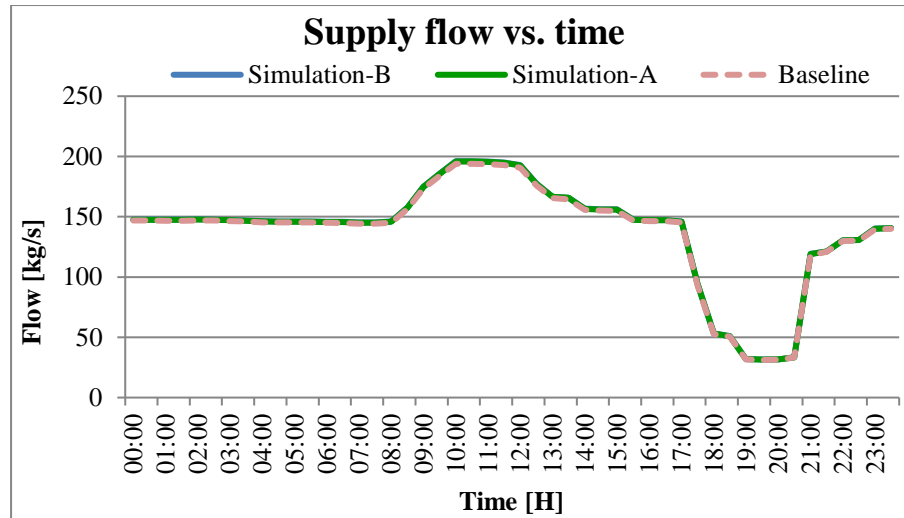


Figure 76: Pipe dimension increase comparison – Simulation-B – flow vs. time

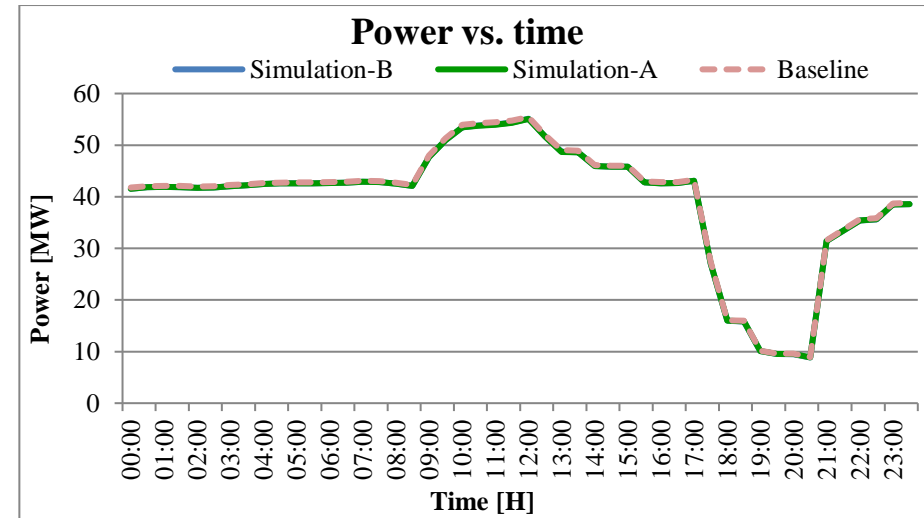


Figure 77: Pipe dimension increase comparison – Simulation-B – power vs. time

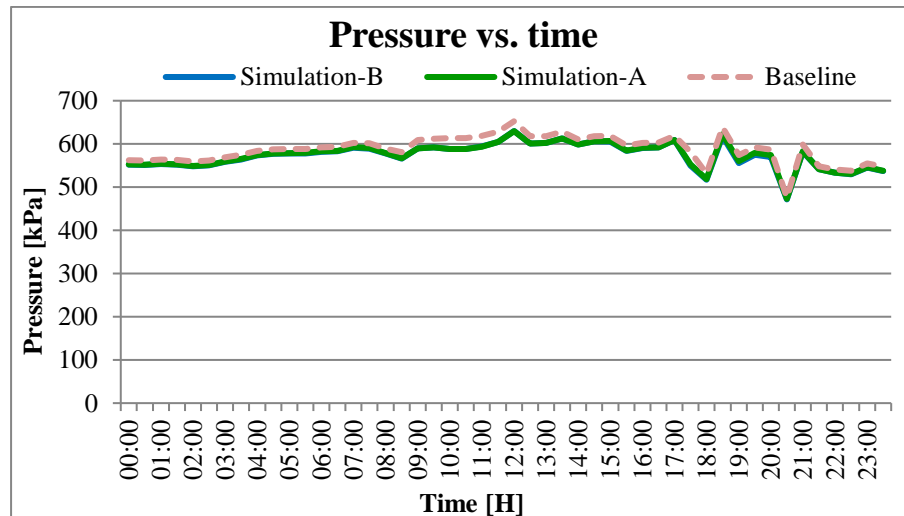


Figure 78: Pipe dimension increase comparison – Simulation-B – pressure vs. time

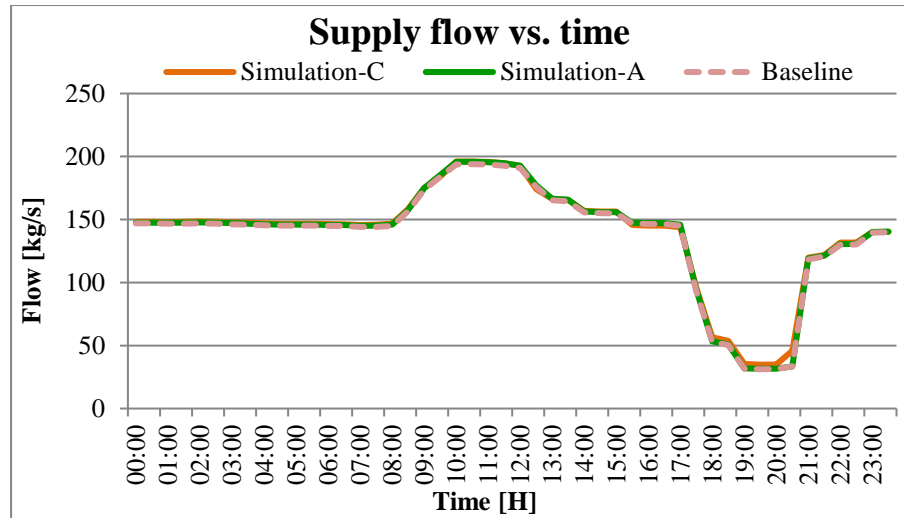


Figure 79: Pipe dimension increase comparison – Simulation-C – flow vs. time

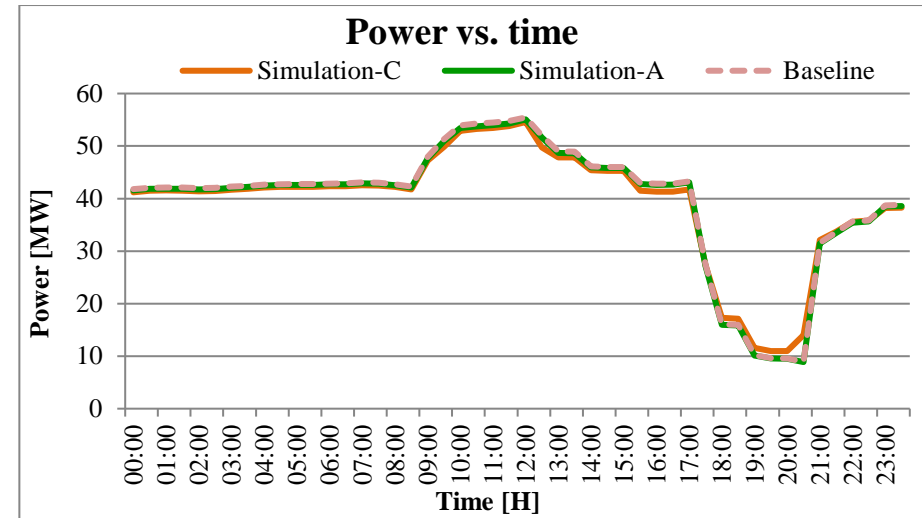


Figure 80: Pipe dimension increase comparison – Simulation-C – power vs. time

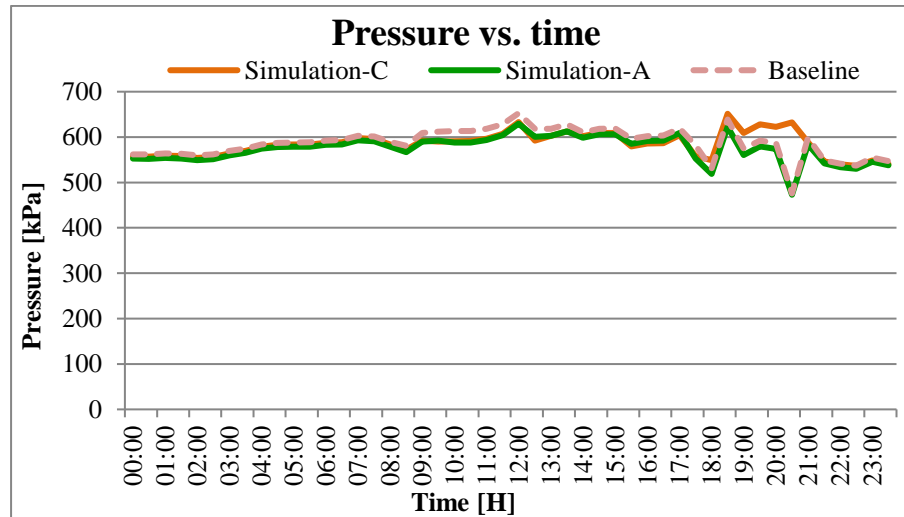


Figure 81: Pipe dimension increase comparison – Simulation-C – pressure vs. time

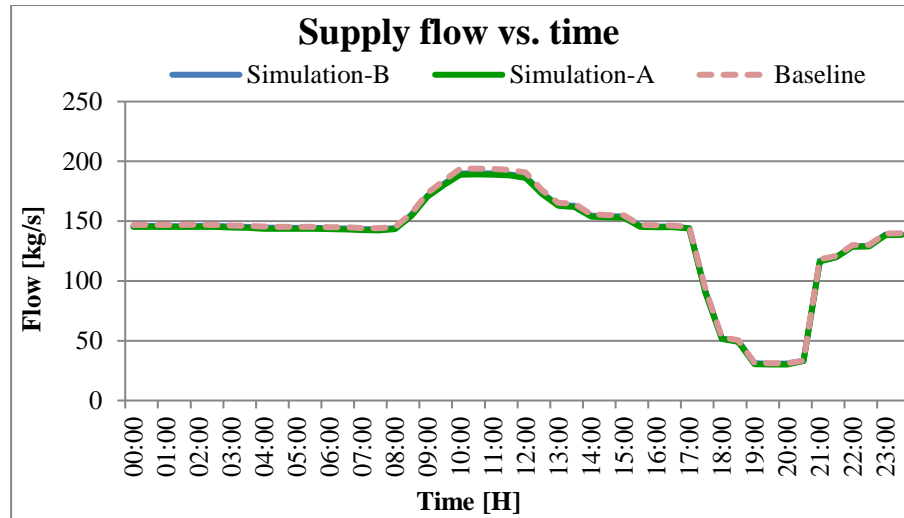


Figure 82: Pipe dimension decrease comparison – Simulation-B – flow vs. time

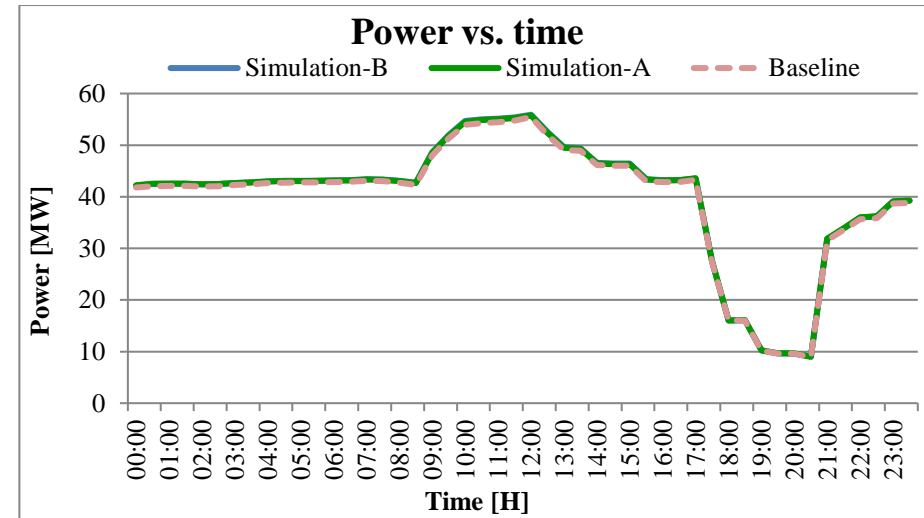


Figure 83: Pipe dimension decrease comparison – Simulation-B – power vs. time

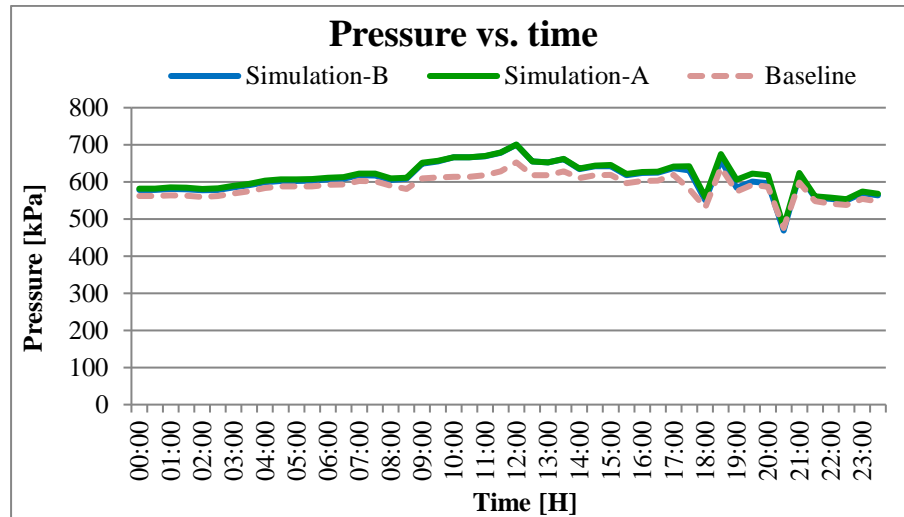


Figure 84: Pipe dimension decrease comparison – Simulation-B – pressure vs. time

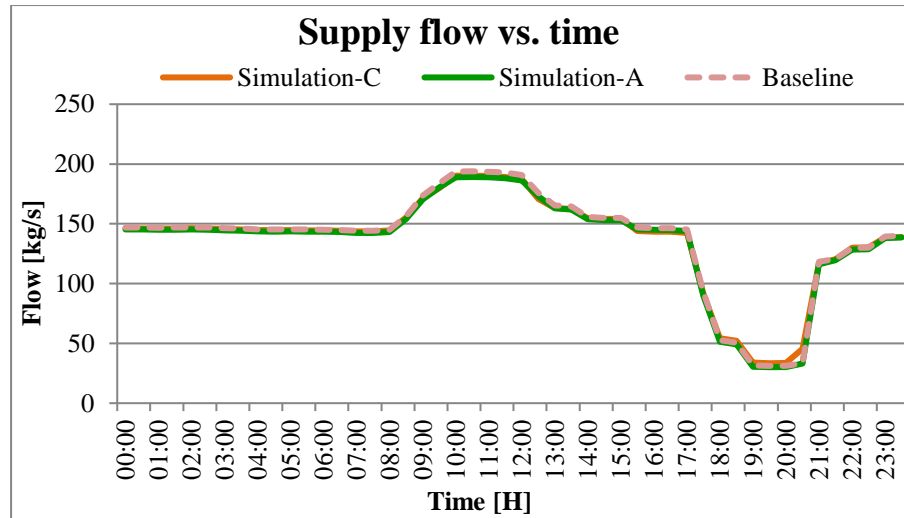


Figure 85: Pipe dimension decrease comparison – Simulation-C – flow vs. time

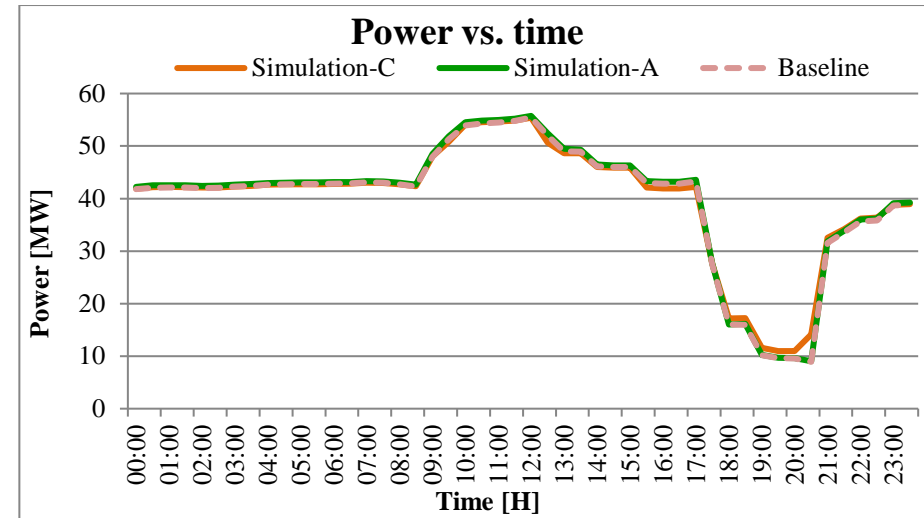


Figure 86: Pipe dimension decrease comparison – Simulation-C – power vs. time

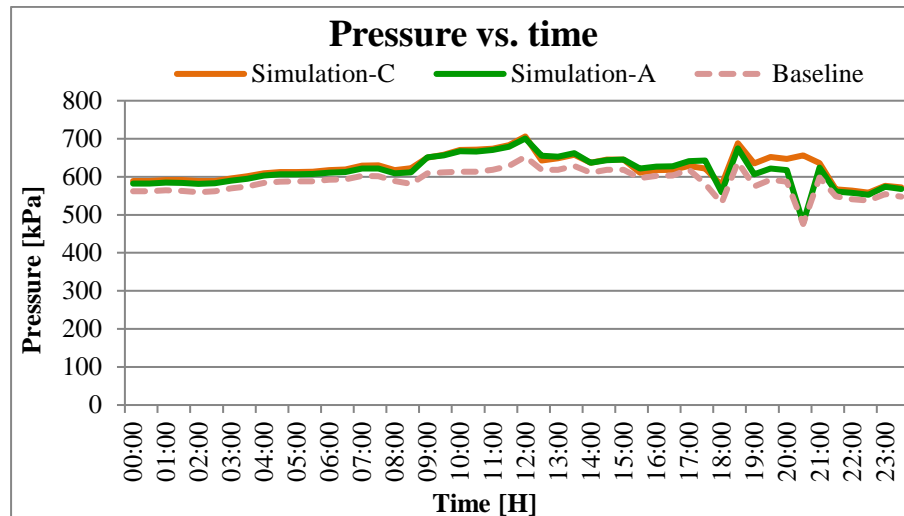


Figure 87: Pipe dimension decrease comparison – Simulation-C – pressure vs. time

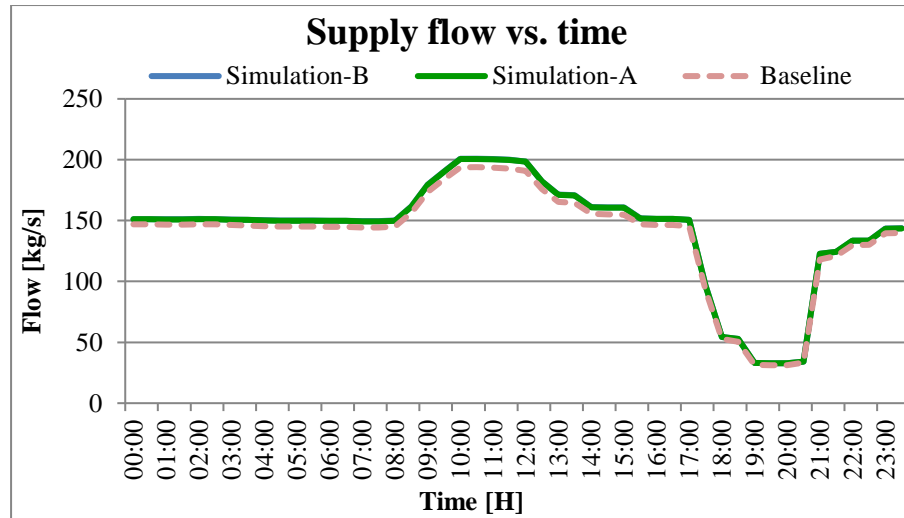


Figure 88: Multiple parameter increase comparison – Simulation-B – flow vs. time

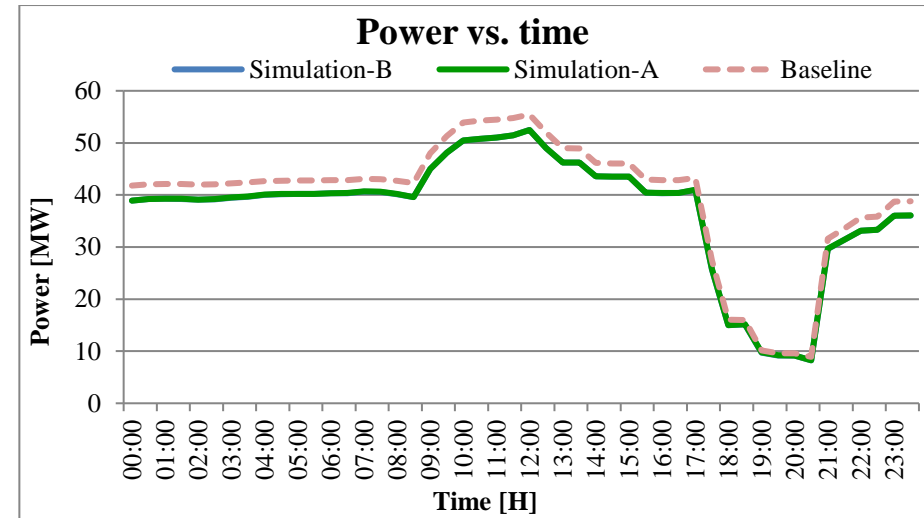


Figure 89: Multiple parameter increase comparison – Simulation-B – power vs. time

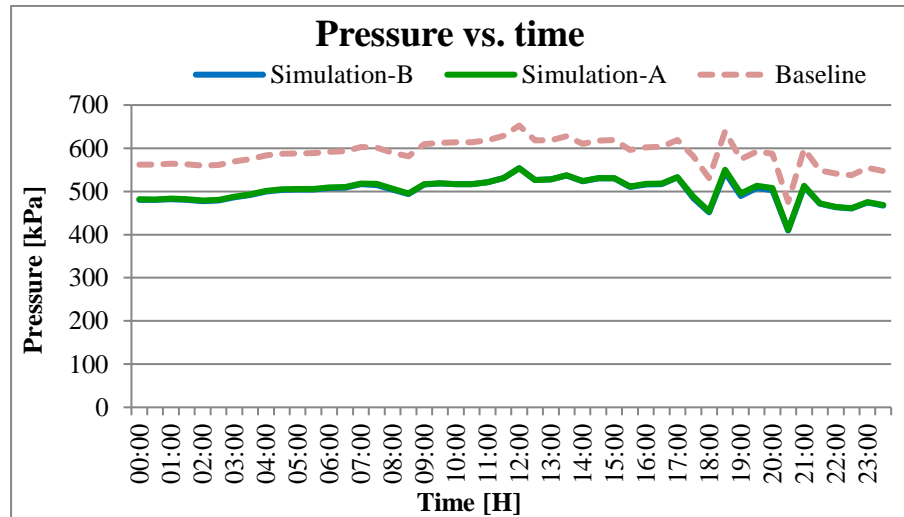


Figure 90: Multiple parameter increase comparison – Simulation-B – pressure vs. time

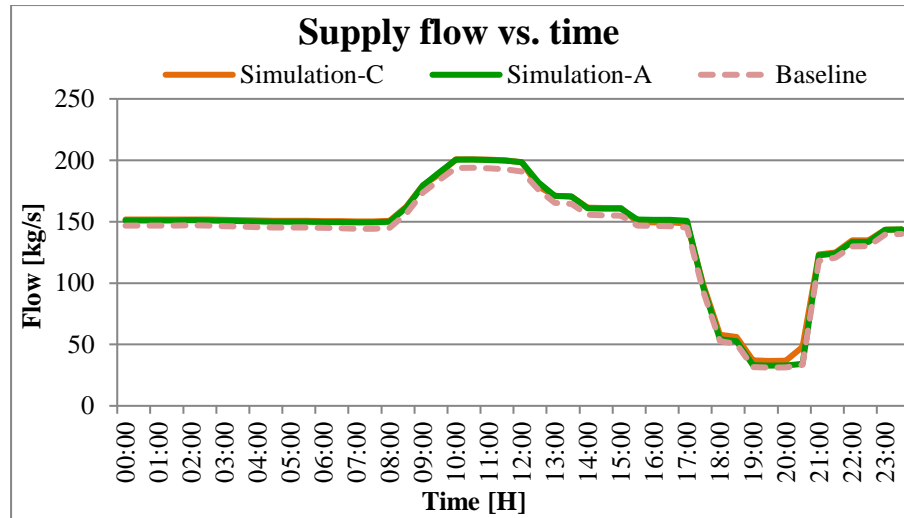


Figure 91: Multiple parameter increase comparison – Simulation-C – flow vs. time

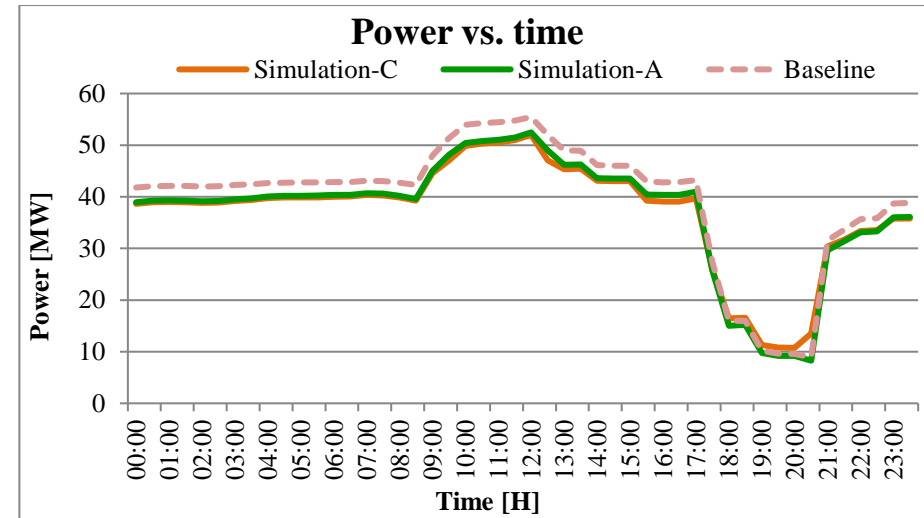


Figure 92: Multiple parameter increase comparison – Simulation-C – power vs. time

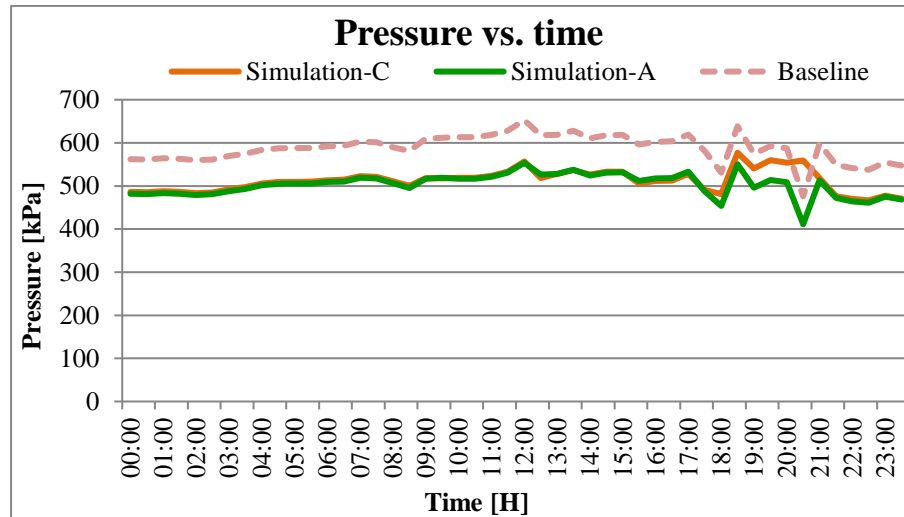


Figure 93: Multiple parameter increase comparison – Simulation-C – pressure vs. time

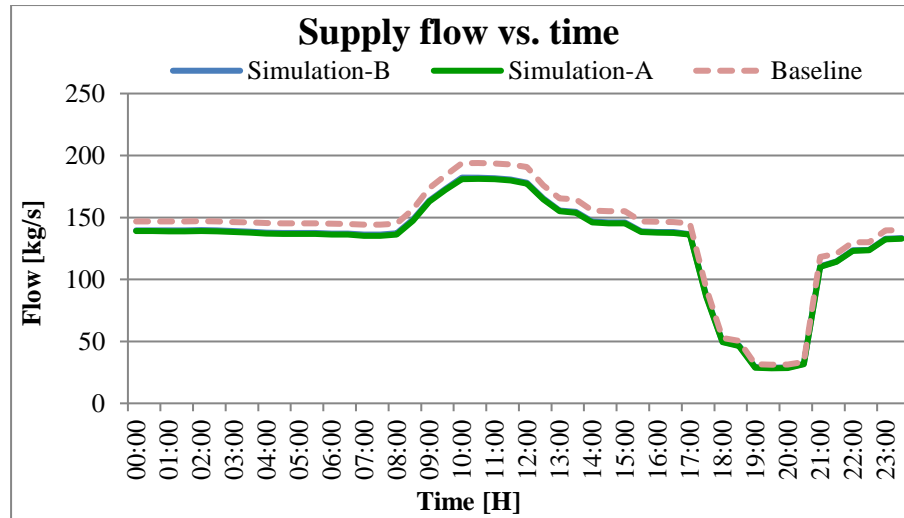


Figure 94: Multiple parameter decrease comparison – Simulation-B – flow vs. time

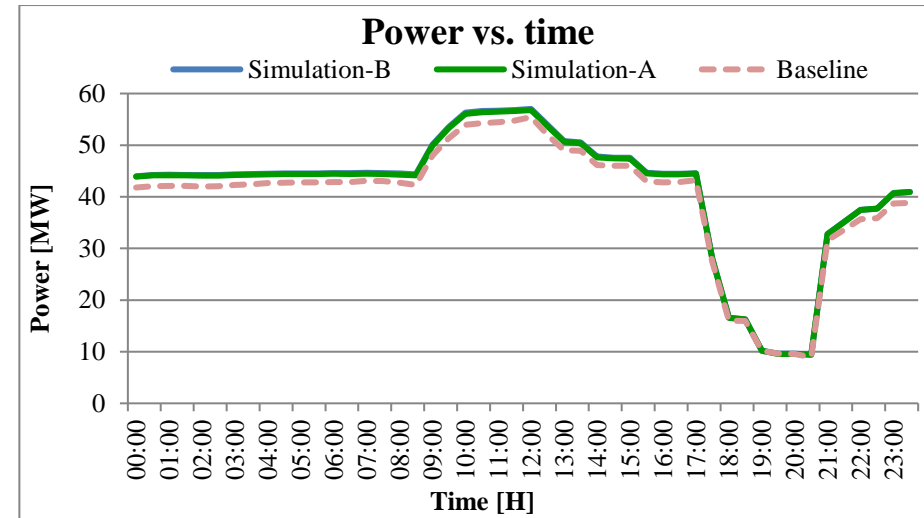


Figure 95: Multiple parameter decrease comparison – Simulation-B – power vs. time

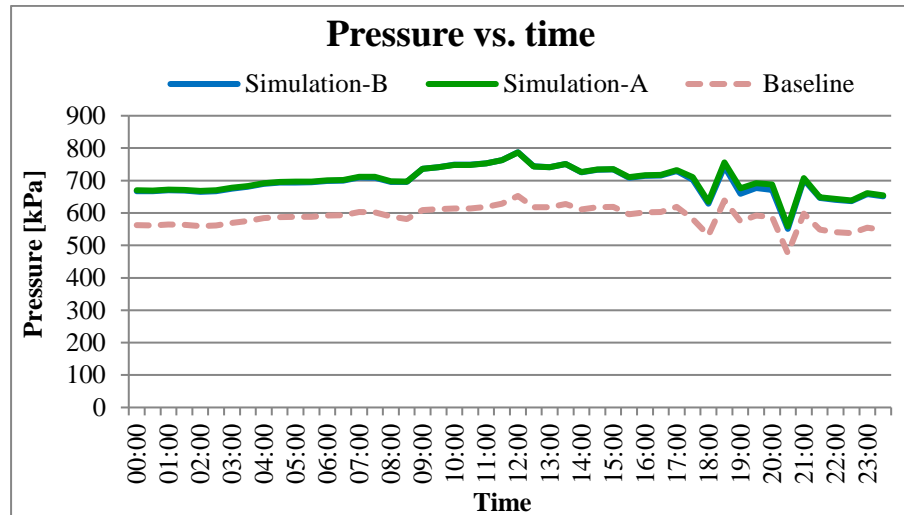


Figure 96: Multiple parameter decrease comparison – Simulation-B – pressure vs. time

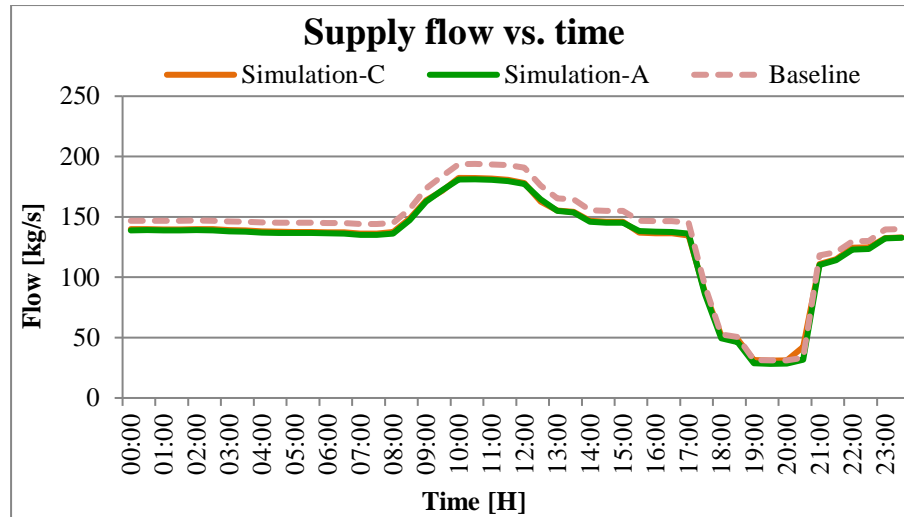


Figure 97: Multiple parameter decrease comparison – Simulation-C – flow vs. time

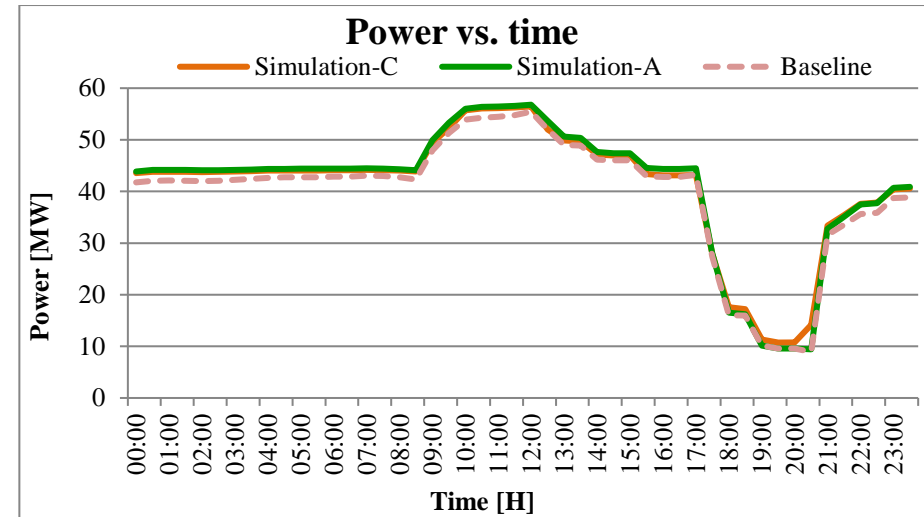


Figure 98: Multiple parameter decrease comparison – Simulation-C – power vs. time

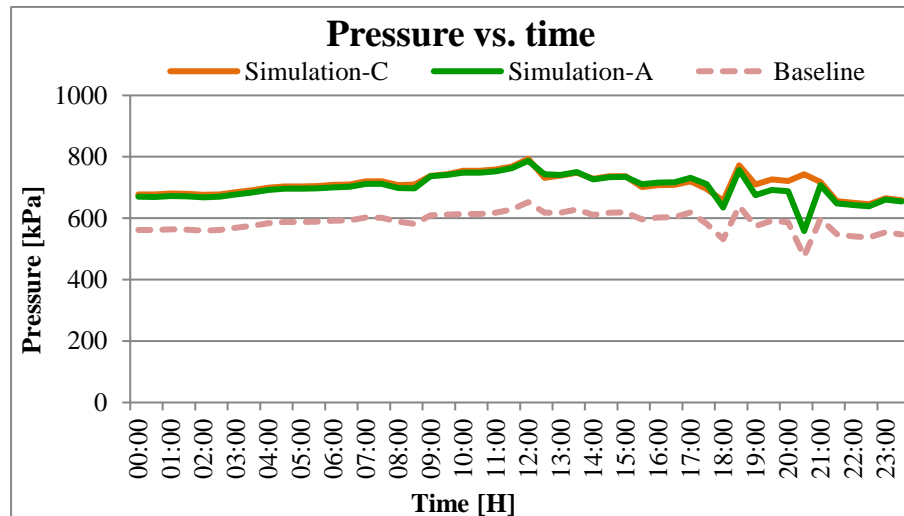


Figure 99: Multiple parameter decrease comparison – Simulation-C – pressure vs. time

Appendix J

Detailed results analysis of simulation components

1. Flow demand variation

Table 42 and Table 43 display the maximum percentage difference obtained from an individual compressor(s) after variation of the flow demand. Table 42 and Table 43 also display the combined average percentage error of all the compressor houses.

a) Simulation-B versus Simulation-A

Table 42: Simulation-B – flow demand variation – max percentage error

	Compressor house	Maximum error [%]	Average error [%]
Increased supply flow	CH14#	0.81	0.28
Increased power usage	CH11#	1.62	0.94
Increased supply pressure	CH14#	3.19	1.96
Decreased supply flow	CH14#	1.12	0.41
Decreased power usage	CH11#	0.71	0.36
Decreased supply pressure	CH11#	1.66	1.26

The maximum percentage error results illustrated in Table 42 display a maximum error of only 3.19% and an average percentage error maximum of 1.96% for all scenarios of Simulation-B.

b) Simulation-C versus Simulation-A

Table 43: Simulation-C – flow demand variation – max percentage error

	Compressor house	Maximum error [%]	Average error [%]
Increased supply flow	CHCentral#	30.43	0.70
Increased power usage	CHCentral#	28.18	0.41
Increased supply pressure	CHCentral#	4.53	1.56
Decreased supply flow	CHCentral#	30.20	0.56
Decreased power usage	CHCentral#	26.62	0.50
Decreased supply pressure	CHCentral#	3.48	1.56

The maximum percentage error results illustrated in Table 43 display a maximum error of 30.43% for Simulation-C. This, however, is because of the low flow rates of CHCentral#.

The corresponding average error obtained from the total flow remains only 0.70%. The total flow from CHCentral# contributes very little to the compressed air network flow. Any small errors would, therefore, result in a substantial percentage error. The maximum average percentage error, however, resulted in only 1.56%.

2. Supply pressure variation

Table 44 and Table 45 display the maximum percentage difference obtained from an individual compressor(s) after variation of the compressor supply pressure set point. Table 44 and Table 45 also display the combined average percentage error of all the compressor houses.

a) Simulation-B versus Simulation-A

Table 44: Simulation-B – supply pressure variation – max percentage error

	Compressor house	Maximum error [%]	Average error [%]
Increased supply flow	CH7#	11.71	0.97
Increased power usage	CH7#	12.22	1.21
Increased supply pressure	CH14#	2.35	1.57
Decreased supply flow	CH7#	182.53	29.93
Decreased power usage	CH7#	248.77	33.76
Decreased supply pressure	CH14#	0.85	0.15

The maximum percentage error results illustrated in Table 44 display a maximum error of 248.77% and an average percentage error maximum of 33.76% for all scenarios of Simulation-B.

The higher percentage error is a result of the interconnected compressed air network that receives compressed air from other shafts. During simulation, the supply pressure is sufficient near compressor house CH7# because of air supplied from other shafts. To maintain its required supply pressure, the compressors of compressor house CH7# will reduce its air supply. This results in a difference in compressor house output accuracy.

However, as seen in Table 44, the decreased supply pressure of all the compressor houses has a maximum percentage error of only 0.85% and an average error of only 0.15%. This is

because compressor house CH7# is the only outlier in the simulated results. All other compressor house results fall within acceptable accuracies.

b) Simulation-C versus Simulation-A

Table 45: Simulation-C – supply pressure variation – max percentage error

	Compressor house	Maximum error [%]	Average error [%]
Increased supply flow	CHCentral#	30.30	0.71
Increased power usage	CHCentral#	27.48	0.16
Increased supply pressure	CHCentral#	3.81	1.37
Decreased supply flow	CH7#	48.03	0.21
Decreased power usage	CH11#	36.32	1.68
Decreased supply pressure	CH14#	0.80	0.43

The maximum percentage error results illustrated in Table 45 display a maximum error of 48.03% for Simulation-C. This again is caused by air being supplied by other compressor houses in the interconnecting compressed air network during simulation of this scenario. The maximum average percentage error, however, resulted in only 1.68%.

c) Pipe dimension variation

Table 46 and Table 47 display the maximum percentage difference obtained from an individual compressor(s) after variation of the pipe diameters. Table 46 and Table 47 also display the combined average percentage error of all the compressor houses.

a) Simulation-B versus Simulation-A

Table 46: Simulation-B – pipe dimension variation – max percentage error

	Compressor house	Maximum error [%]	Average error [%]
Increased supply flow	CH14#	0.51	0.21
Increased power usage	CHCentral#	0.74	0.46
Increased supply pressure	CH11#	1.32	1.08
Decreased supply flow	CH14#	1.88	0.50
Decreased power usage	CH11#	1.64	0.60

	Compressor house	Maximum error [%]	Average error [%]
Decreased supply pressure	CH14#	4.11	1.92

The maximum percentage error results illustrated in Table 46 display a maximum error of only 4.11% and an average percentage error maximum of 1.92% for all scenarios of Simulation-B.

b) Simulation-C versus Simulation-A

Table 47: Simulation-C – pipe dimension variation – max percentage error

	Compressor house	Maximum error [%]	Average error [%]
Increased supply flow	CHCentral#	30.55	0.55
Increased power usage	CHCentral#	26.66	0.41
Increased supply pressure	CHCentral#	3.29	1.71
Decreased supply flow	CHCentral#	29.93	0.87
Decreased power usage	CHCentral#	28.04	0.37
Decreased supply pressure	CH11#	4.52	1.31

The maximum percentage error results illustrated in Table 47 display a maximum error of 30.55% for Simulation-C. This is caused by the low flow contribution CHCentral# has on the total mine compressed air total flow as discussed previously. The maximum average percentage error, however, resulted in only 1.71%.

d) Multiple parameter variations

Table 48 and Table 49 display the maximum percentage difference obtained from an individual compressor(s) after simultaneous variation of all the parameters. Table 48 and Table 49 also display the combined average percentage error of all the compressor houses.

a) Simulation-B versus Simulation-A

Table 48: Simulation-B – multiple parameter variation – max percentage error

	Compressor house	Maximum error [%]	Average error [%]
Increased supply flow	CH14#	0.43	0.18

	Compressor house	Maximum error [%]	Average error [%]
Increased power usage	CH11#	1.05	0.72
Increased supply pressure	CH14#	1.77	1.37
Decreased supply flow	CH14#	2.16	0.61
Decreased power usage	CH11#	1.09	0.40
Decreased supply pressure	CH14#	3.02	1.65

The maximum percentage error results illustrated in Table 48 display a maximum error of only 3.02% and an average percentage error maximum of 1.65% for all scenarios of Simulation-B.

b) Simulation-C versus Simulation-A

Table 49: Simulation-C – multiple parameter variation – max percentage error

	Compressor house	Maximum error [%]	Average error [%]
Increased supply flow	CHCentral#	30.61	0.61
Increased power usage	CHCentral#	27.21	0.35
Increased supply pressure	CHCentral#	3.74	1.74
Decreased supply flow	CHCentral#	29.71	0.79
Decreased power usage	CHCentral#	27.19	0.37
Decreased supply pressure	CHCentral#	4.13	1.41

The maximum percentage error results illustrated in Table 49 display a maximum error of 30.61% for Simulation-C. This is again caused by the low flow contribution CHCentral# has on the total mine compressed air total flow. The maximum average percentage error, however, resulted in only 1.74%.

Appendix K

Method verification results comparison

Table 50: Mine-B 24-hour raw data

Time [Hour]	Power [MW]	Pressure [kPa]	Flow [m³/s]
00:00	7.89	494.47	26.56
01:00	7.97	502.85	26.67
02:00	7.95	512.18	26.70
03:00	7.97	519.60	26.69
04:00	7.94	533.22	26.44
05:00	7.99	549.87	26.19
06:00	8.04	551.91	26.27
07:00	7.99	506.31	26.84
08:00	7.88	471.56	26.83
09:00	8.33	453.83	27.55
10:00	9.53	508.96	29.18
11:00	9.42	512.70	29.15
12:00	9.03	533.04	28.45
13:00	8.84	548.53	27.82
14:00	8.69	562.08	27.03
15:00	8.48	548.66	27.05
16:00	7.65	531.94	25.80
17:00	7.70	541.65	25.91
18:00	7.84	548.91	26.14
19:00	7.86	580.30	25.74
20:00	7.88	537.84	26.70
21:00	7.89	532.28	26.48
22:00	7.91	522.28	26.54
23:00	7.92	501.68	26.80

Table 51: Mine-B power usage comparison

Time [Hour]	Actual power [MW]	Simulated power [MW]	Error [%]
00:00	7.89	8.18	3.57%
01:00	7.97	8.44	5.60%
02:00	7.95	8.35	4.80%
03:00	7.97	8.13	2.02%
04:00	7.94	8.23	3.55%
05:00	7.99	8.22	2.84%
06:00	8.04	8.45	4.84%
07:00	7.99	7.39	8.07%
08:00	7.88	7.27	8.44%
09:00	8.33	7.20	15.60%
10:00	9.53	9.35	1.97%
11:00	9.42	9.43	0.17%
12:00	9.03	9.13	1.08%
13:00	8.84	8.82	0.18%
14:00	8.69	8.44	3.01%
15:00	8.48	8.03	5.69%
16:00	7.65	7.36	3.84%
17:00	7.70	7.33	4.96%
18:00	7.84	7.37	6.40%
19:00	7.86	9.35	15.95%
20:00	7.88	7.87	0.16%
21:00	7.89	7.19	9.73%
22:00	7.91	8.01	1.24%
23:00	7.92	8.32	4.84%
Avg.	8.19	8.16	4.94%

Table 52: Mine-B flow comparison

Time [Hour]	Actual flow [m³/s]	Simulated flow [m³/s]	Error [%]
00:00	26.56	26.81	0.95%
01:00	26.67	27.37	2.57%
02:00	26.70	26.99	1.07%
03:00	26.69	26.34	1.30%
04:00	26.44	26.43	0.03%
05:00	26.19	26.17	0.08%
06:00	26.27	26.75	1.81%
07:00	26.84	24.58	9.19%
08:00	26.83	24.76	8.36%
09:00	27.55	24.82	10.98%
10:00	29.18	29.58	1.38%
11:00	29.15	29.70	1.86%
12:00	28.45	28.65	0.70%
13:00	27.82	27.70	0.42%
14:00	27.03	26.55	1.78%
15:00	27.05	25.69	5.29%
16:00	25.80	24.17	6.76%
17:00	25.91	23.97	8.10%
18:00	26.14	23.97	9.07%
19:00	25.74	28.67	10.21%
20:00	26.70	25.40	5.10%
21:00	26.48	23.71	11.68%
22:00	26.54	26.03	1.96%
23:00	26.80	27.10	1.12%
Avg.	26.90	26.33	4.24%

Table 53: Mine-B pressure comparison

Time [Hour]	Actual pressure [kPa]	Simulated pressure [kPa]	Error [%]
00:00	494.47	494.47	0.00%
01:00	502.85	502.85	0.00%
02:00	512.18	512.18	0.00%
03:00	519.60	519.60	0.00%
04:00	533.22	533.22	0.00%
05:00	549.87	549.87	0.00%
06:00	551.91	551.91	0.00%
07:00	506.31	506.31	0.00%
08:00	471.56	471.56	0.00%
09:00	453.83	453.83	0.00%
10:00	508.96	508.96	0.00%
11:00	512.70	512.70	0.00%
12:00	533.04	533.04	0.00%
13:00	548.53	548.53	0.00%
14:00	562.08	562.08	0.00%
15:00	548.66	548.66	0.00%
16:00	531.94	531.94	0.00%
17:00	541.65	541.65	0.00%
18:00	548.91	548.91	0.00%
19:00	580.30	580.30	0.00%
20:00	537.84	537.84	0.00%
21:00	532.28	532.28	0.00%
22:00	522.28	522.28	0.00%
23:00	501.68	501.68	0.00%
Avg.	525.28	525.28	0.00%